# ABSTRACT

| | |
|---|---|
| Title of Dissertation: | IDENTIFICATION OF A NOVEL ANTI-APOPTOTIC GENE OF *MYCOBACTERIUM TUBERCULOSIS* |
| | Benjamin Edgar Hurley, Doctor of Philosophy, 2012 |
| Dissertation Directed By: | Associate Professor Volker Briken<br>Department of Cell Biology and Molecular Genetics |

Over the next 20 years, more than 36 million people are expected to die of *Mycobacterium tuberculosis* (Mtb) related illness. We may prevent this only by learning as much as possible about the Mtb-mediated exploitation of the human immune system and successfully implementing that knowledge to combat the pathogen. One Mtb virulence mechanism involves inhibition of host apoptosis. An Mtb laden macrophage will attempt cell suicide, subsequently destroying any intracellular bacteria. In prior work, a large gain-of-function screen identified Mtb genomic regions involved in host apoptotic suppression; one such region is "K20." A loss-of-"gain-of-function" (LoGoF) screen involving *in vitro* transposon (Tn) mutagenesis of a K20 expressing vector identified individual gene(s) of K20 potentially responsible the virulence phenotype. This LoGoF screen found two unique K20 Tn-clones that consistently induced significant host apoptosis. These

Tn's disrupted expression of K20 genes *Rv2666* ( probable truncated transposase) and *Rv2667* ( possible Clp ATPase).

A *Himar1* Tn mutant of *Rv2666* was obtained through the TARGET mutant library project. Upon infection of human macrophages, Tn*Rv2666* induced significantly more host apoptosis than wild type (WT) and complement, confirming *Rv2666* as an anti-apoptotic gene of Mtb. There are no current publications suggesting a specific role for transposase-based virulence in Mtb; Rv2666 may affect an anti-apoptotic phenotype by modulating transcription of factors important for the suppression of host apoptosis.

The second LoGoF identified gene, *Rv2667*/*clpC2*/*clpX'*, was not available through TARGET; a recombinant Δ*clpC2* mutant was generated. Comparing induced host apoptosis of Δ*clpC2* infected macrophages to WT revealed *Rv2667*/*clpC2* has no essential role as an anti-apoptotic gene of Mtb. Δ*clpC2* was further characterized to explain the discrepancy between the initial LoGoF data and the Δc*lpC2* Mtb results. Study of Δ*clpC2* determined that it bears no significant differences with WT in terms of *in vitro* growth, host necrosis-induction, *in vivo* survival and induced host TNFα secretion levels. However, Δ*clpC2* induces significantly more host IL-1β release than WT Mtb. The reason for this effect is unknown; ClpC2 may aid Mtb pathogenicity by limiting host inflammation, thus permitting infecting Mtb a "head start" against a host adaptive immune response.

# LAY ABSTRACT

Pulmonary tuberculosis (TB), primarily caused *Mycobacterium tuberculosis* (Mtb) infection, kills over two million people every year. Curable in most cases, the misuse of antibiotics, often due to sporadic access to adequate health care in third-world locales, has given rise to drug-resistant Mtb. These Mtb super-strains essentially return us to a pre-antibiotic era in terms of limiting patient TB treatment and are cause for great concern in all nations, developing and industrialized. Creation of a vaccine is one of the best methods we have for total disease eradication.

On that note, we may be able to generate an effective vaccine by exploiting cellular apoptosis, or "cell suicide." In the same way that defective, pre-cancerous cells of a person's body seem to altruistically sacrifice themselves in order to prevent cancer from spreading, white blood cells such as macrophages will self-destruct when infected with pathogens such as Mtb. Apoptosis of a host macrophage kills the bacteria within; this event also helps to generate a long-term memory response to prevent future infections. Understandably, Mtb employs several tactics of its own to prevent host apoptosis and protect itself.

An effective anti-TB vaccine may be created by genetic modification of Mtb. In this case, scientists will target the Mtb genes responsible for prevention of host apoptosis and remove them, attenuating the bacteria. When this attenuated Mtb strain is used as a vaccine, great amounts of host apoptosis will result, leading to a robust long-term immune system memory response and, hopefully, provide humanity with a vaccine that will eliminate TB once and for all. This dissertation explores that concept and specifically identifies an anti-apoptosis gene of Mtb, *Rv2666*.

# *IDENTIFICATION OF A NOVEL ANTI-APOPTOTIC GENE OF MYCOBACTERIUM TUBERCULOSIS*

By

Benjamin Edgar Hurley

Dissertation submitted to the Faculty of the Graduate School of the
University of Maryland, College Park, in partial fulfillment
of the requirements for the degree of
Doctor of Philosophy
2012

Advisory Committee:
Professor Volker Briken, PhD, Chair
Professor Najib El-Sayed, PhD
Professor Kevin McIver, PhD
Professor Daniel Stein, PhD
Professor Philip DeShong, ScD

# Acknowledgments

I would like to express my deep gratitude to Dr. Volker Briken for his continuous patience and encouragement throughout my graduate career at the University of Maryland. Dr. Briken has been instrumental in keeping me goal-focused and driven when things seemed overwhelming. The journey through any doctoral program is quite difficult, and everyone should be so lucky to have a mentor like Dr. Briken to guide them.

I also must acknowledge Dr. Amro Bohsali, whose continuous upbeat demeanor and advice I'll certainly miss after leaving UMD. Hilarious to hang out with, a natural businessman and a great friend, I'd wish him the best in the future, but I know he doesn't need it. I'd also like to thank Dr. Serdar Gurses, one of the kindest people I've ever known and whose good-natured assistance (in the lab and out) could always be counted on. Dr. Hana Abdalla has been a tremendous source of inspiration during my time here and her advice has been spot-on without fail. Gaya Hettiarachchi's sense of humor will be missed and her and incredible work-ethic is something to which I aspire. I'd like to thank Swati Shah; incredibly considerate of others and a very thoughtful researcher; I've been extraordinarily lucky to have her as a labmate and co-collaborator on so much of the work I've accomplished here. I wish to thank Lalitha Srinivasan, a brilliant lady whose relentless enthusiasm for science (in the face of grad school no less) has been inspiring. Jeff Quigley's incredible attention to detail has never failed to amaze me and his relaxed, good-humored disposition has made him a pleasure to work with.

I'd also like to thank the other members of my thesis committee, Dr. DeShong, Dr. El-Sayed, Dr. McIver and Dr. Stein. Through probing questions, suggestions and advice, I can honestly say I feel like they've helped think as a better scientist. I'd like to acknowledge Dr. Alan Sher (National Institute of Health) and Dr. Bruno Andrade (NIH), who provided the monocytes and technical advice that made much of this dissertation possible. On the same note, I want to thank Dr. Petros Karakousis (Johns Hopkins University) and Michael Pinn (JHU) who donated macrophages and much of their time to make this research possible. Many thanks are given to Kenneth Class, for training in flow cytometry, and Dr. Karen Swanson, whose instruction in fluorescence microscopy was invaluable. I'd like to express my gratitude to Dr. Michelle Brooks, whose help with the red-tape of grad school has been a life saver. Also, much thanks to Carol Rosenberg and Serena Golden, who proof-read this entire document and didn't complain at all.

Finally I'd like to thank my family- my parents, Mark and Gerrie Hurley, my grandmothers, Hazel Hurley and Erna Kist, and Amy, Lorenzo and Nora Bennett. Their love and constant support have made the completion of this journey possible, and I would like to dedicate this publication to them.

# Table of Contents

Acknowledgments ..... ii
Table of Contents ..... iv
List of Tables ..... viii
List of Figures ..... ix
List of Abbreviations ..... xi
Chapter 1: Introduction ..... 1
1.1 TB: A Historical and Cultural Perspective ..... 1
1.1.1 TB: Prehistoric Origins ..... 1
1.1.2 TB: Ancient civilizations through the modern era ..... 4
1.2 TB: Pathology ..... 6
1.3 TB: Epidemiology ..... 7
1.4 TB: Treatment and prevention of TB, clinical approaches ..... 10
1.4.1 Treatment of TB: Prehistoric approaches through the Enlightenment era ..... 10
1.4.2 Treatment of TB: Dawn of the modern medical era, vaccination and antibiotics ..... 11
1.4.3 Treatment of TB: Problems of the present day ..... 14
1.4 Summary and conclusion of introductory remarks ..... 16
Chapter 2: Background ..... 17
2.1 Mycobacteria ..... 17
2.1.1 *M. tuberculosis* (Mtb) ..... 17
2.1.2 *M. bovis* and *M. bovis*-BCG ..... 18
2.1.3 Other mycobacterial model species used in our studies ..... 19
2.2 Experimental systems: cell lines and model organisms ..... 21
2.2.1 THP-1 cell line ..... 21
2.2.2 Primary human monocyte-derived macrophages (HMDMs) ..... 22
2.2.3 Murine model system ..... 25
2.2.4 Hartley guinea pig model ..... 27
2.3 Mtb survival strategies ..... 28
2.3.1 Mtb phagolysosome fusion inhibition ..... 29
2.3.2 Mtb response to reactive nitrogen intermediates (RNI) and reactive oxygen intermediates (ROI) ..... 29
2.4 Mtb survival strategy: prevention of host-cell apoptosis ..... 30
2.4.1 Apoptosis as a host defense mechanism against Mtb: innate immunity ..... 31
2.4.2 Apoptosis as a host defense mechanism against Mtb: acquired immunity/cross-presentation ..... 32
2.4.3 Virulent mycobacteria species suppress host apoptosis ..... 33
2.4.4 Host-apoptosis: A potential means to an improved vaccine ..... 35
2.5 *M. tuberculosis*: transposases and Clp proteases ..... 36
2.5.1 Transposases ..... 36
2.5.2 *M. tuberculosis* Clp proteases ..... 39

Chapter 3: Materials and Methods ..... 42
3.1 Bacterial strain maintenance and media ..... 42
3.1.1 H37Rv work ..... 42
3.1.2 CDC 1551 work- Tn*Rv2666* and complement generation ..... 43
3.1.3 *M. kansasii* and *M. smegmatis* studies ..... 44
3.2 Δ*clpC2* recombinant mutant construction and complementation ..... 45
3.2.1 Δ*clpC2* recombinant mutant construction ..... 45
3.2.2 Δ*clpC2* mutant complementation ..... 48
3.3 *In vitro* transposon mutagenesis for Loss-of-Gain-of-Function (LoGoF) screening ..... 48
3.4 Electroporation of plasmids ..... 51
3.5 THP-1 cell culture maintenance and differentiation. ..... 52
3.6 THP1 infection and cell death quantification ..... 52
3.7 Southern blot analysis ..... 53
3.8 Genomic DNA isolation- Mycobacteria ..... 53
3.9 Reverse transcription PCR (RT-PCR) ..... 55
3.10 RNA isolation- Mycobacteria ..... 56
3.11 Growth curve measurement ..... 57
3.12 SCID mice aerosol infections ..... 57
3.12.1 Aerosol infection of SCID mice ..... 58
3.12.2 Colony forming unit (CFU) determination ..... 58
3.13 Human monocyte derived macrophages (HMDMs) ..... 59
3.13.1 Human monocyte derived macrophages: culturing ..... 59
3.13.2 Human monocyte derived macrophages: infection ..... 60
3.13.3 Human monocyte derived macrophages: hypodiploid staining cell death quantification ..... 60
3.14 Alveolar guinea pig macrophages ..... 61
3.14.1 Obtaining and culturing of guinea pig macrophages ..... 61
3.14.2 Infections of guinea pig alveolar macrophages ..... 61
3.14.3 Infections of guinea pig peritoneal macrophages ..... 62
3.15 Adenylate kinase (AK) release assay ..... 63
3.16 Colony forming units (CFUs) study ..... 64
3.17 ELISA assays ..... 64
3.17.1 TNFα ELISA ..... 64
3.17.2 IL-1β ELISA ..... 65
3.18 Apoptotic cell death quantification ..... 66
3.18.1 Terminal deoxynucleotidyl transferase dUTP nick end labeling (TUNEL) assays ..... 66
3.18.2 Hypodiploid quantification ..... 67
3.19 Statistical analysis ..... 68
Chapter 4: Identification of anti-apoptotic gene(s) for a set genomic region of *M. tuberculosis* ..... 69
4.1 Results: Identification of anti-apoptotic gene(s) for a set genomic region of Mtb ..... 69
4.1.1 The K20 genomic region of Mtb confers an anti-apoptotic phenotype to high-apoptosis inducing mycobacteria ..... 69

4.1.1.1 The K20 genomic region confers an anti-apoptotic phenotype guinea pig alveolar, but not peritoneal, macrophages ..... 72
4.1.2 *Loss-of*-Gain-of-Function (LoGoF) screen identifies possible anti-apoptotic genes of Mtb ..... 75
4.1.2.1 LoGoF screen in $mc^2$-155 background identifies two possible anti-apoptotic genes of Mtb ..... 78
4.1.2.2 LoGoF screen in *M. kansasii* identifies two possible anti-apoptotic genes of Mtb ..... 79
4.1.3 A transposon mutant of *Rv2666* suggests anti-apoptotic role for the gene ..... 85
4.1.4 Complementation of Tn*Rv2666* confirms anti-apoptotic role and identifies *Rv2666* as contributing to the K20 phenotype ..... 88
4.1.5 Creation and confirmation of *clpC2* abrogation mutant ..... 92
4.1.6 Δ*Rv2667*/*clpC2* is dispensable for a salient role in modulating host anti-apoptosis effects by Mtb ..... 95
4.2 Discussion: Identification of anti-apoptotic gene(s) for genomic region of Mtb ..... 98
4.2.1 The K20 genomic region of Mtb displays an anti-apoptotic phenotype in several host models. ..... 100
4.2.2 *Loss-of*-Gain-of-Function (LoGoF) screening approach to identify possible K20 GoF phenotype genes of Mtb ..... 103
4.2.2.1 *Loss-of*-Gain-of-Function (LoGoF) screen in $mc^2$-155 background identifies possible K20 GoF phenotype genes of Mtb ..... 104
4.2.2.2 LoGoF screen in *M. kansasii* identifies two possible anti-apoptotic genes of Mtb ..... 105
4.2.3 *Rv2666* is an Mtb gene contributing to the K20 anti-apoptotic GoF phenotype ..... 107
4.2.3.1 The *Rv2666* gene of Mtb and the Tn*Rv2666* transposon mutant: overview ..... 108
4.2.3.2 Loss-of-function (LoF) study confirms anti-apoptotic role for the *Rv2666* gene ..... 110
4.2.6.1 Generation of a *clpC2* deficient strain of Mtb, details and relevant issues ..... 119
5.1.6.2 LoF study of a *clpC2* deficient strain of Mtb ..... 122
Chapter 5: Characterization of pathogenicity of *clpC2* abrogation mutant ..... 126
5.1 Results: Characterization of pathogenicity of *clpC2* abrogation mutant ..... 127
5.1.1 Altering *clpC2* expression has no effect on *in vitro* growth of Mtb in complete media, overexpression of *clpC2* in minimal media results in defective replication ..... 127
5.1.2 ClpC2 plays no salient role in mediating late-stage *in vivo* host necrosis ..... 132
5.1.3 ClpC2 has no noticeable effect on *in vivo* replication of Mtb ..... 135
5.1.4 ClpC2 has no role in altering TNFα secretion by HMDMs, but *clpC2* deletion elicits a significant increase in host Il-1β release ..... 139
5.2 Discussion: Characterization of pathogenicity of an Mtb *clpC2* abrogation mutant ..... 142

5.2.1 Abrogation of *clpC2* has no effect on *in vitro* growth in complete or defined media; overexpression of the gene in minimal media generates an observable growth defect ..... 143
5.2.2 ClpC2 plays no salient role in mediating late-stage *in vivo* host necrosis manipulation ..... 145
5.2.3 Δ*clpC2* shows no difference in intracellular survival compared to WT Mtb or complemented mutant ..... 148
5.2.4 Mtb *clpC2* has no apparent role in altering host TNFα secretion, but deletion elicits a significant increase in host Il-1β release ..... 149
Chapter 6: Summary and Conclusion ..... 155
6.1 Novel *in vitro* host models identified for the study of Mtb-host apoptosis interactions ..... 156
6.2 Loss-of-gain-of-function screening is a novel and viable method of anti-apoptotic gene identification ..... 159
6.3 Identification of *Rv2666* as a novel anti-apoptosis gene of Mtb, and a unique function for a transposase-like gene of Mtb ..... 161
6.4 *Rv2667* /*clpC2* not an anti-apoptotic gene of Mtb, but does affect host IL-1β secretion ..... 162
Chapter 7: Future Directions ..... 166
7.1 Future directions: model systems ..... 166
7.2 Future directions: screens to identify anti-apoptotic genes of Mtb ..... 169
7.3 Future directions: *Rv2666*, an anti-apoptotic gene of Mtb ..... 173
7.3.1 *Rv2666*: confirmation of phenotype by *in vivo* studies within animal model ..... 174
7.3.1 *Rv2666*: confirmation of potential role as a transcription factor of anti-apoptotic genes of Mtb ..... 174
7.4 Future directions: *Rv2667*/*clpC2*, an Mtb gene affecting host-IL-1β secretion ..... 176
7.4.1 *Rv2667*/*clpC2*: confirmation, and possible extension, of host cytokine secretion phenotype of interest ..... 176
7.4.2 *Rv2667*/*clpC2*: studying potential ATPase or chaperone activity ..... 178
7.4.3 *Rv2667*/*clpC2*: study gene expression and regulation with respect to Mtb virulence ..... 179
Supplemental Figures ..... 181
Supplemental Tables ..... 185
Bibliography ..... 187

# List of Tables

Supplemental Table ST1. Genes of the K20 Region: size, position, orientation and predicted function. ..... 185
Supplemental Table ST2. Individual LoGoF mutants. ..... 186

# List of Figures

Figure 1. Coevolution of *Homo sapiens sapiens* and MTBC. ..... 3
Figure 2. Global instances of TB in 2010 according to WHO. ..... 9
Figure 3. The AES and specialized phage transduction creation of Δ*clpC2*. ..... 47
Figure 4. Creation of LoGoF K20 transposon mutants. ..... 50
Figure 5. The K20 genomic region of Mtb confers an anti-apoptotic phenotype when used to transform the high-apoptosis inducing *M. kansasii*. ..... 71
Figure 6. Hartley guinea pig alveolar macrophages infected with *M. kansasii*-K20 and *M. kansasii*-null vector. ..... 73
Figure 7. Hartley guinea pig peritoneal macrophages infected with *M. kansasii*-K20 and null-vector. ..... 74
Figure 8. Schematic representation of the K20 LoGoF transposon mutant pool. ..... 77
Figure 9. LoGoF mutants sgR*v2666* and sg*Rv2667* are slightly higher inducers of host death than K20 in the $mc^2$155 background. ..... 80
Figure 10. LoGoF mutants sg*Rv2666* and sg*Rv2667* induce more host apoptosis than unaltered K20 in the Mkan background. ..... 83
Figure 11. Detailed transposon insertion map of the 4 LoGoF clones screened in Mkan. ..... 84
Figure 12. The *Himar1* transposon mutant of *Rv2666* induces increased host cell apoptosis compared to WT Mtb. ..... 87
Figure 13. Complementation of Tn*Rv2666* confirms anti-apoptotic role and identifies *Rv2666* as contributing to K20 phenotype. ..... 90
Figure 14. PCR confirms abrogation and complementation of *clpC2*. ..... 94
Figure 15. RT-PCR of purified bacterial RNA from WT Mtb, Δ*clpC2* and Δ*clpC2*-complement confirms *clpC2* gene expression level. ..... 94
Figure 16. Infection of HMDMs with WT Mtb and Δ*clpC2* indicates no significant differences in host apoptosis induction. ..... 96
Figure 17. Infection of alveolar guinea pig macrophages with WT Mtb and Δ*clpC2* indicates no significant differences in host apoptosis. ..... 97
Figure 18. Murine alveolar macrophage cell line (MH-S) is not a viable option for the study of Mtb-mediated suppression of host apoptosis. ..... 102
Figure 19. GM-CSF differentiated HMDMs infected with GoF vector transformed *M. kansasii* exhibit K20 GoF phenotype. ..... 114
Figure 20. *In vitro* growth curves of WT Mtb, Δ*clpC2* and two complements of Δ*clpC2* in complete and Sauton's minimal media studying kanamycin inclusion effect. ..... 130
Figure 22. No significant differences in necrosis of HMDMs infected with WT Mtb or Δ*clpC2* at days 3 and 10 post-infection. ..... 134
Figure 23. No significant differences in CFU counts during early and late-stage HMDM infection with WT Mtb, Δ*clpC2* and complement. ..... 138
Figure 24. Host secretion of cytokines TNFα and IL-1β is differentially affected by infection with WT Mtb, Δ*clpC2* and complemented mutant. ..... 141

Figure 25. Necrosis of HMDMs at 24 hours post-infection: a quality control experiment for IL-1β ELISA results. ..... 151
Figure 26. SCID mice infected with Mtb and Δ*clpC2*..... 154
Figure 27. Infection of Hartley alveolar guinea pig macrophages with WT Mtb and Δ*Rv3167c* indicates significant differences in host apoptosis. ..... 158
Figure S1. THP-1 cell line infection with Tn*Rv2666* mutant and complement confirm host anti-apoptosis phenotype and exclude necrosis. ..... 181
Figure S2. Southern blot confirmation of *clpC2* gene abrogation. ..... 182
Figure S3. sg*Rv2666* LoGoF and Tn*Rv2666* insertion points. ..... 183
Figure S4. sg*Rv2667* LoGoF clone insertion points and location of targeted homologous recombination arms within *Rv2667*/*clpC2* interior. ..... 184

# List of Abbreviations

AK – Adenylate kinase
ATP – Adenosine triphosphate
B6 – C57black6 mice
CD4+ T cells – Helper T cells
CD8+ T cells – Cytotoxic T cells
CFU – Colony forming units
Clp- Caseinolytic (Clp) protease
DAPI – 4',6-diamidino-2-phenylindole
DC – Dendritic cell
EDTA – Ethylenediaminetetraacetic acid
ELISA – Enzyme linked immunosorbent assay
EEA1 – Early endosome antigen 1
ESAT6 – Early secreted antigen 6
ETOH – Ethanol
FBS – Fetal bovine serum
GC – Guanine-cytosine
GM-CSF –Granulocyte macrophage colony stimulating factor
GoF- Gain-of-function assay
$H_2O_2$ – Hydrogen peroxide
HMDM- Human monocyte derived macrophage
hrs - Hours
IL – Interleukin
IL-1Ra – IL-1 receptor agonist
IR – Immune response
IS – Transposon insertion element
KO – Knock-out/gene abrogation mutant
LAM – Lipoarabinomannan
LAMP – Lysosomal associated membrane protein
LoGoF – Loss-of-'GoF'
LXA4 – Lipoxin A4
M1 – Classically activated macrophage
M2 – Alternatively activated macrophage
ManLAM – Mannose capped LAM
$mc^2$-155 – High competency strain of *M. smegmatis*
M-CSF – Macrophage colony stimulating factor
MDR – Multi-drug resistant
MHC – Major histocompatibility complex
min - minutes
Mkan – *M. kansasii*
MOI – Multiplicity of infection
Msmeg – *M. smegmatis*
Mtb – *M. tuberculosis*
MTBC – mycobacterium TB complex
NADH – Nicotinamide adenine dinucleotide

nt – Nucleotide (as a unit of length)
OD – Optical density
PBS – Phosphate buffered saline
PCR – Polymerase chain reaction
PFA – Paraformaldehyde
PGE2 – Prostaglandin E2
PI – Propidium iodide stain
PknE – Protein kinase E
PMA – Phorbol 12-myristate 13-acetate
pNPP – p-Nitrophenyl Phosphate
POI – Point of insertion (transposons)
RBC – Red blood cell
RD – Region of difference
RLU – Relative light unit
RNI – Reactive nitrogen intermediates
ROS – Reactive oxygen species
rpm – Rotations per minute
RT-PCR – Reverse transcriptase PCR
SECA2 – Protein translocase ATPase
SCID – Severe combined immunodeficiency
SD – Standard deviation
TB – Pulmonary tuberculosis
Th1 – CD4+ T helper cell type 1
Th2 – CD4+ T helper cell type 2
TLR – Toll like receptors
Tn – Transposon-mutant
TNFα – Tumor necrosis factor alpha
TNFR – TNFα receptor
TUNEL – Terminal deoxynucleotidyl transferase dUTP nick end labeling
UI – Uninfected
WT – Wild type
XDR – Extensively-drug resistant

# Chapter 1: Introduction

## 1.1 TB: A Historical and Cultural Perspective

### 1.1.1 TB: Prehistoric Origins

Pulmonary tuberculosis (TB) is one of the oldest diseases specifically plaguing mankind. *Mycobacterium tuberculosis* (Mtb) is the primary causative agent of pulmonary TB in humans; however, other mycobacterial species have also been known to cause TB. The entire cluster of organisms responsible for TB is referred to as belonging to the *Mycobacterium tuberculosis* complex (MTBC); MTBC is generally considered to be composed of the species Mtb, *M. africanum*, *M. pinnipedii*, *M. microti*, *M. bovis*, and *M. caprae* [1]. Recent work has suggested that the MTBC cluster, or its immediate progenitors, arose in concert with early Paleolithic era hominids, prior to the existence of hunter-gatherer *Homo sapiens sapiens* in what is now East Africa [1][2]. Specifically, it is believed the Mtb species arose from a clonal expansion event occurring during an evolutionary bottleneck approximately 35,000 years before present [1]. Until recently, *M. bovis* was considered to be the parent species of Mtb. However current bioinformatics work has suggested that *M. bovis* has branched from a human specific pathogen as a result of cohabitation of humans and cattle during the earliest time of bovine domestication and herding, approximately 13,000 to 15,000 years ago [3] (Figure 1).

In 2001, Rothschild *et al*. identified fragments of MTBC DNA in the skeletal tissue remains of an ancient Pleistocene era bison radiocarbon dated at nearly 18,000

years old [4]. The earliest current biochemical indication of human Mtb infections comes from the remains of a mother and child living about 8,500 years ago in the ruins of Atlit-Yam, a Neolithic settlement that is now submerged in the Eastern Mediterranean Sea. Researchers concluded that both individuals had been infected with Mtb prior to their deaths. Tissue for both was well-preserved in mud and brackish sea water; by testing the samples the investigators were able to identify Mtb specific DNA fragments and mycolic acids exclusive to the MTBC within the ancient tissue [5]. Greater detail regarding the phylogenetic origins of Mtb and the earliest days of the pathogen's niche in prehistoric civilizations will surely come to light as the techniques of forensic anthropology and paleomicrobiology continue to improve.

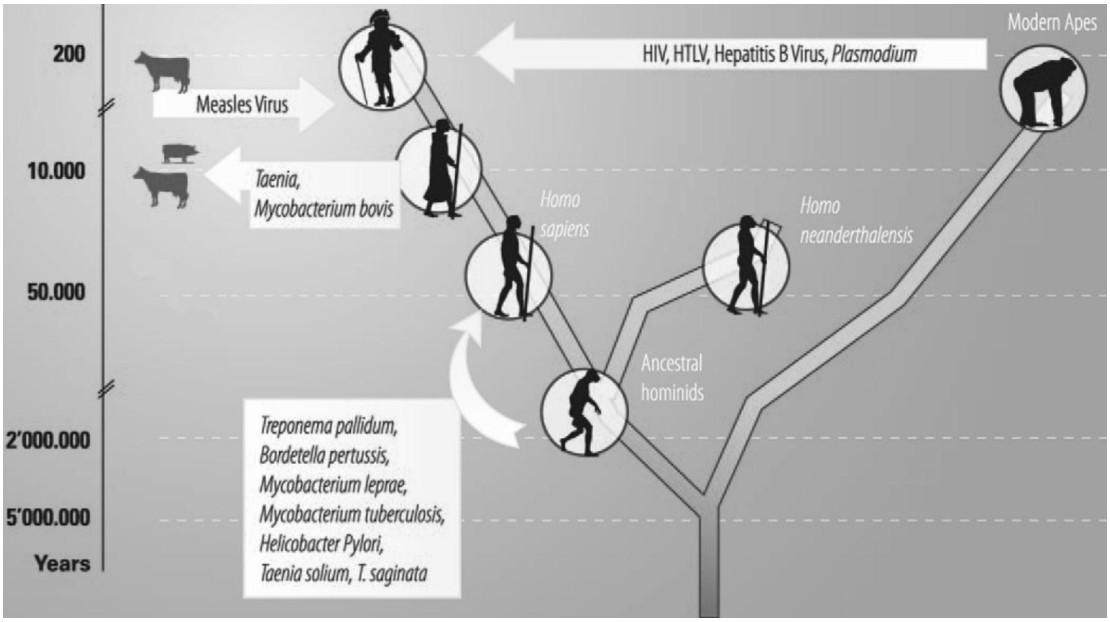


**Figure 1. Coevolution of *Homo sapiens sapiens* and MTBC.**
The *Mycobacterium tuberculosis* complex (MTBC) is generally considered to be composed of the species Mtb, *M. africanum*, *M. pinnipedii*, *M. microti*, *M. bovis*, and *M. caprae*. It is believed the Mtb species specifically arose from a clonal expansion event occurring during an evolutionary bottleneck approximately 35,000 ago [1]. *M. bovis* may have branched from a human specific pathogen during early bovine domestication, approximately 13,000 to 15,000 years before present. (Figure is obtained from [2] and is keeping with the terms of the Creative Commons Attribution License.)

### 1.1.2 TB: Ancient civilizations through the modern era

Mtb has had an enormous and well-evidenced impact on the course of human history. Many ancient Egyptian mummies have been identified as carriers of the Mtb pathogen or the closely related *M. africanum* species [6]. Thousand-year-old Andean mummies of South America were also burdened with the disease in their lifetime [7], suggesting the indigenous peoples of the Americas brought the pathogen with them when crossing the Bering Strait ages ago. Various ancient Sanskrit texts describe a disease similar to modern-day TB and recommend treatments of milk, rest, alcohol and relocation to higher altitudes [8]; interestingly these are some of the very same of treatments recommended for TB through the early 20$^{th}$ century. The ancient scholars Pliny the Younger, Hippocrates and Aristotle all wrote about a disease that shared the hallmarks of TB [9]. What held true for the ancient Greeks of the Mediterranean held true for the rest of Europe as well. For thousands of years, endemic TB was one of the leading causes of death and morbidity. For a 200-year period between the 17$^{th}$ and 19$^{th}$ centuries, TB was known as the "Great White Plague"; it killed one in 100 Londoners in 1660 and 25 percent of the European population at its peak in the 19$^{th}$ century [10].

TB had a significant impact on European mythology and literature. It is believed that the idea of the vampire, gaunt and ashen, began with the wasting and atrophy of TB victims who were occasionally buried during a period of extended unconsciousness and, when later excavated, were found to have scratched the insides of their coffins in an attempt to escape.

A slow death from TB led to emaciation and a characteristic pallor in victims; morbid paleness and sallow features were considered to be marks of great beauty by European culture during much of the last millennium [11]. Additionally, TB or "the Consumption," as it became commonly known was oddly romanticized as a condition that conferred a great burst of artistic innovation and ability just prior to claiming the lives of the affected. Of course, this old wives' tale is more a testament to the ubiquity of the disease across all social classes and educational ranks than any indicator of actual creative benefit. Frederic Chopin, Anton Chekov, Voltaire, several members of the Brontë family, Stephen Crane, Robert Louis Stevenson and George Orwell all died of pulmonary TB. The great poets Alexander Pope and Giacomo Leopardi both suffered from "Pott's disease," the disseminated form of Mtb infection that spreads into victims' vertebral bones and leads, in extreme cases, to severe physical disability, cosmetic deformity and great suffering [12]. Those unfortunate individuals burdened by extreme cases of TB during the pre-antibiotic era typically suffered the additional psychological fallout caused by severely limited physical mobility and great social ostracism.

The lack of effective TB treatments persisted through the early 20$^{th}$ century. TB was the second-leading cause of death in the United States in the year 1900, with about 200 of every 100,000 records deaths due to the illness [13]. The advent of a moderately successful vaccine, much-improved sanitation and effective antibiotics later reduced the lethality of pulmonary TB within industrialized nations, though the disease still persists throughout the developing world [14].

## 1.2 TB: Pathology

Mtb is typically spread when an infected individual aerosolizes the bacteria by forceful coughing, and bystanders inhale the aerosolized droplets. The inhaled bacillus travels to the pulmonary alveoli where it is phagocytosed by alveolar macrophages. By employing a range of survival mechanisms to prevent lysosomal digestion and immune system detection, the pathogen establishes itself within the host macrophage, where it begins to replicate.

The progression of the TB disease often depends on the individual immune response of the host, with about 10% of infected individuals progressing to an active form of TB. A case of TB is "active" if Mtb has established itself and is actively replicating within the infected individual's lungs; active TB is the disease state characterized by outward clinical manifestations of the disease. A patient in this disease state may experience a host of symptoms, including local tissue inflammation, necrosis and lesions, a hacking cough producing blood and sputum, severe weight loss, weakness, fatigue and often death, if the disease is allowed to progress without antibiotic treatment. An individual who is infected with the pathogen but demonstrates no obvious, outward signs of pathology has "latent TB;" this is typically characterized by an asymptomatic dormancy of the bacterial infection. The immune response (IR) of a person with latent TB has contained the contained the pathogen and prevented it from disseminating, but has not completely eliminated the infection [15]. This host IR-mediated quarantine of the infection often produces a granuloma.

A granuloma, a hallmark characteristic of TB infection, is formed by what seems to be a complex balancing act of host-pathogen interactions. (Incidentally, it is from this granuloma, or "tubercle," that we derive the name for tuberculosis disease [16].) Macrophages infected with Mtb will migrate to the epithelial layer [17]; simultaneously, activated $CD4^+$ T cells will

migrate to the site of infection, where they will recruit additional macrophages [15]. The site of infection quickly becomes a hot-spot of host inflammation and chemoattractant signaling. Newly arriving macrophages, neutrophils and monocytes will surround the infected macrophage from all sides, with a three-dimensional wall of leukocytes ultimately containing the infection without actually eliminating it; the infected macrophage may become a lipid-filled foamy macrophage [18]. Lymphocytes will surround this layer creating a hypoxic fibrous cuff, which is the granuloma [17].

It is important to note that the separation between the active and latent states of TB infection is dynamic. At any point, a latent infection may "awaken" or a granuloma may collapse or turn necrotic and cavitate, releasing the pathogen into the surrounding tissue. The occurrence of the latent to active shift is especially likely when an infected individual has become immunocompromised. This is sometimes the case when an individual contracts HIV/AIDS, becomes weakened with advanced age or is treated with anti-inflammatory compounds [19, 20]. In the some cases of uncontrolled TB infection, the bacteria may disseminate from the lungs to the liver, spleen and central nervous system, often leading to TB meningitis in infected children [21, 22]. In the most severe instances, the bacteria may even spread to an individual's spine, specifically to the intervertebral joints, which produces a painful and debilitating clinical condition referred to as Pott's disease or tuberculous spondylitis [23].

## 1.3 TB: Epidemiology

*Mycobacterium tuberculosis* (Mtb), the pathogen primarily responsible for pulmonary tuberculosis (TB), has infected roughly one-third of the world's population and is responsible for nearly 2 million deaths each year [14]. Though only

about 10% of those immunocompetent infected individuals will experience the active disease state in their lifetimes, the other approximately 1.8 billion individuals harboring latent infections will continue to fall victim to the disease, should they become immunocompromised at some point in their lifetime. Most of these new TB infections occur in developing regions of the world (Figure 2). A of political stability, poor access to health care and sanitation issues often exacerbate the spread of TB and limit the ability of medical workers to adequately contain, treat and prevent the disease. Compounding the manner, TB is often a central factor in claiming the lives of individuals who are infected with HIV. People who have both HIV and TB are at twice the risk of dying from TB as those who are infected with TB alone [24]. The current syndemic of HIV-TB occurring in developing nations compounds the problem even further [14, 17, 25]. At the current pace of TB-HIV syndemic growth, the World Health Organization-established goal of TB elimination by the year 2050 will not be achieved without significant advancements in prevention, diagnosis and treatment of the disease [24, 25].

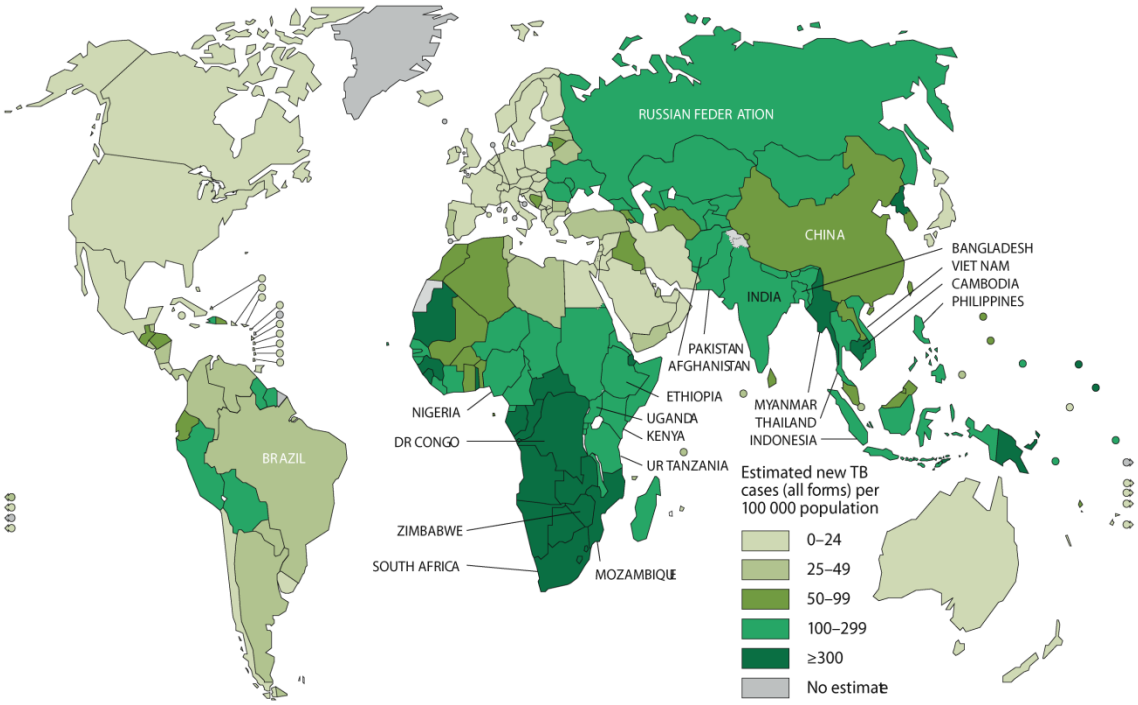


**Figure 2. Global instances of TB in 2010 according to WHO.**
World Health Organization (WHO) Global TB control report 2011 highlighting new reported instances of TB per 100,000 within a population. Gray scale identifies concentration of cases. Adapted from [14].

## 1.4 TB: Treatment and prevention of TB, clinical approaches

### 1.4.1 Treatment of TB: Prehistoric approaches through the Enlightenment era

In ancient Greece, the physicians and philosophers of the day recognized TB as a collection of symptoms composing a condition they referred to as phthisis. These men did not agree on the specific cause of phthisis. Hippocrates believed the disease was inherited, as the condition often seemed to occur in families and within small, related communities [9]. (Incidentally, Hippocrates recognized phthisis as one of the greatest diseases of his time and considered it absolutely terminal. He barred his pupils from attempting to treat victims, as their eventual deaths would damage the reputation of the attending physician.) The vast majority of the ancient Greeks agreed that phthisis was hereditary, with the notable exception of Aristotle, who contended that the disease was actually contagious [9]. It would be roughly 2,200 years before Robert Koch would prove Aristotle correct.

By the European Middle Ages, understanding and treatment of TB, much like the rest of science, had progressed very little since the heyday of the toga. One "treatment" of sorts was a proto-faith healing practice known as the "King's Touch." The general idea was that a person afflicted with phthisis could be cured of their disease when a king or queen, with healing powers ordained by God, laid hands upon the infected individual [26].

The Age of Enlightenment brought new focus and attention to how people thought of TB. Investigators into human anatomy discovered small, granular tubercles in the lungs of deceased individuals who had succumbed to phthisis. The physicians and scientists of the day believed these tubercles were responsible for

phthisis and subsequently blamed the tubercles themselves; the novel term "tuberculosis" arose to describe the condition from this discovery. The actual cause for the lung tubercles was still unknown at this time.

### 1.4.2 Treatment of TB: Dawn of the modern medical era, vaccination and antibiotics

By the 19th century, science had made relatively large leaps in understanding the disease. In 1865, Jean Antoine Villemin was able to infect rabbits with tuberculosis by injecting them with portions of tubercles obtained from cadavers, thus establishing the transmissible nature of tuberculosis. A few years later, Robert Koch conclusively identified the causative agent of TB as the bacillus *Mycobacterium tuberculosis* by testing the sputum samples of tuberculosis patients with a novel staining technique he developed. (To place the importance and impact of his discovery into greater context, at the time he made his announcement on March 24th, 1882, 1 in every 7 human deaths was attributable to tuberculosis.) Koch received the 1905 Nobel Prize in *Physiology or Medicine* and would be remembered as one of the fathers of microbiology for establishing his famous "Koch's postulates."

Although understanding of the disease and its transmission progressed greatly in the 19th century, the actual treatments for tuberculosis were lagging. As TB became generally accepted as contagious, containment and prevention became the focus of the day. Across the industrialized nations, sanatoriums were constructed to house individuals with obvious, active cases of TB. These sanatoriums were often built in high altitude locales, with the belief that the thinner air would assist patients' recovery. As mentioned, operating principle behind sanatoriums was one of

containment first and foremost. These facilities were run as semi-quarantine from the general public as well as a form of treatment for a patient. The medical consensus of the day believed that an infected individual's body should be able to heal itself, or at least wall-off or contain the bacteria within tubercles, if given fresh air, much food and plenty of rest. This "cure" was very similar to treatments prescribed in Ayurvedic texts of ancient India, indicating that TB treatment had progressed very little in over 2,000 years [8]. Sanatoriums also functioned as hospice homes for the terminally ill; it was generally understood that few people in sanatoriums ever fully recovered.

At the same time, public sanitation was greatly improved during the late 19$^{th}$ and early 20$^{th}$ centuries. Health-activist groups such as the National Tuberculosis Association, now the American Lung Association, raised funds to build sanatoriums and educate the public on proper hygiene to limit the spread of TB [27]. The NTA's anti-TB and hygiene propaganda was so effective that it contributed immensely to the decline of the public-use spittoon in the United States [27].

Although the late 19$^{th}$ century brought great strides in understanding of the TB disease and public sanitation, very little improvement had been made in preventing infection and colonization by the Mtb pathogen or in treating those people who were already infected. It was to that end that Albert Calmette and Camille Guérin began developing a vaccine for TB. In order to do this, Camette and Guérin subcultured *M. bovis* on an artificial media for 13 years. Camette and Guérin's *M. bovis* strain eventually lost its innate virulence for humans and became an attenuated strain.

Once the strain was no longer able to establish disease in laboratory animals, a vaccine was created. In 1921, the Bacille Calmette-Guérin, or BCG, vaccine was first used in humans. Theirs is the "parent" of the same strain that is still used to create vaccines in many modern nations. BCG has been quite successful in preventing the disseminated form of TB in children [28]; however, there is a very high degree of variability in the ability of the vaccine to prevent pulmonary TB [29]. Some studies estimate that the variable effectiveness of BCG in this capacity ranges from 80 to 0% [30], with the broad range considered to be at least partially dependent on environmental and/or genetic factors [31].

Even with the development of this moderately effective vaccine, there was still a great need for an effective treatment to aid those already infected. That need would be filled by the development of antibiotics.

Antibiotics were an accidental discovery. While working in his laboratory in 1928, Alexander Fleming noted a blue-green mold had grown on a Petri dish that was being used to culture *Staphylococcus*. Fleming noted that the contaminating mold was preventing the growth of the bacteria. He purified the *Penicillium notatum* mold and was subsequently awarded the 1945 Nobel Prize in *Physiology or Medicine* for isolating the world's first successful antibiotic. Around the same time that Fleming received his Nobel Prize, Selman Waksman's lab at Rutgers University isolated streptomycin from *Streptomyces griseus,* which functions by binding to the 30S subunit of the bacterial ribosome, ultimately blocking protein translation. In 1952, Dr. Waksman was awarded the Nobel Prize in *Physiology or Medicine* for his work in finding the first antibiotic compound capable of treating TB. That same year brought

the first oral antibiotic, isoniazid, which treats actively-replicating Mtb by blocking mycolic acid synthesis. It is still one of the primary drugs being used to treat TB. 1967 saw the advent of rifampicin, another first-line antibiotic still in use, which blocks prokaryotic mRNA synthesis by inhibiting a bacterial RNA polymerase beta-subunit. The two other major compounds used in the treatment of TB, pyrazinamide and ethambutol, came in 1952 and 1961, respectively.

In 1950, TB was the eighth leading cause of death in the United States; in comparison, vascular disease was the ninth greatest cause of death that same year. By 1985, there were only 1,752 TB-related fatalities in the U.S. [32]. Anti-TB antibiotic compounds have been proven quite successful at treating individuals infected with most strains of Mtb. However, the typical course of drug treatment is up to 9 months of daily dosages of drugs that tend to be rather hepatotoxic; even longer treatments with additional drugs may be required in some cases. Additionally, some bacteria may evade the bactericidal treatment by virtue of their inaccessibility within a patient's granulomas. The major anti-TB drugs only target actively replicating bacteria, further compounding this problem; latent-phase bacteria are much more likely to evade destruction [33, 34]. The emergence of antibiotic-resistant Mtb is rapidly becoming a major threat to global public health.

### 1.4.3 Treatment of TB: Problems of the present day

The increased use, and subsequent misuse, of antibiotics to treat TB has created a corresponding rise in antibiotic-resistant Mtb. Lack of strict adherence to prescribed antibiotic regimen has spawned new strains of Mtb. These super-strains are resistant to both first-line antibiotics (isoniazid and rifampicin) and second-line drugs (such as fluoroquinolones,

amikacin, capreomycin and kanamycin), leading to classification of these strains as MDR-TB (multi-drug resistant TB) and XDR-TB (extensively drug resistant TB), respectively [14]. XDR is considered particularly threatening and each case is individually treated, sometimes with surgical removal of infected lung tissue being the only option remaining. Cases of XDR essentially return the ability of physicians to treat Mtb to the days before antibiotics existed. The rapidly increasing prevalence of these MDR and XDR strains is a great cause for concern in both developing countries with endemic levels of TB and in the industrialized world. This increased alarm extends to those nations such as the United States that have had the benefit of improved hygiene and widespread access to healthcare and thus no substantial mortality/morbidity from TB.

In a recent example from within the United States, in 2007, Andrew Speaker, a newly-married personal injury lawyer from Atlanta, Georgia, was diagnosed with TB and warned by medical professionals that he should avoid travel. Speaker ignored their advice and traveled to Greece for a postnuptial vacation. Shortly thereafter, further testing by the Center for Disease Control revealed Speaker's strain of Mtb to be drug resistant. Initially classified as XDR, but later proven to be MDR, Speaker fled Greece, flew to Canada and sneaked across the border into the U.S., where he was taken into custody and placed into quarantine [35] to receive appropriate medical treatment [36]. Though Speaker's particular strain was not as deadly as initially thought, the extensive media coverage of the entire debacle, especially "TB Andy's" flights across the Atlantic Ocean that put hundreds of lives at risk, did a great deal to raise awareness of the dangers Mtb still poses to even the wealthiest of nations.

## 1.4 Summary and conclusion of introductory remarks

The efficacy of first line antibiotics has progressively diminished as the prevalence of multi-drug resistant (MDR) TB and extreme-drug resistant (XDR) TB rises throughout the world. The variable effectiveness of the BCG vaccine and the increasing prevalence of MDR-TB and XDR-TB demonstrate the urgent need for new methods of preventing or treating Mtb infections. As previously mentioned, a large portion of new TB cases originate from individuals acting as a reservoir of infection. Within the infected individual, there is an "activation" of latent TB, which is then transmitted by exhalation to uninfected hosts.

Currently, the vast majority of TB treatment compounds are designed to inhibit the growth of Mtb, as entirely preventing infection itself is quite impractical. By targeting active, replicating bacteria, these anti-TB drugs decrease the overall bacterial burden, lessening the number of individual cases of active TB and, correspondingly, instances of individuals harboring latent TB. In light of BCG's obvious shortcomings, it seems only reasonable to approach the TB "vaccination problem" by examining or retooling BCG in a manner that complements the pharmaceutical approach. Current vaccine development projects should aim to prevent Mtb colonization of pulmonary alveoli and generate long-term immunological memory; one of the best ways of doing this is by understanding, exploring, and exploiting the various mechanisms and survival strategies an Mtb bacillus employs as it attempts to hijack a macrophage and shelter itself within a host. Our current needs for improved treatments such as superior antibiotics and, especially, an effective vaccine against Mtb is as urgent today as it was in the era of Dr. Robert Koch.

# Chapter 2: Background

## 2.1 Mycobacteria

### 2.1.1 *M. tuberculosis* (Mtb)

Mtb is a pathogenic species of mycobacteria that is the primary agent of pulmonary TB. The bacterium is a rod shaped bacillus 1.0-4.0μm in length and between 0.3-0.6μm in width. Technically considered a Gram positive species due to the lack of an outer cell membrane, Mtb has a thick waxy cell wall composed of a great deal of mycolic acid, which makes the bacteria resistant to Gram staining; acid-fast staining, such as Ziehl-Neelsen stain, is typically employed as a suitable alternative. In addition to mycolic acid, the cell wall contains peptidoglycan, arabinogalactan, lipoarabinomannans and phosphatidylinositol mannosides. The complex make-up of the Mtb cell wall assists the pathogen in resisting medicinal and noxious compounds, as well as protecting the bacteria in the potentially hostile environment of a host phagosome [37].

The genome of the Mtb H37Rv laboratory strain is composed of 4,411,529 nucleotides (nt) in a circularized chromosome and contains an estimated 4,000 genes [38]; Mtb Erdman, another common lab strain, has a chromosome that is 4,392,353nt in size and codes for approximately 4,250 genes [39]. Both of these lab strains have guanine-cytosine (GC) content of 65.6%. In terms of rate of replication, Mtb is relatively slow-growing with a doubling time of about 24 hrs *in vitro* [40]. The bacteria produces a roughly-textured cream-colored colony when plated onto solid media.

The clinical isolate CDC1551 is another strain commonly used to study Mtb. The strain was isolated following a US-based TB outbreak in 1995, near the Tennessee-Kentucky border [41]. Reports have suggested CDC1551 is typically hypervirulent relative to Mtb strains H37Rv and Erdman in most laboratory uses [42].

### 2.1.2 *M. bovis* and *M. bovis*-BCG

*M. bovis* is a member of the *Mycobacterium* TB complex (MTBC), along with Mtb and a handful of other virulent mycobacteria species (*M. africanum*, *M. pinnipedii*, *M. microti*, and *M. caprae*) that are capable of giving rise to pulmonary TB. Mtb is the primary causative agent of TB in humans, and *M. bovis* can be considered the primary agent of TB in cattle, though the pathogen is cable of bovine to human zoonotic transfer. Years before pasteurization of dairy products became common, *M. bovis* was responsible for a large number of cases of human TB, particularly in children [43]. Incidentally, it was the subculturing and attenuation of *M. bovis* by Albert Calmette and Camille Guérin that gave us the BCG vaccine which has been effective at preventing the disseminated form of Mtb infection in children. This attenuation has been primarily attributed to the loss of RD1 [44, 45], or "region of difference 1" which contains 9 specific genes: *Rv3871*, *Rv3872* (*PE35*), *Rv3873* (*PPE68*), *Rv3874* (*esxB*), *Rv3875* (*esxA*), *Rv3876*, *Rv3877*, *Rv3878* and *Rv3879c*. A deletion of these corresponding genes from Mtb generates a virulence phenotype more similar to BCG than WT Mtb, establishing the loss of RD1 as important for the attenuation of *M. bovis* [44].

BCG (and to a lesser extent *M. bovis*) is of interest to researchers for obvious reasons. In addition to a great deal of genetic similarity, Mtb and *M. bovis* employ similar infection and survival strategies, life cycles and counter-immunity mechanisms. Additionally, BCG is a Bio-Safety Level 2 (BSL2) pathogen, which means it is classified as "relatively safe" for research scientist usage, while Mtb is classified as a BSL3 pathogen. Working with BCG significantly lowers the equipment and training costs associated with mycobacterial research. Finally, one of the more provocative notions in Mtb vaccine research is the idea that a much more effective vaccine against Mtb may be created by retooling the BCG vaccine [46], something that may be much safer than attempting to create a new recombinant vaccine against TB by genetic manipulation and attenuation of an Mtb species [47, 48]. A sort of hybrid-variation of this theme has been attempted with promising results. A Danish group has recently shown in CB6F1 mice [49] and cynomolgus macaques [50] significantly reduced rates of clinical disease, increased survival and lowered latent TB reactivation when given both the standard BCG vaccine and a recombinant booster employing the Mtb antigens Ag85B and ESAT-6 (both Mtb secreted proteins) and Rv2660c (Mtb stress-induced protein).

### 2.1.3 Other mycobacterial model species used in our studies

The *Mycobacteria* genus consists of many species beyond the aforementioned Mtb and *M. bovis* species. This group of organisms consists of a wide variety of pathogenic, opportunistic pathogenic and nonpathogenic organisms. Many of these less virulent species are useful as model organisms for the study of Mtb and its

pathogenesis. For the Briken lab, our study of mycobacterial-mediated suppression of host apoptosis makes two particular model species tremendously valuable: *M. smegmatis* and *M. kansasii*.

*M. smegmatis* (Msmeg), first isolated in 1884 from ulcers of patients with syphilis, is one of the most widely employed model species used in the study of Mtb, for a variety of reasons. Msmeg is considered to be a nonpathogenic species and can be employed in research laboratories with only BSL1 precautions. This greatly reduces the initial cost of specialized facilities, employee health monitoring and safety equipment generally associated with Mtb research. Additionally, Msmeg replicates relatively quickly, with a doubling time of about four hrs, versus the approximately 24 hour doubling time of Mtb [51]. Both of these factors make the organism a preferred model for many TB researchers. There also exists specially developed laboratory strains such as Albert Einstein College of Medicine's "$mc^2155$" strain; this strain specifically chosen and propagated for its excellent transformation efficiency [52]. These properties make Msmeg an excellent Mtb model species, especially for use in early stage, high volume screening and any desired molecular cloning or expression work where rapid results are desired [53].

The opportunistic pathogen *M. kansasii* (Mkan) is another useful organism for modeling Mtb. It was initially isolated from human pulmonary secretions, and it is believed that impure tap water may act as a reservoir of transmission [54]. Mkan seems to lie somewhere between Msmeg (nonpathogenic) and *M. bovis* (obligate pathogen) on a scale of mycobacterial virulence in humans; it is typically an opportunistic pathogen [55, 56, 57]. It is classified as BSL2 pathogen and, compared

to Msmeg, has greater homology with the more virulent mycobacterial species such as Mtb. While Mkan is relatively slow-growing (it replicates with a doubling time of about 20-24 hrs), it shares greater life cycle similarity with other pulmonary TB producing organisms (compared to the nonpathogenic Msmeg-mc$^2$155, our fast-growing Mtb model). The species is thus quite useful for studying many of the survival, persistence and virulence mechanisms of more highly-pathogenic species under more controlled, less hazardous research conditions. Moreover, the increased genetic homology with Mtb (relative to Msmeg) often makes Mkan a "more stringent" model for screening and expression work, which has been quite important for the mycobacteria-mediated host anti-apoptotic phenotype of interest to the Briken lab [53].

## 2.2 Experimental systems: cell lines and model organisms

As the primary residence of Mtb, the human alveolar macrophage would be the ideal cell type for exploring host-pathogen interactions. However, the only way to obtain these particular macrophages is by branchoalveolar lavage, a process that is difficult, time-consuming, relatively expensive and rather uncomfortable for a donor. With that in mind, we must employ alternative models suitable for studying Mtb pathogenesis.

### 2.2.1 THP-1 cell line

THP-1 cells (an acute myelomonocytic leukemia cell line) [58] are routinely employed in mycobacterial infection studies. They possess a relatively rapid replication time of about 24 hrs and have C3b and Fc receptors, enabling enhanced phagocytosis of complemented bacteria, they also lack immunoglobulins. Resting THP-1s can be driven to an activated state by an

added stimulator such as phorbol myristate acetate (PMA). In terms of simulating *in vivo* infections with Mtb, PMA-activated THP-1s will effectively phagocytize complemented mycobacteria and subsequently apoptose in a manner similar to primary macrophages. The consistency of the cell line *in vitro* apoptosis-induction response and the ability to quickly grow large quantities of the THP-1s make them ideal for screening and large-scale studies of mycobacteria-induction/suppression of host apoptosis interactions [53]. As a tumor cell line, THP-1s are wonderful a model for rapid, large scale experiments, but the correlation to real world *in vivo* conditions may cause some to question the validity of observed outcomes; therefore, it is necessary to establish observed phenotypes in primary macrophages as well.

### 2.2.2 Primary human monocyte-derived macrophages (HMDMs)

In order to best recreate an *in vitro* approximation of alveolar macrophage infection by Mtb, TB researchers often culture macrophages from a pool of undifferentiated human monocytes. Primary human monocyte-derived macrophages (HMDMs) are obtained by drawing blood from a donor, isolating the buffy coat (leukocytes) by ficoll centrifugation separation, plating undifferentiated monocytes and then driving these monocytes to $CD14^+$ macrophage maturation by culturing them with cytokines such as Granulocyte-Macrophage Colony Stimulating Factor (GM-CSF) or Macrophage Colony Stimulating Factor (M-CSF) for roughly a week [59]. These monocytes themselves are derived from $CD34^+$ myeloid progenitor cells within the bone marrow; monocytes enter the blood stream and migrate to various tissues, where they can differentiate into a variety of specialized resident macrophage types. Two of these polarized, macrophage subtypes are classified by the established "Th1/Th2" nomenclature system as "M1" and "M2," with M1 macrophages having a

"classically activated macrophage subtype" and M2 macrophages possessing an "alternatively activated" macrophage response to stimuli. As a rule of thumb, M1 macrophages act as effectors of Th1-type immune response (IR); they are proficient manufacturers of inflammatory cytokines such as IL-6, TNFα and IL-1β, and quickly generate substantial quantities of reactive oxygen species (ROS) and reactive nitrogen intermediates (RNI) [60]. The M2 polarized macrophages are quite different. M2 cells have a variable ability to generate an inflammatory response and typically produce low levels of IL-1β and caspase-1 and high levels of the IL-1 receptor agonist (IL-1Ra), all in stark contrast to M1 polarized macrophages [60, 61]. The M2 macrophage will typically play role a in Th2-type response and promote foreign body encapsulation and destruction [62]. In terms of culturing HMDMs, it has been previously reported that culturing monocytes in a media supplemented with human GM-CSF will produce a M1-like macrophage while monocytes cultured in the presence of human M-CSF generate M2-like macrophages.

When culturing HMDMs to maturity, M-CSF and GM-CSF are both commonly, and separately, used to differentiate monocytes into macrophages. Evidence established by Komuro *et al*. [59], suggests that in terms of general "fried-egg" morphology and surface antigen expression ($CD14^{low}$, $CD71^{+}$, c-$fms^{low}$) GM-CSF cultured HMDMs have greater similarity to alveolar macrophages than M-CSF derived HMDM. M-CSF cultured HMDM may be more analogous to peritoneal macrophages with their "spindle-shape" morphology, and surface antigen expression levels (c-$fms^{high}$, $CD14^{high}$). Furthermore, the group noted that alveolar macrophages and GM-CSF HMDMs are both strong scavengers of $H_2O_2$ by way of a pronounced basal level of catalase activity and induction, while M-CSF HMDMs have intrinsically lower catalase expression levels. Subsequently, M-CSF derived macrophages are

approximately 50-fold more sensitive to exogenous $H_2O_2$ than either GM-CSF HMDMs or alveolar macrophages. At the same time, relatively large amounts of $H_2O_2$ are generated by the addition of heat-killed *S. aureus* to M-CSF HMDMs, while GM-CSF HMDMs do not exhibit this effect [59].

Taken together, the data suggest that GM-CSF generated HMDMs may be more analogous to native alveolar macrophages than M-CSF generated HMDMs in terms of *in vitro* culturing and subsequent experimentation behaviors. This line of thought is in agreement with accepted literature suggesting GM-CSF is essential for the generation of human alveolar macrophages [63, 64] and that M1-like macrophages (GM-CSF derived HMDMs) promote a Th1 type immunity activation when faced with a mycobacterial challenge, while similarly challenged M2-like macrophages (M-CSF derived HMDM's) fail to efficiently promote and sustain a Th1-type immune response [65]. We would therefore assume GM-CSF to be the preferred HMDM differentiating cytokine for the *in vitro* modeling of Mtb/host interactions. However, a major point of contention arises where the specific needs of the Briken lab are concerned. It has been established that M-CSF generated HMDMs require the continued presence of the cytokine in order to survive; the removal of M-CSF will allow for apoptosis of the macrophage. In contrast, GM-CSF created HMDMs are much more resistant to apoptosis upon removal or depletion of the cytokine [66]. This poses a dilemma for research groups, such as the Briken lab, who are interested in the study of host/pathogen interactions and subsequent host-apoptosis outcomes. The Briken lab tested various HMDM differentiation approaches in several pre-experimental optimization studies (B. Hurley, data not shown); it was ultimately decided that GM-CSF differentiation of monocytes is not a viable option for our study of Mtb-mediated anti-apoptotic effects. Real world *in vivo* cytokine differentiation of

monocytes into mature alveolar macrophages is likely a dynamic spectrum of competing and collaborating cytokine interactions; rapidly fluctuating cytokine doses with varying durations of exposure, ultimately dependent on the tissue microenvironment, only further complicates the *in vitro* modeling efforts of Mtb researchers.

### 2.2.3 Murine model system

The murine model is the most commonly employed animal model in Mtb studies. Within the various genetic backgrounds of the mouse model, C57Black/6 (B6 hereafter) may be the mouse most commonly used to model human disease [67, 68]. The B6 strain is inbred, so upon Mtb infection, every animal should theoretically produce an immunological response similar to its litter mates and any other B6 mice used in follow-up experiments. The relative ease of breeding B6 mice and the availability of a wide range of transgenic mutants within this genetic background also contribute to their ubiquity as animal models [67]. In order to distinguish B6 from other strains, it is helpful to classify them by their response to a bacterial infection, as this is how the usefulness of a particular strain in Mtb infection studies will be gauged.

Generally speaking, it is believed that B6 mice generate a Th1-type ("cell-mediated immunity": macrophage, IFN-gamma, and TNF-beta associated) of response to *Leishamania major*, while a strain such as Balb/C generates a Th2-type ("humoral-mediated immunity": B-cells, various interleukins) of response [69, 70]. The Balb/C strain itself is another commonly used strain. Balb/C mice tend to be more docile in temperament than the aforementioned B6 strain [67], but unlike in B6 mice few transgenic and substrain models exist.

One of the most important substrains of the Balb/C line is the severe combined immune deficiency (SCID) mouse. "SCID" is a general term used to describe several different

substrains of Balb/C mice, generally homozygous for a "Prkdc$^{SCID}$" mutation on chromosome 16, which results in a lack of V(D)J recombination. This particular mutation results in lymphoid organs 10% of normal size and a lack of functional T and B cells, meaning the animal possesses an immature immune system with no true humoral response and a cell-mediated immunity that is more-to-less compromised depending on the particular SCID substrain [67]. SCID mice are consequently excellent animal models for studying T cell subsets as well as exploring cell-mediated immunity in an environment of limited variables. SCID mice, therefore, provide an animal model system for studying the mycobacterial/host interaction in a controlled, relatively short-term manner.

In this experimental scenario, SCID mouse infection-survival and morbidity progression outcomes can be taken as indication of virulence at the level of cell-mediated immunity- an extrapolation that is especially striking when the evidence is considered in tandem with corresponding *in vitro* work. However, it has been suggested that the murine model may not be the best animal model for mycobacterial infection studies, due to the inability of the mouse to form a "true granuloma," defined as the granuloma that occurs in humans and other primates [71]. While the mouse is relatively inexpensive, reproducible and wel-characterized [68], and mimics the sterilizing effect of the first-line anti-TB drugs rifampin and pyrazinamide in Mtb infection, the murine granuloma itself is formed of fairly loose cellular aggregates, making murine histology quite different from human granulomas [72]. Some researchers have suggested this issue diminishes the value of the mouse as a TB model; these scientists suggest turning to other model species to more thoroughly explore the mycobacterial infection/macrophage apoptosis link [68].

### 2.2.4 Hartley guinea pig model

Other TB modeling species, which better approximate the Mtb-granuloma seen in humans, would be non-human primates [73, 74], rabbits [75, 76] and guinea pigs [77, 78]. Of these three species, the guinea pig is by far the most practical animal model for any "early stage" experimentation not currently seeking vaccine/treatment approval from the Food and Drug Administration. The "Hartley" strain is currently the guinea pig breed most commonly used in laboratory work.

In terms of value as an accurate model of Mtb infection, guinea pig experimentation is arguably superior to the murine model due to its formation of a "true granuloma," which more accurately represents the granuloma histology seen in human infections. Specifically, the guinea pig produces a caseous granuloma, which is histologically reminiscent of the human granuloma and distinct from the loose aggregates of cells seen in the murine "granuloma." Also, the murine "granuloma" lacks tissue hypoxia; hypoxia is a hallmark of human granulomas and occurs within the granulomas of guinea pigs and rabbits [79]. The primary difference in the human and guinea pig granulomas seems to occur at the point of late-stage necrosis, in which granulomas in humans will liquefy and cavitate, ultimately resulting in lesions leading to increased aerosol transmission [72]. Studies involving the guinea pig as a viable animal model of TB have not been limited to survival studies and *in vivo* work; recently, David McMurray's group has demonstrated the usefulness of guinea pig macrophages in *in vitro* studies [77].

One of the most interesting studies has indicated differing roles for alveolar and peritoneal macrophage based on responses to *in vitro* infections with heat-killed mycobacteria [77]. Guinea pigs (both naïve and BCG-vaccinated) were sacrificed, and alveolar and

peritoneal macrophages were collected. The macrophages were infected with live or heat-killed Mtb. Alveolar macrophages demonstrated no change in $H_2O_2$ production, no significant increase in MHC class II expression and a "post-vaccine" Th1-type cytokine response (IL-12 expression) that did not significantly rise above the basal levels of response seen in naïve animals; peritoneal macrophages tended to have much greater $H_2O_2$ production, significantly greater MHC class II expression and elevated IL-12 production compared to naïve animals (however, the *overall* levels of cytokine production were greater in the alveolar macrophages).

The data seem to indicate that BCG vaccination of guinea pigs and/or treatment with recombinant guinea pig TNFα or IFNγ provided significantly greater enhancement of cytokine-induced functions in peritoneal macrophages compared to alveolar macrophages. The McMurray group proposes that alveolar macrophages are likely constitutively activated *in situ* due to regular contact with inhaled environmental substances [77], which would lead to diminished shifts in cytokine production when stimulated with mycobacteria under *in vitro* conditions. They suggest that this may not be an *in vitro* experimental artifact, but rather that a diminished alveolar macrophage-generated cytokine response to exogenous antigens *in situ*, may be important for limiting inflammatory damage to lung tissue.

## 2.3 Mtb survival strategies

Believed to have evolved as a human specific pathogen, Mtb has developed many measures to counter the human immune system. Notably, the inhibition of phagosome/lysosome fusion [80] and interference with the macrophage-generated toxicity of reactive nitrogen intermediates [81] have been two of best-characterized survival mechanisms employed by Mtb.

### 2.3.1 Mtb phagolysosome fusion inhibition

To take other examples of this virulence tactic, the cell wall lipid mannose-capped lipoarabinomannan (manLAM) and the Mtb PknG kinase are two mechanisms Mtb uses to inhibit phagolysosomal fusion. The manLAM component of Mtb has been extensively researched. It seems to function by inhibiting host Vps34, a PI3-kinase, which prevents PI3P from accumulating; this disables recruitment of early endosome antigen 1 (EEA1), a tethering molecule that interacts with SNARE and is necessary for endosomal trafficking [80, 82]. PknG, a eukaryotic-like serine/threonine protein kinase, is not a requisite for *in vitro* growth, but is necessary for survival within the host macrophage. Mtb expressing a kinase-disabled form of PknG are quickly transferred to lysosomes and destroyed following phagocytosis [83]. Also, PknG has been detected in the cytosol of host macrophages infected with live but not killed mycobacteria [83]. Moreover, a lysosomal associated membrane protein (LAMP) labeling study has indicated that *M. smegmatis*, which does not express PknG, seems to block phagolysosomal fusion when transformed with a *pknG* expressing; compared to WT *M. smegmatis*, the $PknG^{+}$ bacteria shows lower levels of LAMP staining [83]. For both mechanisms, the halt of phagosomal maturation allows for protection of the bacteria and provides an opportunity for replication and further mycobacterial colonization.

### 2.3.2 Mtb response to reactive nitrogen intermediates (RNI) and reactive oxygen intermediates (ROI)

Another well-characterized antimicrobial mechanism of the macrophage is the production of RNIs and nitric oxide. RNIs are believed to control Mtb infection, and RNI knock-out mice demonstrate an increased susceptibility to Mtb [84]. The

peroxiredoxin-alkyl-hydroperoxide-reductase subunit C (AhpC) protein seems to play a role in protecting Mtb by catalytically catabolizing peroxynitrate anions, a powerful oxidant that forms as a reaction product of nitric oxide and superoxide anion [81]. In a later study, the same group found that AhpC, along with Lpd, SucB and AhpD, forms an antioxidant complex that possesses peroxynitrite reductase activity [85]. Shortly thereafter, a large-scale transposon screen identified seven genes that aid Mtb in RNI resistance [86]. More recently, OsmC was shown to be important for protecting Mtb from oxidative stress by contributing significant peroxide reductase activity to the pathogen [87].

Additionally, the Mtb protein Lsr2 is a dimer that protects the pathogen from ROI-mediated DNA damage; it does this by binding adenine-thymine rich portions of the Mtb chromosome and physically protecting the bacterial nucleic acids in that region from harm [88, 89]. As with mechanisms preventing phagolysosomal fusion, Mtb is protected and afforded a chance to replicate. These two survival strategies are hardly the full extent of Mtb defensive maneuvering; one of the Mtb virulence mechanisms of greatest interest to the Briken lab is the suppression of host-macrophage apoptosis.

## 2.4 Mtb survival strategy: prevention of host-cell apoptosis

In the give-and-take world of host-pathogen interaction, it stands to reason that hosts will have developed countermeasures to override Mtb's attempts at concealment and to prevent the bacteria's replication and ensuing colonization. One manner in which the host macrophage accomplishes this is by the induction of apoptosis, a well-controlled form of cell suicide [90, 91, 92, 93, 94]. The beneficial result of an infected macrophage inducing and coordinating a

well-regulated self-destruction stands in sharp contrast to necrosis, which is a relatively chaotic event that occurs when cells die as a result of an unregulated physical or chemical occurrence. Correspondingly, it is believed that Mtb possesses mechanisms adapted to counter this particular host defense mechanism, preventing the programmed cell death of its host and ensuring the survival of the pathogen.

### 2.4.1 Apoptosis as a host defense mechanism against Mtb: innate immunity

In terms of Mtb infection, apoptosis can be considered a significant component of the innate immune response (IR), in that macrophages undergoing the controlled cell-suicide process destroy the invading intracellular mycobacteria [90]; the unregulated event of infected macrophage necrosis does not result in obliteration of the bacteria [93, 95]. This seemingly altruistic role played by the apoptotic infected macrophage is a successful defense strategy that has been observed in other bacteria burdened cells [96]; *Shigella flexneri*, *Yersinia spp*. and *Salmonella spp*. have all been shown to induce macrophage apoptosis following infection.

Numerous papers have indicated that infection of macrophages with mycobacteria often results in host cell death. This host cell death can take the form of apoptosis (a host-mediated cell suicide that is bactericidal) or necrosis. Necrosis can be a pathogen-mediated form of host death resulting in unregulated cell lysis that causes contents of the cell to spill out into the extracellular space, resulting in local tissue damage and a hyper-inflammatory response. This further propagates the spread of the bacterial pathogen into newly recruited macrophages and neutrophils and assists the pathogen in avoiding immunosurveillance [97, 98].

The degree of pulmonary virulence of a mycobacterial strain can be used as an indicator of expected host death outcome. That is, the more virulent a bacterium the less apoptosis (and

more necrosis [99] it induces; less virulent mycobacteria will induce more apoptosis and less necrosis. This has been demonstrated within Mtb; virulent H37Rv actively induces necrosis [100, 101] and suppresses apoptosis, while the avirulent H37Ra does not have this phenotype [95]. This rule of thumb extends to other mycobacterial species and attenuated strains as well; *M. smegmatis* [53], *M. kansasii* [53, 91] and BCG [91] have all been established as "high-inducers" of host cell apoptosis. The inability of these organisms to suppress apoptosis makes them useful model organisms for gain-of-function (GoF) screens that attempt to identify anti-apoptotic virulence genes of Mtb [53].

### 2.4.2 Apoptosis as a host defense mechanism against Mtb: acquired immunity/cross-presentation

As in innate immunity, the apoptosis of infected macrophages also plays a critical role in acquired immunity by way of cross-presentation of mycobacterial antigens. A series of events occurs in the course of macrophage apoptosis: cytoplasmic shrinkage occurs, the chromosomes condense, chromatin degradation occurs and the cell membrane begins to form small blebs, ultimately resulting in the creation of apoptotic bodies. These newly formed apoptotic bodies are then rapidly captured by proximal antigen presenting cells (APCs), such as dendritic cells (DCs), as a way of averting a situation in which these cellular contents might generate an inappropriate immune response [102]. If a mycobacterial bacillus was contained within the macrophage at the time of its apoptosis, then mycobacterial antigens would likely be contained within the apoptotic bodies. These antigenic molecules, phagocytosed and processed by the proximal DC, can be presented by major histocompatibility complex (MHC) molecules on the surface of the DC [103]. If this DC is concurrently expressing the requisite costimulatory molecules, induced by the ligation of Toll-like receptors (TLRs) by pathogen-associated

molecular patterns (PAMPs) derived from additional antigenic mycobacterial products also contained within the apoptotic bodies [104], then T cells specific to the presented mycobacterial antigen will achieve activation when coming into contact with said DC, and this cross-priming will ultimately lead to an advantageous and desirable adaptive immune response for the host [103]. The theory of macrophage apoptosis inducing cross-presentation and cross-priming adaptive immunity was supported by a 2006 study under *in vivo* conditions. In this study, $CD8^+$ T cells were activated by inoculating mice with apoptotic vesicles obtained from macrophages infected with pro-apoptotic Δ*secA2* mycobacteria; the vesicle inoculated, cross-primed mice were subsequently protected against later challenge by Mtb [105]. The benefits and safety of a similarly retooled, pro-apoptotic Δ*secA2*-based recombinant vaccine were also seen in immunocompromised mice [106] and were found to be safe when tested in immunosuppressed SIV-infected infant macaques [47].

### 2.4.3 Virulent mycobacteria species suppress host apoptosis

A correlation can be drawn between the specific, qualitative degree of virulence associated with an infecting mycobacterial strain and the apoptotic rate of host macrophages. More virulent strains of mycobacteria (the causative agents at work in pulmonary TB) such as *M. tuberculosis* H37Rv, *M. tuberculosis* Erdman, and *M. bovis*, have previously been shown to induce significantly less apoptosis in host macrophages than the more avirulent strains *M. tuberculosis* H37Ra, *M. bovis* BCG, and *M. kansasii* [91]. While the colony forming units (CFU) of intracellular virulent strains increased, the CFU of intracellular avirulent strains decreased suggesting that the apoptosis of infected macrophages may help reduce the quantity of intracellular mycobacteria [91].

Within Mtb, several different gene products have been reported as contributing an

anti-apoptotic phenotype to the bacteria. Genes such as *nuoG* [53], *pknE* [107], *secA2* [106], *Rv3165c* (S. Gurses, unpublished), *Rv3167c* (S. Gurses, unpublished), *sigH* [108]and *Rv3654c-55c* [94] have all been shown to encode players operating in the Mtb-mediated inhibition of host apoptosis. NuoG seems to operate as part of the Mtb type I NADH complex and may function by neutralizing host NOX2 activity [109]. PknE is involved in countering host induced nitric oxide stress [110],[107]. SecA2 is an important secretion mechanism for Mtb and when it is functionally disrupted [111], the anti-apoptotic mechanism SodA cannot be exported thus the host is able to induce apoptosis [112]. SodA will convert host superoxide to $H_2O_2$ once it has been secreted by the pathogen. $H_2O_2$ can then be cleared by Mtb KatG [113]. Rv3165c and Rv3167c have been recently characterized by Briken lab member Serdar Gurses; a working model suggests the two proteins function together as a membrane integrated signal transduction receptor and a corresponding transcription factor that will act in a stress-response capacity. SigH is an important stress response factor [108] and is essential for *in vivo* infection of primates [114]. Rv3654c and Rv3655c seem to be proteins that are secreted from Mtb into the cytoplasm of the host and suppress apoptosis by inhibition of the extrinsic pathway [94]; the same research group that reported an anti-apoptotic phenotype for these two proteins recently identified another secreted virulence factor, Rv3364c, that seems to operate by binding to host serine protease cathepsin G and preventing caspase-1 activation, thus preventing host programmed cell death [115]. Taken together, it seems that prevention of ROS or nitric oxide species is the central goal of these Mtb anti-apoptotic mechanisms; this may be the key strategy in Mtb's suppression of host

apoptosis or it may be one of many different approaches the pathogen employs and may simply be the most noticeable of the virulence apoptosis-modulating tactics in play. As one might expect, some Mtb proteins, such as Rv0183 [116] , have been shown to actually induce greater levels of host apoptosis; this, of course, only serves to further highlight the tumultuous push-pull relationship between pathogen and host [117].

### 2.4.4 Host-apoptosis: A potential means to an improved vaccine

In light of BCG's obvious shortcomings, it seems only reasonable to approach the TB "vaccination problem" by examining or retooling BCG in a manner that complements the pharmaceutical approach. Current vaccine development projects should aim to effectively prevent Mtb colonization of pulmonary alveoli and generate long-term immunological memory; one of the best ways of doing this is by understanding, exploring, and exploiting the various mechanisms and survival strategies Mtb employs as it attempts to hijack macrophages and harbor itself within a host.

The background literature previously discussed has highlighted the importance of host cell apoptosis as a protective response to mycobacterial infection. Identification of the specific genes of Mtb responsible for "inhibition of host apoptosis" counter-measures would be quite beneficial; these genes could be studied, reconfigured, and employed in the production of novel vaccine strains which could induce high levels of host macrophage apoptosis. Thus any recombinant vaccine strains created would be expected to generate a greater degree of host cellular immunity via apoptosis with subsequent increases in cross-presentation to $CD8^+$ T cells; this will ultimately produce a vaccine superior to BCG by generating a more desirable immune response and long-term memory to the pathogen [106, 111, 118]. Additionally, the

identification and characterization of Mtb apoptosis-inhibiting genes and gene products will likely reveal many new targets for the generation of novel anti-mycobacterial pharmaceuticals.

In January of 2012, a study was published in *Clinical and Vaccine Immunology* showing that a highly attenuated, pro-apoptotic Mtb strain (Δ*secA2*-based) was a both safe and effective preventative measure against Mtb when tested in immunosuppressed infant macaques. Such a vaccine should theoretically be safe for use in children and, critically, those individuals infected with HIV and most susceptible to infection by Mtb [47].

## 2.5 *M. tuberculosis*: transposases and Clp proteases

Mtb transposases and Clp proteases factor heavily into this dissertation. A brief summary of both follows.

### 2.5.1 Transposases

Transposases (Enzyme Commission number 2.7.7.) are enzymes that catalyze the movement of transposons, regions of nucleic acids, from one place in to another; this cut-and-paste mechanism often occurs within a genome, but will occasionally jump between genomes of the same species, or even into entirely new species [119]. The transposition typically involves three mechanisms: the transposase enzyme, the transposon and a target region of DNA to accept the insertion. These three elements function by a "cut-and-paste" mechanism in which a transposases act as the enzymes catalyzing a reaction where DNA is double-nicked, the transposon element is excised with a hairpin formation, the transposon "breaks free" of its point of origin and transposases carry the element to a new, suitable nucleic acid region where it is physically inserted. The discovery and characterization of transposons and transposition is generally associated with Barbara McClintock, who was awarded the 1983 Nobel Prize in

*Physiology or Medicine* for her work. Transposases have been called the most prevalent genes found in nature [120].

A computational analysis group published a 2010 study in which the authors had analyzed over $10.0 \times 10^6$ protein encoding genes and gene-tags from a wide variety of sequenced eukaryotic, bacterial, viral and archaeal genomes. The group found that genes encoding transposases were the most abundant and commonly occurring genes in their genome pool [120]. This was, of course, a study limited to currently annotated genes, and was therefore subject to the biases inherent in such an approach. However, the authors' central premise, that transposase genes are both ancient and ubiquitous, is certainly valid.

Transposase genes can be found in all currently known forms of biological life; they can be considered the archetypal "selfish gene." It is believed that some transposases are maintained within their host genomes due to some survival advantage conferred upon the host, that their existence may be more "symbiotic" and less "parasitic" than the term "selfish gene" might imply. The advantage transposases offer a host is probably derived from their mobile nature; as they promote nucleic acid rearrangement and, subsequently, genetic diversity. It is believed transposases may do this by the induction of advantageous mutations, bringing novel genes into a genome or enhancing the fitness of a host. Specifically, insertion of a transposon into a new region may disrupt an encoded gene, disrupt a native repressor or promoter or may increase distance between a regulatory element and the associated gene, which may significantly alter gene expression. Additionally, many transposase and transposon elements are associated with a constitutive promoter [121] or possibly a promoter inducible by environmental stress [122]. Some transcription factors [123], certain centromere-binding proteins [124], and regulatory elements playing essential roles in programmed DNA deletion

[125] have been shown to have evolved from transposase genes. For immunologists, the transposition-inducing proteins RAG1 and RAG2 are known to be essential for generating immunodiversity [126, 127].

In mycobacteria, there are at least 12 established insertion (IS) elements [128]. Very few publications specifically exploring and characterizing Mtb transposases currently exist. The vast majority of literature details methods in which IS-elements may be used for clinical diagnostics or, more recently, large-scale phylogenetic analyses of the relationship between strains and species of mycobacteria. The IS*6110* elements appear to be exclusive to MTBC, and the detection of IS*6110* has been used as a tool for clinical diagnosis of Mtb infection [129, 130, 131]; however, recent detection of an IS6110-like element in *M. smegmatis* has suggested that horizontal transfer of genetic material between co-habiting mycobacterial species can and does occur [132]. Additionally, a recent publication has linked the important Mtb hypoxia response system, DosR/DevR, to proximal transposase genes in nine distinct blocks throughout the Mtb genome. Perhaps important for our interests, a significant portion of the K20 genomic region of interest to this dissertation encodes transposase and phage-related elements. *Rv2666*, a predicted truncated transposase gene for IS*1081*, is relatively proximal to several phage integrase-related genes, *Rv2650c* to *Rv2659c*, as well as transposase genes which precede these phiRV2 prophage genes. It has been suggested that this particular region of the Mtb chromosome was apparently a hot-spot for many mobile elements at some point in the evolution of Mtb [133]. This particular region may have been a switch site of GC-skew (sGCS) for Mtb at one time [134]. Little has been done to characterize this region, leaving plenty of room for future studies.

### 2.5.2 *M. tuberculosis* Clp proteases

The intracellular regulation and recycling of aberrant and misshapen protein by protease activity is absolutely essential for the survival of all organisms. Abrogation of *clpP* and *clpX* in *E. coli* has been observed to lead to an over 50-fold increase in frameshift mutations. This phenotype can primarily be attributed to the role of Δ*clpP* (29 fold), with Δ*clpX* showing a slight (2 fold) increase and Δ*clpA* showed no discernible increase in frameshift mutations [135]. Protease importance is even more readily apparent in pathogens such as Mtb that spend a significant portion of their life cycle dealing with the ramifications of phagocytosis by alveolar macrophages and subsequent acidification of the intraphagosomal space. The activity of the Clp proteases of Mtb is an essential part of the organism's arsenal for dealing with the relatively high-stress conditions of the intraphagosomal space.

Recently, investigators employing transposon site hybridization (TraSH) screening of Mtb Tn-mutant libraries have shown that protease subunits ClpP1/Rv2561c and ClpP2/Rv2460c, ATPase subunits ClpX/Rv2457c and ClpC1/Rv3596c, and clpB/Rv0384c are all essential for the *in vitro* growth of Mtb [136, 137, 138]. Additionally, studies examining the Clp ATPase subunits clpX and clpC1, and the Clp proteolytic subunits clpP1and clpP2 have all provided additional levels of evidence supporting the essentiality of these genes [139, 140, 141, 142].

Mtb caseinolytic (Clp) protease activity is thought to be composed of two basic elements, a proteolytic subunit (ClpP1 or ClpP2) responsible for substrate lysis and an ATPase subunit (ClpC1, ClpC2 or ClpX) which assists the lytic process by providing substrate specificity in an ATP-dependent manner. The functional protease

is thought to be comprised of two heptameric rings stacked on top of each other creating a chamber that carries out lysis with an active serine protease site. An attached ATPase subunit unfolds the substrate for catalysis in the ClpP lytic barrel [143].

Recent publications have suggested that there may be many different roles for the various Clp family members. Mycobacteria are somewhat unique in that they possess two Clp proteolytic subunits, while the majority of bacteria have only a single Clp proteolytic subunit. Also, most bacteria encode four classes of ATPase (Lon, FtsH, HslUV and Clp) while Mtb only encodes two, (FtsH and Clp) [144]. It has been noted that ClpP1 and ClpP2 are sufficient for the generation of a functional protease capable of peptide lysis; however, the addition of a Clp ATPase provides the complex with a boost of specificity and efficiency [141]. Alternative reports suggest that a complex of ClpC1P2 is the central player in the inactivation of RseA, the anti-sigma factor of the Mtb SigE stress response regulator [145]. Additionally, it was noted that ClpP1 and ClpX could not be substituted for ClpP2 or ClpC1, respectively [145]. Furthermore, studies have shown that ClpP1 overexpression is toxic while corresponding overexpression of ClpP2 seems relatively innocuous from the standpoint of toxicity [142]; additionally, recent publications have suggested that ClpX expression alteration can lead to aberrant bacterial replication due to interactions with FtsZ [140]. All of these studies taken together suggest the various Clp family members are likely functioning in differing capacities in Mtb.

Beyond their well-established role in general cell housekeeping, functional Clp proteases are thought to play important roles in degrading regulators, activating

enzymes, directing various regulators by elimination of repressors and/or possibly carrying out roles similar to helicases [146]. Moreover, Clp protease activity has been shown to be important for the virulence of *Listeria monocytogenes* [147], *Streptococcus pneumonia* [148, 149] and *Salmonella typhimurium* [150]. Also, ClpC1P2 assembly was shown to be important in the activating the Mtb SigE stress response [145] and several papers have established a Clp family stress response orchestrated as part of the ClgR regulon [151][152][108]. However, a Clp family homologue *clpC2*/*Rv2667* was not shown to be part of the ClgR regulon). Rv2667/ClpC2/ClpX' is a Clp protease family outlier in terms of ClgR regulation of the gene; evidence by other groups indicate *clpC2* may be a "black sheep" in the important Mtb Clp protease family [151]; Mehra and Kushal specifically exclude *clpC2* as a Clp-group outlier in their 2009 study of the Mtb stress response [153]. However, one study found *clpC2* expression to be upregulated following reaeration after a period of hypoxia [152], a condition one would expect a following new infection or shift from a latent to an active TB state.

It was recently shown that Mtb is susceptible to antibiotic treatment with cyclomarin, which functions by targeting and inactivating ClpC1function [154]; this compound may also interfere with the other Mtb ATPases ClpC2 and ClpX. ClpP1 and ClpP2 have also been suggested as potential drug targets [142]. These studies make the Mtb Clp protease family an attractive target for future investigations.

# Chapter 3: Materials and Methods

All animal studies were approved by the Institutional Care and Use Committee of The University of Maryland- College Park and were conducted in accordance with the IACUC guidelines and the National Institutes of Health Guide for the Care and Use of Laboratory Animals.

## 3.1 Bacterial strain maintenance and media

### 3.1.1 H37Rv work

*M. tuberculosis* (Mtb) H37Rv (*ATCC* 25618) cultures were maintained in a BSL3 facility. All strains were grown in complete 7H9 media supplemented with 10% ADC and 0.05% Tween-80 unless otherwise stated. Strains were thawed from freezer stocks and maintained at 37 ºC in a shaking incubator at concentrations as near an $OD_{600}$ = 0.600-0.800 as possible (but never higher) for a time of more than 1, but less than 3, week(s) to be considered viable for our experiments. Δ*clpC2*::complement (pMV261 episomal vector) was grown and maintained in 40 µg/mL kanamycin in order to maintain the episomal pMV261 plasmid of interest. All H37Rv recombinant mutants involved were initially selected using appropriate antibiotic, and the antibiotic cassette integrity was maintained by inclusion of the selective antibiotic every second passage of the mutant. Prior to use in infection all cultures were washed in $PBS_{Tween}$, resuspended and centrifuged at a low-speed (80 x g) for 5 min to pellet any bacterial clumps. Bacteria used in the subsequent infection were taken from the resulting supernatant and MOI was calculated from this suspension.

### 3.1.2 CDC 1551 work- Tn*Rv2666* and complement generation

Cultures were maintained in a BSL3 facility under identical conditions to H37Rv cultures. Prior to use in infection all cultures were washed in $PBS_{Tween}$, resuspended and centrifuged at a low-speed (80 x g) for 5 min to pellet any bacterial clumps. Bacteria used in the subsequent infection were taken from the resulting supernatant and MOI was calculated from this suspension.

*M. tuberculosis* strain CDC1551 and mutants were obtained through the TARGET (Tuberculosis Animal Research and Gene Evaluation Taskforce) project [155, 156, 157], a transposon mutant library operated through a collaboration of Johns Hopkins University and Colorado State University. TARGET scientists used *Himar1* based transposon mutagenesis [158] to create a large pool of individual Mtb transposon mutants (Tn) in the CDC1551 strain background and made these Tn-mutants available by request. A Tn-mutant for Mtb gene *Rv2666* (TARGET id: JHU2740A-322) and wild type (WT) CDC1551 were requested and obtained by the Briken lab.

A complement for Tn*Rv2666* was generated by cloning the gene in the streptomycin resistant integrating vector, pDB60. A significant upstream region of the gene was also cloned to ideally include the native promoter; at this time, it is unknown whether this upstream region actually includes an *Rv2666* promoter. Primers (see below) were designed with respective KpnI and EcoRI restriction enzyme sites orientation specific ligation into the pDB60 vector. Plasmid was initially transformed into *E. coli* DH5α, and then plasmid was miniprepped and sequence confirmed. Confirmed plasmid was then used to transform Tn*Rv2666* for

the purpose of genetic complementation. The method of transformation is described below in the "Electroporation of plasmids" section.

*Rv2666* complementation primers:

5' GCTTTTTTTTGGTACCGCCGGTGGGCGTGTCGTAGC 3'

5' GCTTTTTTTTGAATTCATGGCGTTGATGAGCTCGTC 3'

### 3.1.3 *M. kansasii* and *M. smegmatis* studies

*M. kansasii* (strain Hauduroy ATCC 12478) cultures were maintained in a BSL3 facility; *M. smegmatis* strain $mc^2$-155[52] cultures were maintained in a BSL2 facility. All strains were grown in complete 7H9 media supplemented with 10% ADC and 0.05% Tween-80 unless otherwise stated. Strains were thawed from freezer stocks and maintained at 37 ºC in a shaking incubator as near to $OD_{600}$ = 0.600-0.800 as possible for a time of more than one but less than 3 weeks to be considered viable for our experiments. The method of plasmid transformation is seen below in the "Electroporation of plasmids" section. Plasmid transformed *M. kansasii* and *M. smegmatis* strain $mc^2$-155 cultures were grown in 50 µg/mL of hygromycin or 40 µg/mL kanamycin, as the case warranted. Prior to use in infection all cultures were washed in $PBS_{Tween}$, resuspended and centrifuged at a low-speed (80 x g) for 5 min to pellet any bacterial clumps. Bacteria used in the subsequent infection were taken from the resulting supernatant and MOI was calculated from this suspension.

## 3.2 Δ*clpC2* recombinant mutant construction and complementation

The Δ*clpC2* recombinant mutant was constructed within the H37Rv (common laboratory strain) background of Mtb; it carries a hygromycin resistance cassette in the place of a functionally coding copy of the *clpC2*/*Rv2667*/*clpX'* gene seen in WT H37Rv.

### 3.2.1 Δ*clpC2* recombinant mutant construction

The Δ*clpC2* recombinant mutant was generated by specialized phage transduction and subsequent homologous recombination (Figure 3) [159]. An allelic exchange substrate (AES) employed for *clpC2* homologous recombination was created by PCR amplification of two regions flanking the gene including the first and last ~50 base pairs of the *clpC2* (see primer list below). The flanking regions were digested with Van91I (Fermentas) and ligated into p004S vector (a pjsc347 background vector) containing a hygromycin resistance cassette and then sequence confirmed. The AES was linearized with PacI (Fermentas) and ligated into mycobacterial phAE159 phage DNA. The resulting phasmid product was packaged with MaxPlax phage packaging kit (Epicentre) and then *E. coli* HB101 was transformed with the phasmid. Phasmid was screened for correctness and then electroporated into $mc^2155$ *M. smegmatis*; $mc^2$ 155 was mixed with Noble agar, and plated on 7H10 and grown for 4 days at 30 ºC. Plaque formation indicated phage generation. Individual plaques were selected and high-titer phage was obtained by repeating the process with individual plaques at a 30 ºC lytic temperature, then harvesting the high-titer phage by adding MP buffer (50 mM Tris-Hcl, 10 mM

$MgSO_4$, 150 mM NaCl, 2 mM $CaCl_2$) and gently shaking the plates at room temperature for 2 hrs. Purification of the phage by 0.22 µm filtration followed.

10mL of WT H37Rv was grown to mid-log phase and then washed once with 37 ºC MP buffer. The culture was then pelleted at 2,000 x g and resuspended in 1 mL of 37 ºC MP buffer. The prepared Mtb was incubated with the high-titer phage (10 phage : 1 bacterium) for 24 hrs at 37 ºC for transduction. The transduced bacteria were plated onto 37 ºC 7H10 agar plates containing 50 µg/mL of hygromycin for selection of recombinant mutants. Colonies of recombinant mutants were then selected for inoculation at 3-4 weeks post-plating. The Δ*clpC2* mutant of H37Rv was confirmed by PCR of genomic DNA, RT-PCR of RNA and Southern blot (see respective "Methods" sections).

Δ*clpC2* knock-out (KO) generation primers:

5' TTTTTTTCCATAAATTGGATGCCGGCCCGTATACCTTC 3'

5' TTTTTTTTCCATTTCTTGGATGGCGTTGATGAGCTCGTC 3'

5' TTTTTTTTCCATAGATTGGCCGGCTGAGGCGAGCGACCC 3'

5' TTTTTTTTCCATCTTTTGGCGACAATTCGGCCGTCATGG 3'

Δ*clpC2* KO confirmation primers:

5' GCTTCAGCAGCAGGAGATCG 3'

5' AGGTGAGCTCGAGGACCTTG 3'

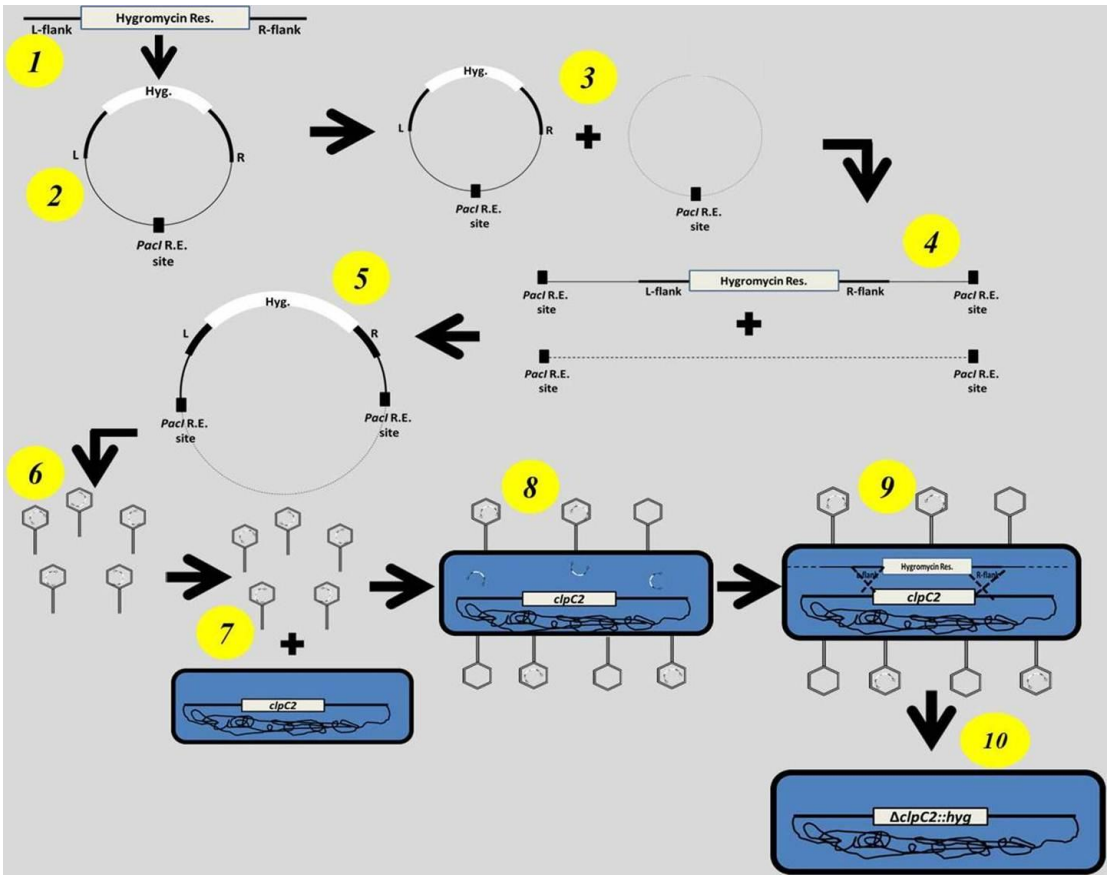


**Figure 3. The AES and specialized phage transduction creation of Δ*clpC2*.**
Null mutant of *clpC2*/*Rv2667* in Mtb was created by introducing a hygromycin antibiotic resistance cassette into the H37Rv genome by specialized phage transduction and homologous recombination. (As described in 3.2)
(1) An allelic exchange substrate (AES) employed for *clpC2* homologous recombination was created by PCR amplification of two regions flanking the gene including the first and last ~50 base pairs of the *clpC2*. (2) The flanking regions were digested with Van91I and ligated into a carrying vector with a hygromycin resistance cassette. (3) AES and phage DNA (4) were cut with PacI (5) and the digested DNA fragments were ligated together. (6) The resulting product was then packaged with a phage packaging kit; a high-titer phage was obtained and purified by filtration. (7) WT H37Rv was grown to mid-log phase and incubated with the high-titer phage (10 phage : 1 bacterium) for 24 hrs at 37 ºC for transduction. The transduced bacteria were plated onto 37 ºC 7H10 agar plates containing 50 µg/mL of hygromycin for selection of recombinant mutants. (8) Phage transduction progresses at 37 ºC for 24 hrs. (9) A *clpC2* abrogation mutant is created upon a homologous recombination event. (10) Δ*clpC2* mutants are selected for (and unsuccessful transductions eliminated) by growing transduced bacteria on media containing 50 µg/mL hygromycin.

### 3.2.2 Δ*clpC2* mutant complementation

A Δ*clpC2* complement was created by cloning *clpC2* tagged with BamHI and EcoRI restriction sites into both a pMV261 episomal expression vector and pMV361 *attB* integrating vector; both complementation vectors feature a kanamycin resistance gene and a *groEL2* constitutive promoter [160]. The resultant plasmids were confirmed by sequencing and used to transform the Δ*clpC2* mutant for complementation. (The transformation method employed is described in "Electroporation of plasmids" section 3.4 below.) Successfully transformed bacteria were selected on plates of 7H10 media containing 40 µg/mL kanamycin. Complementation of Δ*clpC2* was confirmed by PCR and RT-PCR.

*clpC2* complementation primers:

5' GCTTTTTTTTGGATCCGGTCGACACAATGCATAACG 3'

5' GCTTTTTTTTGAATTCACCTTCGCATGATTGCACAC 3'

## 3.3 *In vitro* transposon mutagenesis for Loss-of-Gain-of-Function (LoGoF) screening

**Generation of the K20 LoGoF mutant pool was carried out by Briken lab member Serdar Gurses.* *In vitro* transposon mutagenesis of the original K20 vector was undertaken with a commercially available kit (*HyperMu*™ Transposon Tools, Epicentre Biotechnologies/Illumina, Cat. No. HMI032K). Following the manufacturer's suggested protocol, *HyperMu* transposon insertion elements were randomly inserted into 15 genes of the 19-gene region of the K20 locus. The transposon cassette included a kanamycin resistance maker; this marker was used for the selection of successfully mutated K20. Once transformed, the vector pool was

used to transform susceptible *E. coli*. The resultant transposon mutants were sequenced for single insertion into the genes of interest. A confirmed transposon mutant for each respective K20 gene of interest was selected and subsequently employed in *loss-of*-gain-of-function (LoGoF) screening (see Figure 4).

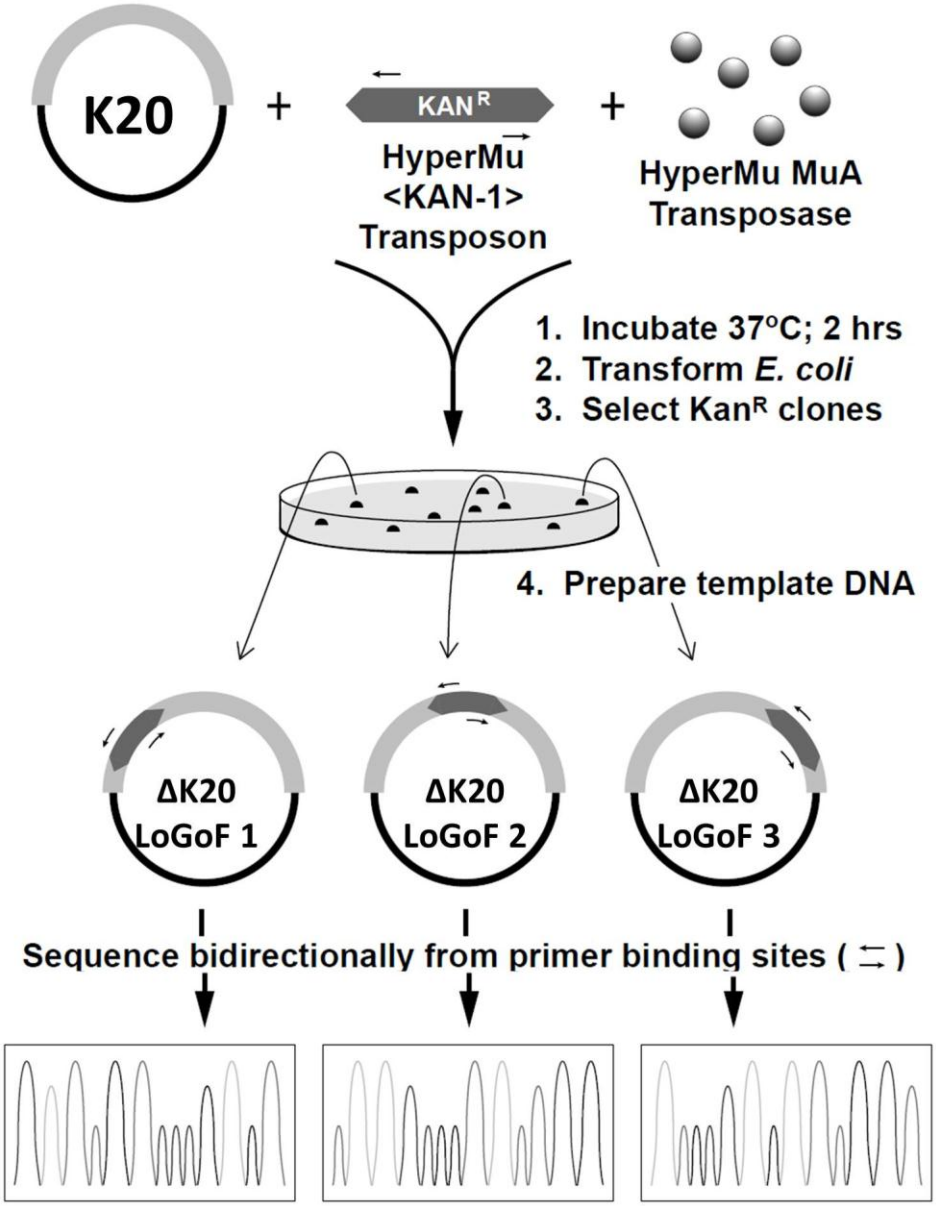


**Figure 4. Creation of LoGoF K20 transposon mutants.**
Briken lab member Serdar Gurses employed *in vitro* transposon mutagenesis of the K20 GoF vector. HyperMu <KAN-1> Transposase™ Kit (Epicentre Biotechnologies/Illumina, Cat. No. HMI032K), a kanamycin-transposon selection/insertion cassette, and the K20 GoF vector were incubated together. Transposon insertion elements were randomly inserted into the 19-gene region of K20 and the altered K20 mutants were used to transform *E. coli*, which was then plated onto kanamycin selection plates. Individual colonies were selected, and episomal DNA was extracted and sequenced with bidirectional primers to determine the point of insertion. Only mutants with an single transposon insertion into a K20 gene were selected from the pool and used in LoGoF screening. (Figure adapted from Epicentre Biotechnologies/Illumina. Technical process carried out by S. Gurses.)

## 3.4 Electroporation of plasmids

For each plasmid electroporation, a 10 mL culture of $OD_{600}$ = ~0.8 of the desired mycobacterial strain was used. The 10 mL culture was pelleted at 2000xg for 10 min at room temperature (or at 4 ºC for all steps concerning $mc^2155$ *M. smegmatis* work unless otherwise noted). The pellet was then washed with 10 mL of a solution composed of 10% glycerol and 0.05% Tween80; this wash and pelleting was repeated 3 times. The fourth pellet was resuspended in 1mL of the washing solution and 400 µl of these bacteria was added to a 2 mm electroporation cuvette to which 2 µl of the desired plasmid had been previously added. The washed bacteria were then electroporated at 2.5 kV/25 µFD/1000 Ω in a BioRad GenePulser Xcell electroporator. Immediately following the pulse, 1ml of complete 7H9 medium was added to the bacteria. The bacteria were allowed to recover at 37 ºC for 4 hrs for $mc^2155$ *M. smegmatis* or 16 hrs for Mtb and *M. kansasii*. The transformed bacteria were then plated onto 7H10 agar plates containing the appropriate concentration of antibiotic for selection (50 µg/mL hygromycin or 40 µg/mL kanamycin or 100 µg/mL streptomycin). The plates were incubated at 37 ºC for 4 days for $mc^2155$ or 3-4 weeks for Mtb and *M. kansasii*; plates were inspected for number of colonies relative to "no plasmid" control electroporations. Successful plasmid uptake was confirmed by PCR.

## 3.5 THP-1 cell culture maintenance and differentiation.

Cyrovials of THP-1 human acute myelomonocytic leukemia cell line (ATCC™ TIB-202) were stored in liquid nitrogen. Individual cyrovials of cells were thawed in a 37 $^{o}$C water bath and then washed once with plain RPMI. Cells were then pelleted at 400 x g and then resuspended in 20 ml of RPMI plus 10% heat inactivated FBS. The THP-1s were grown at 37 $^{o}$C/5% $CO_2$. Great care was taken to ensure the cells were passaged before growing to a confluency beyond 0.8 x $10^6$ cells/mL. In order to infect THP-1 cells, 0.6-1.0 x $10^6$ cells/mL were seeded into wells of a 24 well plate in the presence of 20 ng/mL of PMA for 20 hrs at 37 $^{o}$C/ 5% $CO_2$.

## 3.6 THP1 infection and cell death quantification

PMA differentiated THP-1 cells were infected with a desired MOI of mycobacteria grown to mid-log phase. The infections were carried out for 2 hrs in the case of *M. smegmatis* infections or 4 hrs in the case of *M. kansasii* or Mtb infections. Infection media consisted of RPMI plus 10% AB human serum (Gemini). After the desired infection time, all extracellular bacteria were removed from the wells by 2 washes of sterile PBS and chase media consisting of THP-1 culturing media containing 100 µg/mL gentamicin was added to each well. Infections were allowed to proceed to a desired endpoint at which time the cells were lifted with 37 ºC PBS/ 5 mM EDTA. THP-1 death was then quantified by propidium iodide staining and flow cytometry.

## 3.7 Southern blot analysis

The Δ*clpC2* knockout was additionally confirmed by Southern blotting. The probe was created from the primers used to generate the initial "5'/upstream arm" fragment of the original p004S AES (see Δ*clpC2* recombinant mutant creation section 3.2). The primer sequences employed are provided below. The K20 vector of the original GoF screen served as template for PCR amplification. The probe was labeled using a BrightStar Psoralen-Bioten Kit (Ambion). Genomic DNA was extracted from the clones and uniformly digested with Van91I. Additionally, the original K20 vector was digested with the same enzyme to serve as a probe-control. All digested DNA fragments were separated by agarose gel electrophoresis, and then transferred onto a charged nylon membrane. A denaturing step with 0.4 M NaOH followed. The probe was denatured at 90 ºC for 12 min, then immediately hybridized to the membrane in a 57 ºC water bath for approximately 16 hrs. The labeled membrane was then well washed, and adherent probe was detected with a BrightStar BioDetect Nonisotopic Detection Kit (Ambion). The membrane was exposed to photosensitive film for a period of no less than 15 min; the film was immediately developed.

Probe primers:

5' TTTTTTTCCATAAATTGGATGCCGGCCCGTATACCTTC 3'

5' TTTTTTTTCCATTTCTTGGATGGCGTTGATGAGCTCGTC 3'

## 3.8 Genomic DNA isolation- Mycobacteria

Following methods previously set forth [160], a 10 mL culture of a desired Mtb strain was grown to a high $OD_{600}$ and transferred to a 15 mL conical tube. The

bacteria were then pelleted by centrifugation in a Sorvall "Legend" centrifuge at 2000 x g for 20 min. Culture supernatant was discarded, and the pellet was resuspended in 1mL of GTE (25 mM Tris-HCl (pH 8.0), 10 mM EDTA and 50 mM glucose) solution. The bacterial suspension was then transferred to a 2 mL screw-cap centrifuge tube and centrifuged for 10 min at 2000 x g in an Eppendorf "5415D" table top centrifuge. The resulting supernatant was discarded, and the pellet was resuspended in 450 µL of GTE solution and 50 µL of a 10 mg/mL lysozyme solution, and then incubated at 37 ºC, 5% $CO_2$ overnight. Next, 100 µL of 10% SDS detergent was added and gently mixed; this was followed by the addition of 50 µL of 10 mg/mL proteinase K (Fermentas) and a 55 ºC heat block incubation for 45 min. After the incubation, 200 µL of 5 M NaCl was gently mixed in order to block the binding of DNA to cetrimide. 160 µL of CTAB ($dH_2O$, NaCl, and 10% cetrimide) heated to 65 ºC was added, mixed and incubated in a heat block at 65ºC for 10 min. An equal volume of chloroform-isoamyl alcohol (24:1) was added; the mixture was gently shaken, and then spun at maximum speed in for 5 min. Following centrifugation, 900 µL of the aqueous layer was transferred to a fresh microcentrifuge tube. The chloroform-isoamyl extraction was repeated with 800 µL of the aqueous layer reclaimed and transferred to a fresh microcentrifuge tube. A 70% volume of isopropanol was added and mixed until DNA precipitated. A 5 minute incubation at room temperature was followed by a 10 minute centrifugation at maximum speed. The supernatant was removed and the DNA pellet was washed once with 70% ETOH. A 5 minute centrifugation at maximum speed followed. The supernatant was

aspirated and the DNA pellet was allowed to air dry for 15 min, and then resuspended with 50 µL $dH_2O$.

## 3.9 Reverse transcription PCR (RT-PCR)

Purified total RNA was generated from bacterial cultures of interest following a standard methodology (see "RNA isolation- Mycobacteria section 3.2.10). Complementary DNA (cDNA) was then generated from 500 ng of this RNA using a Phusion® RT-PCR Kit (Fisher) for reverse transcription (RT) following the manufacturer's provided protocol. "Reverse Transcriptase" negative controls were consistently employed in all cDNA generation reactions to ensure the lack of genomic DNA contamination in the RNA preps. Following RT-PCR, the resultant cDNA was employed in a traditional PCR to confirm the presence or absence of expression of the *clpC2* gene; *sigA* primers were employed as an expression control (see below). A C1000 Thermal Cycler (BioRad) was used for all PCR work.

*sigA* primers:

5' CGTCAAGCACGCAAGGA 3'

5' TCGCTAAGCTCGGTCAT 3'

*clpC2* primers:

5' GCTTCAGCAGCAGGAGATCG 3'

5' AGTGCCAGCAGCAGGTGTTC 3'

## 3.10 RNA isolation- Mycobacteria

Mycobacteria cultures of interest were grown in complete 7H9 growth media to $OD_{600}$= 0.8, or late log phase. Cultures were pelleted by centrifugation for 10 min at 2,000 x g. Bacteria were resuspended by pipetting in chilled TRIzol Reagent (Invitrogen); the suspension was added to a chilled 2 mL screw-cap tube containing RNase free zirconia beads. Lysis was carried out by a Biospec Mini-Beadbeater 8 operating at maximum speed for a period of 10 min. A 5 minute incubation at room temperature followed to allow for complete dissociation of nucleoprotein complexes. A 20% volume of chloroform was added to each tube, which was then hand-shaken for 30 seconds. A second room temperature incubation of 2-3 min followed. The sample was then centrifuged at 12,000 x g for 15 min at 4 °C. The aqueous phase was extracted, and the chloroform extraction and 4 °C centrifugation was repeated. The resultant aqueous phase was mixed with an equivalent volume of isopropanol, and incubated at room temperature for 10 min. A 12,000 x g spin for 10 min at 4 °C followed. The supernatant was removed, and the RNA pellet was resuspended with 50 µl RNase-free water. To ensure complete removal of DNA from the samples, DNase treatment of the samples was carried out by employing a TURBO DNA-free (Ambion) kit. Additionally, "reverse transcriptase negative controls" were consistently employed in all subsequent cDNA generation work to confirm the lack of genomic DNA contamination in the RNA preps.

## 3.11 Growth curve measurement

Cultures of WT H37Rv, Δ*clpC2* and episomal-plasmid Δ*clpC2* complement and integrating Δ*clpC2* complement (previously described) were inoculated in triplicate into 7H9 and Sauton's minimal media at $OD_{600}$=0.01. Duplicate optical density readings were taken at 600 nm every day for 12 consecutive days for all cultures. The pMV261 and based episomal Δ*clpC2* complement was grown in 40 μg/mL kanamycin containing media in order to retain the plasmid; all other cultures were grown without any antibiotic unless stated otherwise.

## 3.12 SCID mice aerosol infections

*(This experiment was carried out by Serdar Gurses and B. Hurley.)* All mice were observed daily and sacrificed once in a moribund state. Disease progression was evaluated by the standards of the University of Maryland Institutional Animal Care and Use Committee (IACUC).

### 3.12.1 Aerosol infection of SCID mice

SCID mice (BALB/c background) were obtained from Jackson Laboratories. 8 SCID mice were infected per strain. Mice were exposed to aerosolized Mtb while contained in a Glas-Col® *Inhalation Exposure System* (A4212). A 5 mL volume of bacteria ($5 \times 10^6$ bacteria/mL) suspended in $PBS_{Tween}$ was employed for each aerosol infection. The following 3-step program was used in all infections:

1) 1,800 seconds of nebulizing time

2) 1,800 seconds of cloud decay time

3) 900 seconds of decontamination time

Following infection, all mice were caged and the nebulizer was cleaned, sterilized and prepped for another round of infection with a separate strain of Mtb.

### 3.12.2 Colony forming unit (CFU) determination

3 mice per condition were sacrificed the following day. Mice were sacrificed by cervical dislocation after being anesthetized with isoflurane. Lungs were excised and coarsely homogenized with scissors. The lung tissue was then thoroughly homogenized in a Stomacher® 80 *Biomaster*. The resulting homogenate was filtered through a strainer into a 50 mL conical tube and centrifuged for 15 min at 2000 x g. The resulting bacterial pellet was resuspended in $PBS_{Tween}$, plated onto 7H10 agar plates and incubated at 37 ºC. The plates were examined for colonies at 3-4 weeks post-plating, and CFU values were established for all Mtb strains.

## 3.13 Human monocyte derived macrophages (HMDMs)

Elutriated human monocytes were obtained through our collaborators Dr. Allen Sher and Dr. Bruno Andrade at National Institutes of Health in Bethesda, MD.

### 3.13.1 Human monocyte derived macrophages: culturing

Monocytes were washed with plain RPMI media and pelleted at 1500 rpm for 5 min at 4 ºC in Sorvall *Legend* centrifuge. An RBC lysis was carried out using 1x lysis buffer (eBioscience.); cell pellets were resuspended in 2 mL of the buffer and incubated at room temperature for 5 min. ACK buffer was diluted with 8mL of plain, chilled RPMI and pelleted at 1200 rpm for 5 min at 4 ºC; the RPMI wash was repeated and cells were pelleted a final time at 1000 rpm for 5 min at 4 ºC. The monocytes were then seeded at a concentration of $0.75 \times 10^5$ cells/mL into 24 well flat-bottom plates in plain RPMI warmed to 37 ºC. The monocytes were allowed to adhere in a 37ºC, 5% $CO_2$ calibrated incubator. After 2 hrs, RPMI was removed from all wells and the adherent monocytes were gently washed once with warmed, plain RPMI. Culturing media was comprised of RPMI, 10% off-the-clot AB human serum (Gemini) and 10 ng/mL Human M-CSF (Peprotech). The monocytes were differentiated to macrophage maturity by culturing in this media for seven days, replacing media with fresh media every two days. Macrophage maturity was verified by CD14 labeling and flow cytometry quantification of sample wells.

### 3.13.2 Human monocyte derived macrophages: infection

HMDMs were washed twice with sterile PBS. A 0.5mL volume of infection media comprised of RPMI and 10% AB human serum (Gemini) was added to each well of HMDMs. Infections were carried out with Mtb strains of interest for 4 hrs. Following infection, HMDMs were gently washed twice with sterile PBS. Then 1 or 2 mL of chase media (1x culturing/differentiation media + 100 µg/mL gentamycin) was added to each experimental well, with the volume depending on the duration of the particular study (1 mL of chase media for studies less than or equal to 5 days; 2 mL of chase media for studies greater 5 days). All empty wells and chamber spaces within the plate were filled with sterile PBS to mitigate evaporation from experimental wells; these reservoirs were topped-off with sterile PBS every 2 days post-infection.

### 3.13.3 Human monocyte derived macrophages: hypodiploid staining cell death quantification

At a desired experimental endpoint post-infection, culture supernatants were collected from the wells of infected HMDMs and uninfected controls. All HMDMs were lifted from the wells following a 37 ºC, 5% $CO_2$, 20 minute incubation with PBS/ 5 mM EDTA/10% trypsin solution. HMDM trypsinization reaction was stopped by adding the previously collected supernatant back in to the respective well of origin. All viable HMDMs and any cellular fragments within the supernatant resulting from induced cell death were then collected by gentle pipetting and added to a 15 mL conical tube for each respective well; post-lifting examination of the 24-well

plate by light microscopy ensured removal of all adherent HMDMs. The HMDMs and cellular fragments were pelleted at 400 x g for 10 min, then resuspended in chilled 70% ETOH and stored at -20 ºC for a minimum of 24 hrs to ensure fixation of the samples. Following complete fixation, cell death was quantified by washing each sample once in PBS, pelleting at 400 x g and then resuspending the pellet in a propidium iodide/RNAse solution (BD Pharmingen) for the purpose of hypodiploid labeling all apoptotic cells. Each well-sample was analyzed by flow cytometry approximately 20 min following the addition of the hypodiploid labeling solution. Rates of apoptosis were assessed by histogram analysis.

## 3.14 Alveolar guinea pig macrophages

### 3.14.1 Obtaining and culturing of guinea pig macrophages

Guinea pig macrophages were obtained through our collaborators Dr. Petros Karakousis and Mr. Michael Pinn of Johns Hopkins University in Baltimore, MD. Hartley guinea pigs were sacrificed by $CO_2$ asphyxiation and tissue was appropriately processed as follows.

### 3.14.2 Infections of guinea pig alveolar macrophages

Lungs were excised from the animal and gently lavaged with sterile, chilled PBS. The cells obtained were pelleted by centrifugation at 400 x g for 10 min and then resuspended in plain, chilled RPMI. Cells were transported to UMD College Park on ice. RBC lysis was carried out with 1x RBC lysis buffer (eBioscience) for 5 min at room temperature. Cells were then washed twice with plain, chilled RPMI. The alveolar macrophages that remained were counted and seeded overnight at 37 ºC, 5% $CO_2$ onto 3-well microscope slides (EMS) at 100,000 macrophages per well.

Seeding media was comprised of RPMI, 5% heat-inactivated FBS, and 1% Pen-Strep antibiotic. Following overnight adherence, wells were gently washed twice with sterile PBS and added infection media comprised of RPMI and 5% FBS. Macrophages were infected with Mtb strains of interest for 4 hrs at 37 ºC, 5% $CO_2$. Following infection, all wells were washed twice with sterile PBS, and a chase media composed of RPMI, 5% heat-inactivated FBS and 100 µg/mL gentamycin was added to each well. At a chosen experimental endpoint, cells were fixed by the addition of 4% PFA and placed at 4 ºC overnight. Apoptosis of macrophages was assessed by TUNEL staining (Roche Applied Sciences) and DAPI labeling (ProLong Anti-fade Gold with DAPI from Invitrogen). Subsequent analysis was carried out by florescence microscopy using a Zeiss Axiovision florescence capable microscope.

### 3.14.3 Infections of guinea pig peritoneal macrophages

Lavage of the peritoneal cavity was carried out by gently flushing the peritoneal cavity with 40 mL of sterile, chilled PBS. The cells obtained were pelleted by centrifugation at 400 x g for 10 min and then resuspended in plain, chilled RPMI. Cells were transported to UMD College Park on ice. RBC lysis was carried out with 1x RBC lysis buffer (eBioscience) for 5 min at room temperature. Cells were then washed twice with plain, chilled RPMI. The alveolar macrophages that remained were counted and seeded overnight at 37 ºC, 5% $CO_2$ onto 24-well tissue-culture treated plates at 500,000 macrophages per well. Seeding media was comprised of RPMI, 5% heat-inactivated FBS and 1% Pen-Strep antibiotic. Following overnight adherence, wells were gently washed twice with sterile PBS and added infection media composed of RPMI and 5% FBS. Macrophages were infected with Mtb strains

of interest for 4 hrs at 37ºC, 5% $CO_2$. Following infection, all wells were washed twice with sterile PBS, and a chase media comprised of RPMI, 5% heat-inactivated FBS and 100 µg/mL gentamycin was added to each well. At a chosen experimental endpoint, cells were fixed by the addition of 4% PFA and placed at 4 ºC overnight. Apoptosis of macrophages was assessed by TUNEL staining (Roche Applied Sciences) and subsequent flow cytometry.

## 3.15 Adenylate kinase (AK) release assay

Host cell necrosis was quantified by an adenylate kinase (AK) release assay. Toxilight® BioAssay (Lonza, Cat # LT07-217) was employed following the manufacturer's suggested protocol. Cell-free aliquots of the desired experimental supernatants were analyzed in a white, bioluminescence compatible, flat-bottom 96-well plate (Optiplate-96™ from Perkin-Elmer) read by a BioTek® "*Synergy*" plate reader. Three 20 µL samples of supernatant from each experimental well were collected and individually measured, unless otherwise stated.

Lysis controls were generated as follows. A single uninfected well per experiment was treated with a detergent to completely lyse all cells present; supernatants from this well were then used in the AK assay as "lysis-positive controls" that approximate the maximum possible AK release per well. This maximum AK release value correlates with total necrosis of all cells in a well.

## 3.16 Colony forming units (CFUs) study

To assess the *in vivo* viability of our bacterial strains, CFU studies were undertaken. Infections of HMDMs were carried out for 4 hrs at MOI of 3 with Mtb strains WT H37Rv, Δ*clpC2* and the complement previously described. All wells were washed twice with sterile PBS, and 2 mL of culturing media (RPMI, 5% off-the clot AB human serum and 10 ng/mL M-CSF) was added. Zero-hour samples, day 3 samples and day 10 samples were collected for each strain by lysing all HMDMs with 0.1% Triton® X-100 detergent and pipetting thoroughly. A dilution series was created for each replicate and then samples were plated onto 7H10 media. Each sample plate was evaluated at 4 weeks post-plating and CFU values were assessed at that time.

## 3.17 ELISA assays

### 3.17.1 TNFα ELISA

ELISA to detect TNFα was performed using the supernatants of HMDMs infected with strains of interest for 4 hrs at an MOI of 3, with a 20 hour chase following. Culture supernatants were collected at 24 hrs post-infection. Clear, flat bottom ELISA plates (Costar) were coated overnight at 4 °C with human anti-TNFα capture antibody (BD Pharmingen Cat. 551220) at [5 µg/mL] in a binding solution of 0.1 M $Na_2HPO_4$, pH adjusted to 6.0. All blocking steps were carried out at room temperature with PBS/0.05% Tween-20/10% FBS. TNFα (BD Pharmingen Cat. 554589) was diluted with infection media and used as concentration standards

ranging from 4,000 pg/mL to 15.6 pg/mL. A volume of 100 µL of supernatant was added into each ELISA well; there were 3 experimental wells per condition and 3 triplicate measures for each of these (n=9 for each condition). Binding was carried out at 4 °C overnight. Detection antibody of biotin anti-human TNFα (BD Pharmingen Cat. 554511) suspended in blocking buffer was added at room temperature for 1 hour. All wells were thoroughly washed, and streptavidin-alkaline phosphatase (Strep-AP) was added for 2 hrs. Wells were soundly washed, and 1 mg/mL of *p*-nitrophenyl phosphate (PNPP), well-suspended in 1.02 M diethanolamine (pH 9.8) substrate buffer, was added to each well. The ELISA plate was then read 10-20 min following substrate addition, in a BioTek® "*Synergy*" plate reader.

### 3.17.2 IL-1β ELISA

ELISA to detect IL-1β was performed using the supernatants of HMDMs infected with strains of interest for 4 hrs at an MOI of 3, with a 20 hour chase following. Culture supernatants were collected at 24 hrs post-infection. Clear, flat bottom ELISA plates (Costar) were coated overnight at 4 °C with human anti- IL-1β capture antibody (BD Biosciences Cat. 51-9002512) in a binding solution of 0.1 M $Na_2CO_3$, pH adjusted to 9.0. All blocking steps were carried out at room temperature with PBS/0.05% Tween-20/10% FBS. IL-1β standard (BD Biosciences Kit Cat. 557953) was diluted with infection media in concentrations ranging from 2,000 pg/mL to 15.6 pg/mL. 100 µL of supernatant was added into each ELISA well; there were 3 experimental wells per condition and 3 triplicate measures for each of these (n=9 for each condition). Binding was carried out at 4 °C overnight. Detection

antibody of biotin anti-human IL-1β (BD Biosciences Cat. 51-9002516) suspended in blocking buffer was added at room temperature for 1 hour. All wells were thoroughly washed, and Strep-AP was added for 1 hour. Wells were soundly washed, and PNPP, well-suspended in substrate buffer, was added to each well. The ELISA plate was then read approximately 10-20 min after substrate addition, in a BioTek® "*Synergy*" plate reader.

## 3.18 Apoptotic cell death quantification

### 3.18.1 Terminal deoxynucleotidyl transferase dUTP nick end labeling (TUNEL) assays

At a desired experimental endpoint post-infection, culture supernatants were collected from the wells of infected HMDMs and uninfected controls. All HMDMs were lifted from the wells following a 37ºC, 20 minute treatment of PBS/5mM EDTA/10% trypsin solution. HMDM trypsinization was stopped by adding the previously collected supernatant back to the respective well of origin. All viable HMDMs and any cellular fragments within the supernatant resulting from induced cell death were then collected by gentle pipetting and added to an individual 15mL conical tube for each well; post-lifting examination of the 24-well plate by light microscopy ensured removal of all adherent HMDMs. Host cell apoptosis was quantified by using "*In Situ* Cell Death Detection Kit: Fluorescein" (Roche Applied Sciences). TUNEL assays were carried out as described by the provided manufacturer's protocol. The percentage of TUNEL positive cells was determined by

counterstaining cells with DAPI (ProLong Anti-fade Gold with DAPI from Invitrogen) and subsequent fluorescence microscopy and quantification of apoptotic percentages.

### 3.18.2 Hypodiploid quantification

At a desired experimental endpoint post-infection, culture supernatants were collected from the wells of infected HMDMs and uninfected controls. All HMDMs were lifted from the wells following a 37 ºC, 20-minute treatment of PBS/5mM EDTA/10% trypsin solution. HMDM trypsinization was stopped by adding the previously collected supernatant back to the respective well of origin. All viable HMDMs and any cellular fragments within the supernatant resulting from induced cell death were then collected by gentle pipetting and added to an individual 15 mL conical tube for each well. Post-lifting examination of the 24- well plate by light microscopy ensured removal of all adherent HMDMs. The HMDMs and cellular fragments were pelleted at 400 x g for 10 min, resuspended in chilled 70% ETOH and stored at -20 ºC for a minimum of 24 hrs for total fixation of the samples. Following fixation, cell death was quantified by washing each sample once in PBS, pelleting at 400 x g and resuspending the pellet in a propidium iodide/RNAse solution (BD Pharmingen) for the purpose of hypodiploid labeling of all apoptotic cells. Each well-sample was analyzed by flow cytometry 20 min after the addition of the hypodiploid labeling solution. Rates of apoptosis were assessed by histogram analysis and comparison.

## 3.19 Statistical analysis

Statistical analyses were performed on three independent experiments each with three experimental replicates unless otherwise noted within individual figure legends. GraphPad Prism 5.0 software was used to create all data figures and was employed to analyze data by ANOVA with Tukey post-test. Error bars indicate standard deviation (±SD) unless otherwise noted. The range of p-values is indicated as follows: * $p = 0.01\text{-}0.5$; ** $p = 0.001\text{-}0.01$ and *** $p \leq 0.001$.

# Chapter 4: Identification of anti-apoptotic gene(s) for a set genomic region of *M. tuberculosis*

Previously, the Briken lab employed a large gain-of-function (GoF) genetic screen in an effort to identify genes within the *M. tuberculosis* genome that mediate apoptotic-suppression [53]. The screen used 312 randomized gene segments from the Mtb genome (average segment size was approximately 40kbp, total clone pool represented a 3x coverage of the total genome) and vector-expressed these regions within the less virulent, fast-growing (4 hrs doubling time), high apoptosis inducing relative species *M. smegmatis* (Msmeg). The GoF vector-carrying Msmeg were used to infect a human cell line (THP-1) which was screened for a reduction in apoptosis compared to an empty-vector control post-infection. Three unique Mtb genomic segments were positively identified- J21, M24 and K20. This dissertation specifically investigates genes of the K20 genomic region of Mtb. Chapter 4 describes the experiments employed and results obtained in the attempt to identify a novel Mtb gene mediating the suppression of host apoptosis.

## 4.1 Results: Identification of anti-apoptotic gene(s) for a set genomic region of Mtb

### 4.1.1 The K20 genomic region of Mtb confers an anti-apoptotic phenotype to high-apoptosis inducing mycobacteria

The K20 genomic region of Mtb (see Supplemental Table ST1) was previously shown to play a role in the inhibition of apoptosis by way of gain-of-function (GoF) screening [53] in *M. smegmatis* (Msmeg) (data by K.K. Velmurugan,

unpublished). Briefly, Msmeg transformed with the K20 GoF vector (Msmeg-K20) induced noticeably less apoptosis (approximately half as much) when used to infect THP-1 cells than Msmeg carrying empty-vector (a pYUB415 expression construct) at 16 hrs post-infection [53], as measured by TUNEL labeling (data not shown). Msmeg is a very potent inducer of host apoptosis; another species of mycobacteria which also induces high levels of host apoptosis was chosen to repeat the assay to confirm the K20 GoF results initially observed.

The relatively slow-growing *M. kansasii* (~20 hrs doubling time) is an opportunistic pathogen which induces high levels of host apoptosis, albeit at a much slower rate than Msmeg. *M. kansasii* generates a "cleaner phenotype" in terms of margins of host apoptosis induction between empty-vector controls and vectors expressing GoF genetic information, as well as variation within sample replicates [53]. The K20 GoF phenotype seen in Msmeg held true when the K20 vector was used in a second, more stringent round of GoF screening [53] in *M. kansasii* (Mkan) (Figure 5, K20 data previously unpublished) (data by K.K. Velmurugan). Mkan transformed with the K20 GoF vector (Mkan-K20) induced less than 20% host apoptosis as measured by TUNEL staining, far less than the 86% host apoptosis induced by Mkan transformed with an empty-vector (CO) control.

As these studies were conducted in PMA differentiated THP-1 cells, it was decided an appropriate animal model would be needed for future characterization of the phenotype. To this end, Hartley guinea pigs were employed; the Hartley guinea pig line is outbred, meaning researchers may anticipate slight animal-to-animal variations during experimentation.

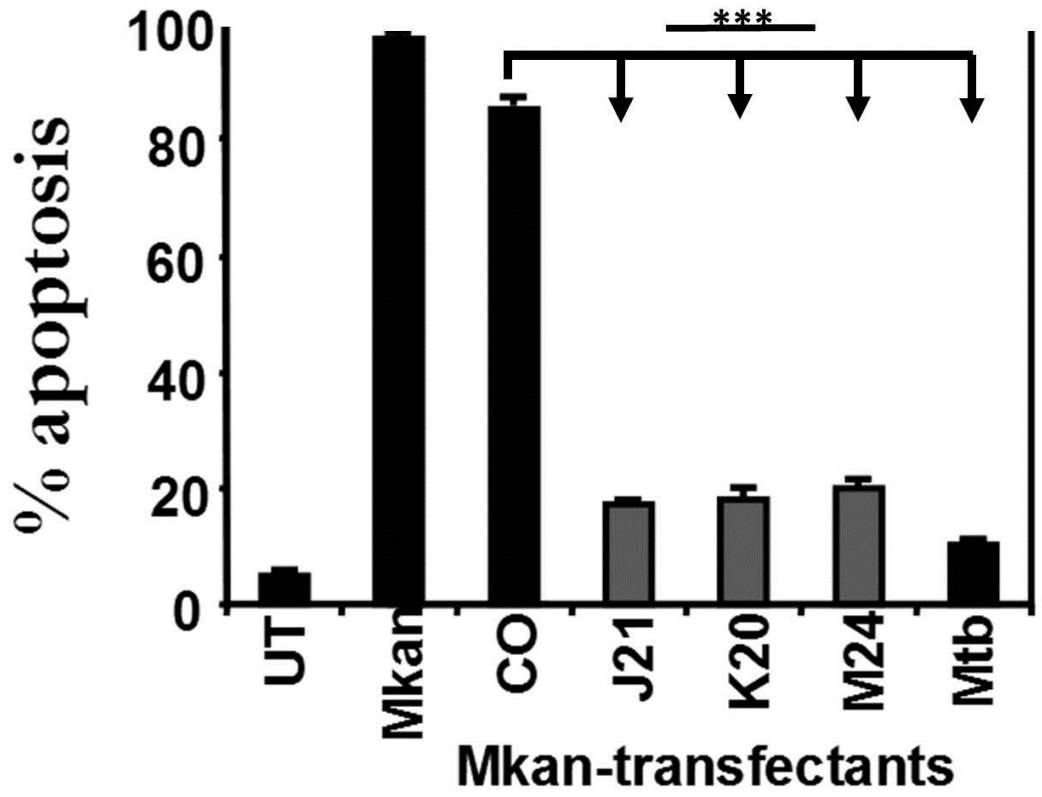


**Figure 5. The K20 genomic region of Mtb confers an anti-apoptotic phenotype when used to transform the high-apoptosis inducing *M. kansasii*.**
A GoF screen carried out in Mkan (with previously unpublished results for K20) [53]. (Figure is courtesy of K.K. Velmurugan.) The J21, K20 and M24 GoF vectors and empty vector (CO) were transformed into Mkan, and used to infect THP-1 cells. Apoptosis induction by the bacteria was compared to uninfected (UT) and Mtb infected cells. Apoptosis of host cells was quantified by TUNEL assay following 5 days of infection. Results are averages of three independent experiments and error bars represent 6 standard deviation (±SD). Statistical significance is relative to levels of apoptosis induced by wildtype *M. kansasii*: ***, $p \leq 0.001$ (ANOVA with Tukey post-test).

#### 4.1.1.1 The K20 genomic region confers an anti-apoptotic phenotype guinea pig alveolar, but not peritoneal, macrophages

Alveolar and peritoneal guinea pig macrophages were obtained with assistance from our collaborators at Johns Hopkins University. Animals were sacrificed, and then the lungs and peritoneal cavity were lavaged. Macrophages were purified and then infected with empty-vector Mkan or Mkan-K20, then lifted, fixed and assayed by TUNEL microscopy a day post-infection (Figure 6). The K20 phenotype was observed in alveolar macrophages; 8.5 ± 4.2% of K20 infected cells were apoptotic versus 43.1 ± 4.5% of empty vector infected cells. While the GoF phenotype was conserved in Mkan-K20 infected alveolar macrophages, there was no difference in Mkan-K20 and empty-vector infections of macrophages obtained by peritoneal lavage (Figure 7).

These observances held true for several animal experiments, with overall numbers varying, likely due to the differing genetic predispositions of the outbred guinea pigs, but the overall trend of the GoF phenotypes remained consistent. The K20 GoF phenotype was conserved in alveolar macrophages, and it was ultimately decided that the Hartley guinea pig would be a suitable animal model for future studies involving the K20 genomic region of Mtb.

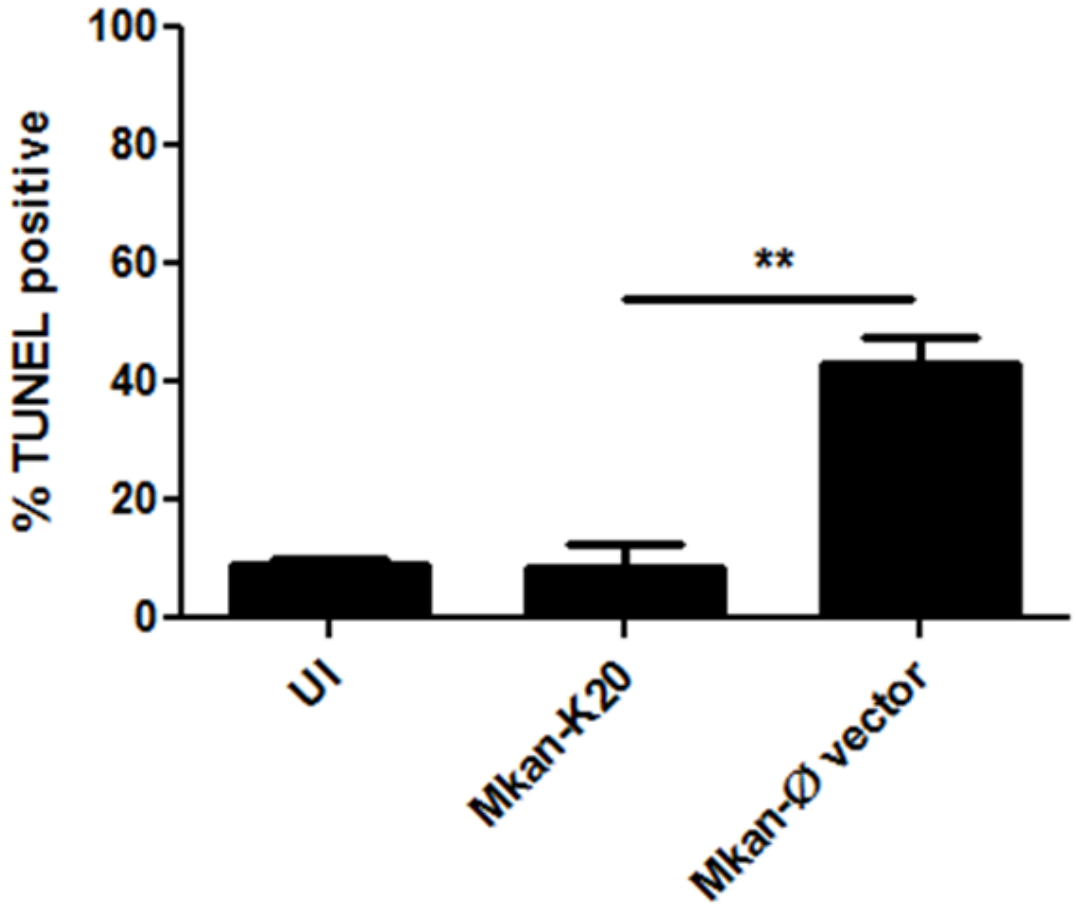


**Figure 6. Hartley guinea pig alveolar macrophages infected with *M. kansasii*-K20 and *M. kansasii*-null vector.**
Alveolar macrophages were infected with Mkan-K20 and null-vector control at MOI of 3 for a 4 hour infection, followed by a 20 hour chase; uninfected controls (UI) were included in all experiments. Alveolar macrophages were seeded on 3 well slides and quantified by TUNEL staining and microscopy, 3 data points/sample; a minimum of 400 cells/well were counted and additionally validated by blinded counts. Representative data from one animal is presented. Statistical significance bar highlights relative differences between Mkan-K20 and empty-vector control induced-apoptosis levels. Error bars show ± SD. ** $p<0.01$ (ANOVA and Tukey post-test).

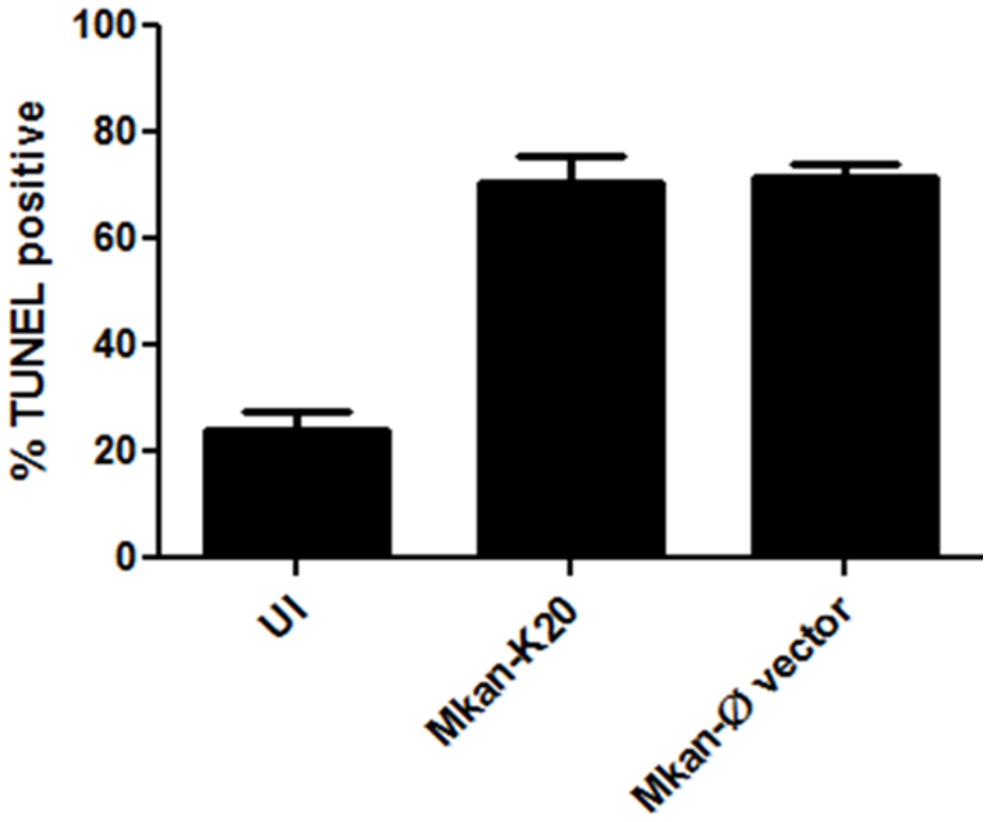


**Figure 7. Hartley guinea pig peritoneal macrophages infected with *M. kansasii*-K20 and null-vector.**
Peritoneal macrophages were infected with Mkan-K20 and null vector control at MOI of 3, for a 4 hour infection followed by a 20 hour chase; uninfected controls (UI) were included in all experiments. Peritoneal macrophages were seeded in 24 well plates and quantified by TUNEL staining and flow cytometry, 3 replicates/sample. Representative data from one animal is presented in this figure. Error bars show ± SD.

### 4.1.2 *Loss-of*-Gain-of-Function (LoGoF) screen identifies possible anti-apoptotic genes of Mtb

Mtb has previously been shown to actively inhibit the apoptosis of host macrophages. This is quite likely a survival mechanism of the pathogen, enabling Mtb to avoid detection by the immune system and retain the shelter of a viable host cell. Genes such as *nuoG* [53], *pknE* [107], *secA2* [106, 111], *Rv3165c* (S. Gurses, unpublished), *Rv3167c* (S. Gurses, unpublished), and *Rv3654c-55c* [94] are all involved in the Mtb-mediated inhibition of host apoptosis. As the Briken lab routinely explores this particular component of host-pathogen interaction, we looked into a potential role for a gene or genes of the K20 genomic region of Mtb in modulating host cell apoptosis.

Having previously established and confirmed an anti-apoptotic role for the K20 genomic region of Mtb in Msmeg and Mkan ([53], data not shown) by way of a gain-of-function, forward genetics approach, our attention turned to identifying the specific gene(s) responsible for the observed GoF phenotype. Importantly, the GoF screen depended on a particular Mtb gene or set of genes carried on an episomal vector to confer an increased ability to suppress host apoptosis by the relatively high-inducing Msmeg and Mkan species.

In the original GoF screen that led to the identification of the K20 genomic region of Mtb, a positive GoF phenotype was indicated when the level of host apoptosis induced by Msmeg or Mkan was reduced by a particular Mtb gene region carried on an expression vector relative to apoptosis levels induced by a genetically-null copy of the expression vector; the Mtb gene regions were all carried on a pYUB415 expression vector, meaning the expression vector provides additional,

extra-chromosomal genetic information to the transformed species that does not naturally occur. All genetic information on this expression vector must be translated and transcribed by the transformed bacteria, meaning Mtb-specific promoters/repressors/etc. carried on the GoF expression vectors may not be recognized by the Mkan and Msmeg; additionally, the gene-products must successfully integrate with the pre-existing machinery of a transformed bacterium in order to effect a GoF phenotype.

In order to capitalize on this effect from another angle, Briken lab member Serdar Gurses employed *in vitro* transposon mutagenesis of K20 (Figure 4) in order to ablate the function of each individual gene carried on the vector and allow for identification of the specific gene(s) responsible for the anti-apoptotic phenotype. To do this, HyperMu Transposase™, a kanamycin-transposon insertion/selection cassette, and the K20 GoF vector were incubated together. The transposon insertion elements were randomly inserted into the 19-gene region of K20, and the altered K20 mutants were used to transform *E. coli*, which was then plated onto kanamycin-containing plates for selection. Individual colonies were selected, and episomal DNA was extracted and sequenced with bidirectional primers to determine the point of transposon insertion. Individual transposon mutants with an insertion occurring in in a single K20 gene were selected from the pool; of this transposon mutant pool, 15 of the 19 total K20 genes were mutated with a single transposon insertion and considered viable tools for future screening (Figure 8 and Supp. Table ST2).

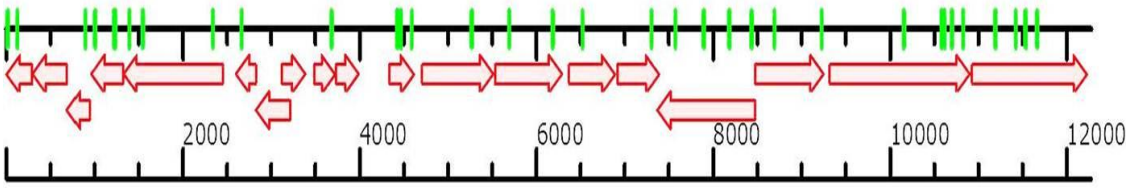


**Figure 8. Schematic representation of the K20 LoGoF transposon mutant pool.** Above is a schematic representation of the K20 genomic region with green, vertical dashes indicating the transposon insertion location for each of the individual transposon mutants generated. Approximate size of each gene (indicated by hollow, open red arrows; lower scale provided in 500nt/tick mark) and gene orientation on (+) genomic strand are indicated; all size and orientation data are *in silico* predictions obtained through "TB Database" website, *tbdb.org* [161]. *Note:* Sequencing results for the original K20 vector (K.K. Velmurugan [53], data not shown) revealed that an additional distal gene, *Rv2617c* (the entire gene and severe truncations of two neighboring genes), is attached to the rest of the K20 region as an unexpected artifact of the Mtb genomic library creation process. The single transposon mutant generated for this particular gene is not indicated in the figure, but was included in the LoGoF screening process.

### 4.1.2.1 LoGoF screen in mc$^2$-155 background identifies two possible anti-apoptotic genes of Mtb

An individual K20 transposon mutant was selected for each of the 15 interrupted genes (Supp. Table ST2). Each transposon (each annotated as "sg*Rv26XX*") mutant was used in the transformation of mc$^2$155, a high-competency lab strain of Msmeg. To carry out the screen, PMA-differentiated THP-1 cells were infected at MOI of 5 for 2 hrs with each of the respective mc$^2$155-K20 transposon mutants mc$^2$155-K20 (carrying the original K20 GoF vector) and mc$^2$155-null vector.

As previously mentioned, the original GoF screen identified *positives* as those expression vectors carrying an Mtb gene cluster conferring an ability to suppress host apoptosis, masking the normally high-apoptosis-inducing phenotype of the given model species of mycobacteria. The K20 transposon mutagenesis screening employed a "*Loss-of*-Gain-of-Function" (LoGoF) strategy, where *positives* are those individual transposon mutants that lose the ability to suppress host apoptosis relative to the original K20 GoF phenotype.

At 16 hrs post-infection, the THP-1 wells were visually inspected by microscopy and assessed by experimentally-blinded observers for obvious, visible differences in degree of cell death (S. Gurses and V. Briken; data not shown). Following the visual scoring, the cells were lifted and stained with propidium iodide (PI) to quantify the level of induced cell death. The LoGoF screen suggests a role in the anti-apoptotic phenotype when a particular transposon mutant induces greater levels of host cell death than the original, unaltered K20 GoF vector. The LoGoF screen in mc$^2$155 was repeated several times, and it was noted that two of the

transposon mutants, sg*Rv2666* and sg*Rv2667*/*clpC2* (Figure 8), consistently induced apoptosis at levels above the K20 GoF background.

However, as demonstrated in Figure 8, the degree of the shift, 26.9 ± 1.9% for sg*Rv2666* and 26.4 ± 2.2% for sg*Rv2667*/*clpC2* versus 20.9 ± 1.8% for K20, was statistically non-significant in the $mc^2155$ model background. However, the difference in cell death induction by K20 and the null-vector control (31.9 ± 2.5%) was a paltry 10%, putting the roughly 6-7% shift of the two LoGoF mutants into a broader context.

### 4.1.2.2 LoGoF screen in *M. kansasii* identifies two possible anti-apoptotic genes of Mtb

As in the initial GoF screen that identified the K20 region as an anti-apoptotic region, the first round of LoGoF screening was carried out in the relatively rapidly growing $mc^2155$ model species. This initial screening was followed by a second round of screening in the much slower-growing Mkan (*ATCC 12478*) species with a limited, more refined pool of LoGoF mutants. As a modeling species of host apoptosis-induction, Mkan generates a "cleaner phenotype," meaning it affords a much greater discrepancy between positive (K20) and negative (null-vector) controls. When this screen was repeated in the Mkan background with the selected LoGoF-vectors of greatest interest, we once again saw the LoGoF mutants sg*Rv2666* and sg*Rv2667*/*clpC2* induce greater levels of host apoptosis than their K20 parent.

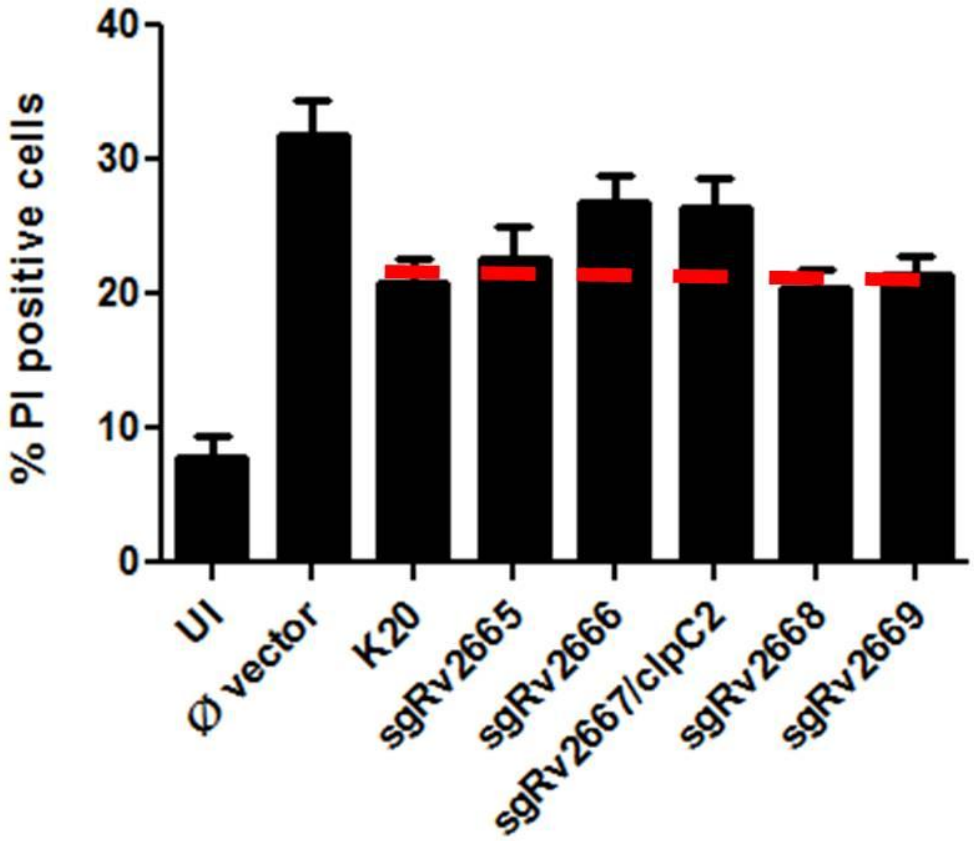


**Figure 9. LoGoF mutants sgR*v2666* and sg*Rv2667* are slightly higher inducers of host death than K20 in the mc$^2$155 background.**
THP-1 cells differentiated with PMA overnight were infected at MOI of 5 for 2 hrs with mc$^2$155-K20, mc$^2$155-null vector, and the listed transposon mutants; all experiments included uninfected (UI) THP-1 control wells. At 30 hrs post-infection, the THP-1 cells were lifted and cell death was quantified by staining with propidium iodide. A threshold was set (horizontal red dashed line) at the level of cell death induced by the original K20 GoF carrying mc$^2$155. Data is pooled from three independent experiments; a minimum of 10 replicates per condition are shown. Error bars indicate ±SD.

Figure 10 presents the results of two such experiments in the Mkan background and includes the Mkan-carrying null-vector, the original K20 GoF vector, the two LoGoF mutants of primary interest and LoGoF mutants of the two genes upstream and downstream of the predicted *Rv2666-Rv2667* operon (see Figure 11). Unlike the insubstantial 10% differences in host apoptosis-induction in $mc^2155$ LoGoF screen, variances in the degree of host-apoptosis induction were far more significant when using the Mkan model species.

In Figure 10, pooled results gave a mean value of 70.6 ± 1.7% for Mkan-null-vector induced death and 20.9 ± 3.9% for Mkan-K20-induced apoptosis. LoGoF mutants of interest, sg*Rv2666* and sg*Rv2667*/*clpC2,* induced 51.6 ± 7.7% and 59. 6 ± 3.4% host apoptosis, respectively. Both LoGoF mutants induced host death at statistically significant levels above Mkan-K20 ($p \leq 0.01$ for *Rv2666* and $p \leq 0.001$ for sg*Rv2667*, both p-values relative to K20 induction levels) and generated non-significant levels of apoptosis relative to empty-vector control. The resulting trend of the Mkan-LoGoF screen was consistent over multiple experiments. Host death was minimally induced by the experimental control LoGoF mutants (corresponding to genes bordering the predicted *Rv2666-Rv2667* operon), sg*Rv2665* (17.5 ± 1.6% host apoptosis) and sg*Rv2668* (35.9 ± 8.1% host apoptosis). The control LoGoF clones did not induce host cell apoptosis at levels significantly varied from the K20 parent vector. These results suggest the specific importance of the *Rv2666* and *Rv2667* genes to the K20 anti-apoptosis phenotype. Overall, the repetition of the LoGoF screen in the Mkan background validated *Rv2666* and *Rv2667*/*clpC2* as potential Mtb

anti-apoptotic genes of interest and confirmed LoGoF-screening results initially observed in the $mc^2155$ model species.

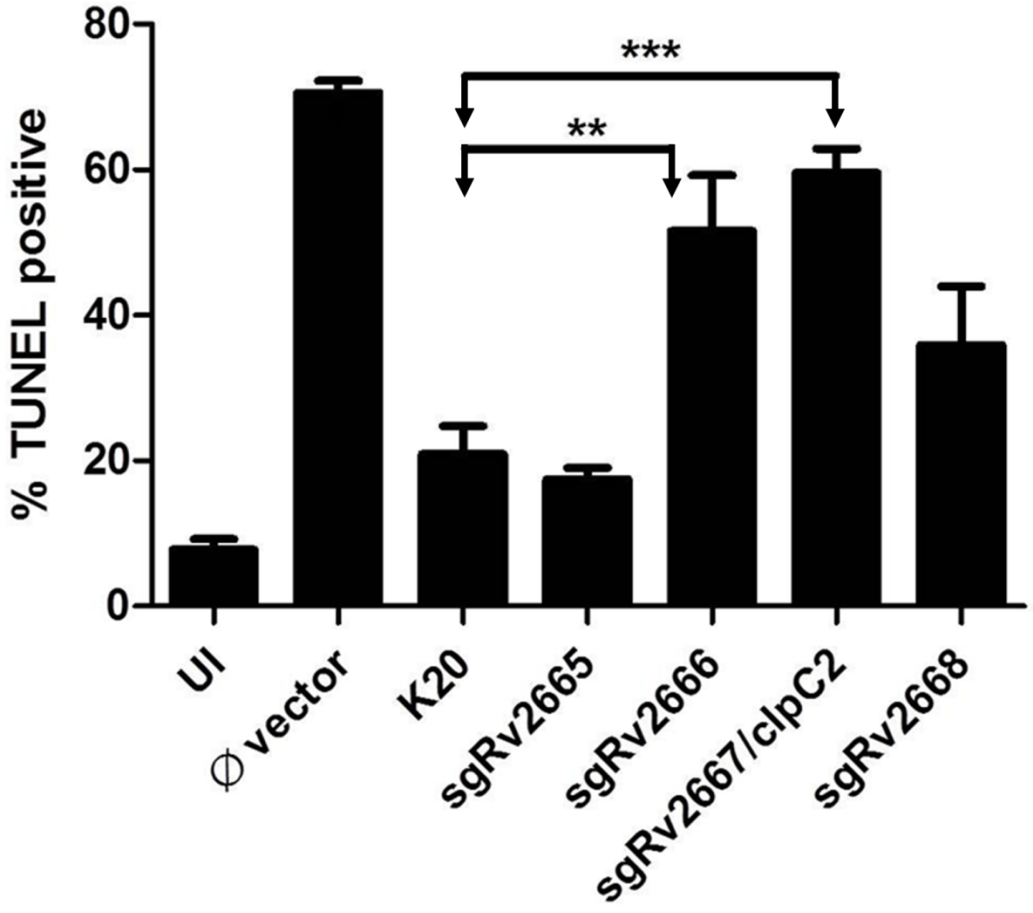


**Figure 10. LoGoF mutants sg*Rv2666* and sg*Rv2667* induce more host apoptosis than unaltered K20 in the Mkan background.**
THP-1 cells differentiated with PMA overnight were infected at MOI of 5 for 4 hrs with Mkan-K20, Mkan-null vector, and the listed transposon mutants; each experiment includes infected (UI) THP-1 control wells. At least 48 hrs post-infection, the THP-1 cells were lifted and apoptosis of THP-1 cells was quantified by TUNEL staining and subsequent analysis by flow cytometry. Data is pooled from two independent experiments at least 48 hour post-infection and is representative of numerous experiments; a minimum of 4 replicates per condition are shown. Error bars indicate ±SD. **, $p < 0.01$ (Mkan-K20 vs. Mkan-sg*Rv2666*); ***, $p \leq 0.001$ (Mkan-K20 vs. Mkan-sg*Rv2667*)

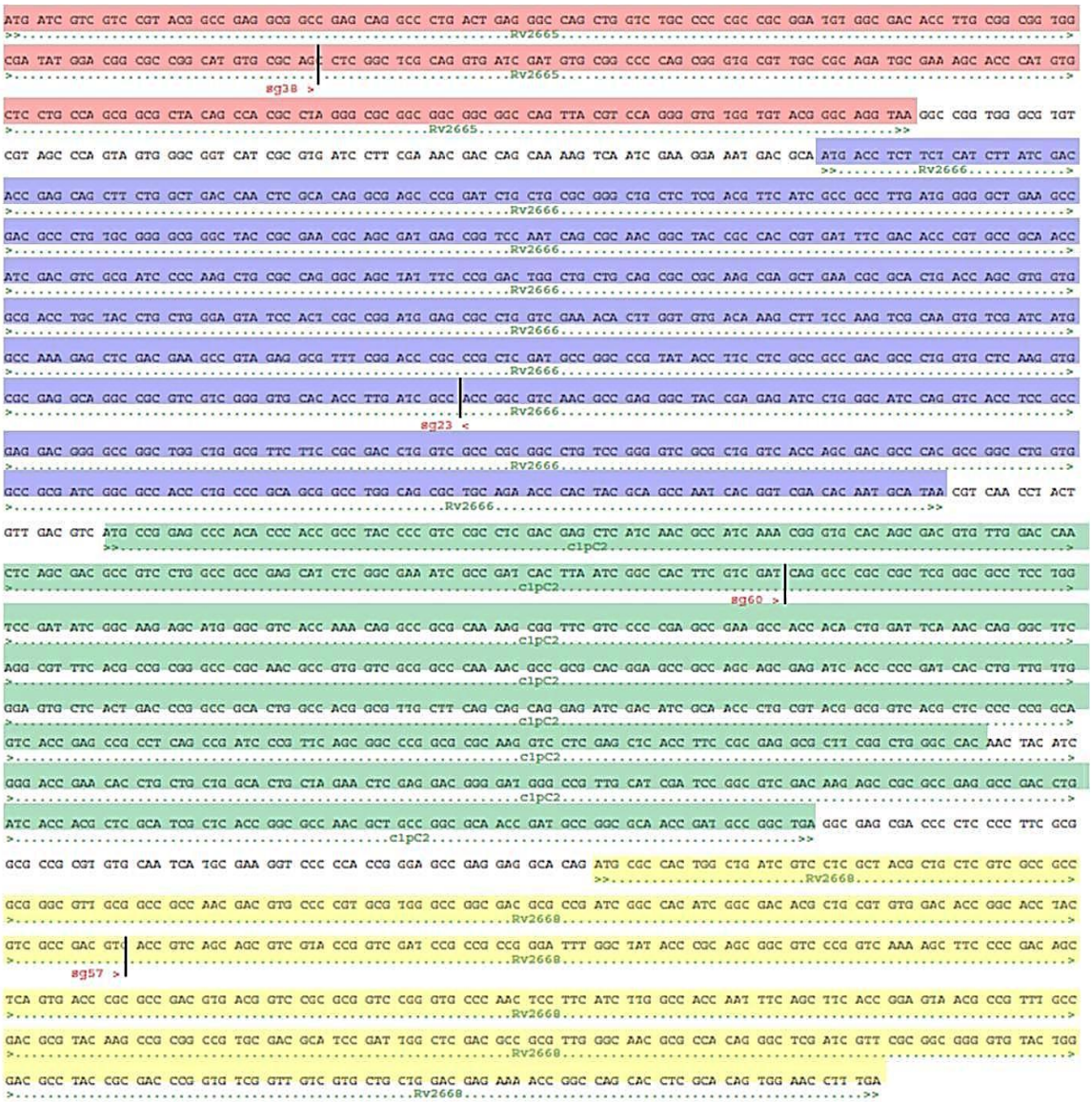


**Figure 11. Detailed transposon insertion map of the 4 LoGoF clones screened in Mkan.**

The above figure reveals individual insertion points for each of the four LoGoF transposon mutants employed in the Mkan screening. Each predicted gene is uniquely color coded in addition to the indicative subscript labels: *Rv2665* (red), *Rv2666* (blue), *Rv2667*/*clpC2* (green) and *Rv2668* (yellow). Vertical black dashes ( ┃ ) indicate specific points of insertion for each of the transposon mutants. *Rv2665*: H37Rv nt pos. 2,982,827+, (pos. 128/282 of the gene); *Rv2666*: H37Rv nt pos. 2,983,632+, (pos. 561/803 of the gene); *Rv2667*: H37Rv nt pos. 2,984,057+, (pos. 161/758 of the gene); *Rv2668*: H37Rv nt pos. 2,984,050+, (pos. 154/521 of the gene). Subscript annotations immediately preceding each dash provide the unique experimental working name (text in red) for the respective LoGoF mutant; a (>) symbol indicates a (+) strand oriented insertion while a (<) symbol indicates a (–) strand oriented insertion.

### 4.1.3 A transposon mutant of *Rv2666* suggests anti-apoptotic role for the gene

Having previously employed a LoGoF screen in two separate modeling backgrounds and following the identification of the putative two gene *Rv2666-Rv2667* operon as carrying the gene(s) of interest, our attention turned to confirming our observation in Mtb. Employing deletion or gene abrogation mutants of Mtb in a loss-of-function (LoF) approach is a direct way of examining any potential anti-apoptotic phenotype. As in all avenues of production, it is inevitably more efficient to employ tools already available than to reinvent the wheel. To that end, we searched lists of available transposon mutants provided by the TARGET (*Tuberculosis Animal Research and Gene Evaluation Taskforce*) research project; the TARGET mutant collection is essentially a very large pool of randomly generated *Himar1* transposon (Tn) mutants created in the CDC1551 Mtb strain background [158]. The collection has been assembled, and is currently maintained, as a collaborative research effort between Johns Hopkins University [155], Colorado State University [156] and other interested institutions. A handful of transposon mutants generated in the K20 genomic region was available by request through the TARGET repository. One of the transposon mutants available within the library of mutants is the 804 nt, hypothetical transpose gene *Rv2666* (BEI catalog number NR-14775; position of transposon insertion is at 322 nt from the putative start site). There was no transposon mutant available in the TARGET library for the other gene of primary interest, *Rv2667*/*clpC2*. The Tn*Rv2666* mutant was employed in a LoF, reverse genetics study to determine the role of *Rv2666* in modulating host apoptosis. Tn*Rv2666* and WT CDC1551 were used to infect human monocyte-derived

macrophages (HMDMs) at an MOI of 5. Infections proceeded for 4 hrs and were followed by a chase period of 4 days. HMDM apoptosis was then quantified by hypodiploid labeling and flow cytometry. Results from two separate experiments are shown in Figure 12.

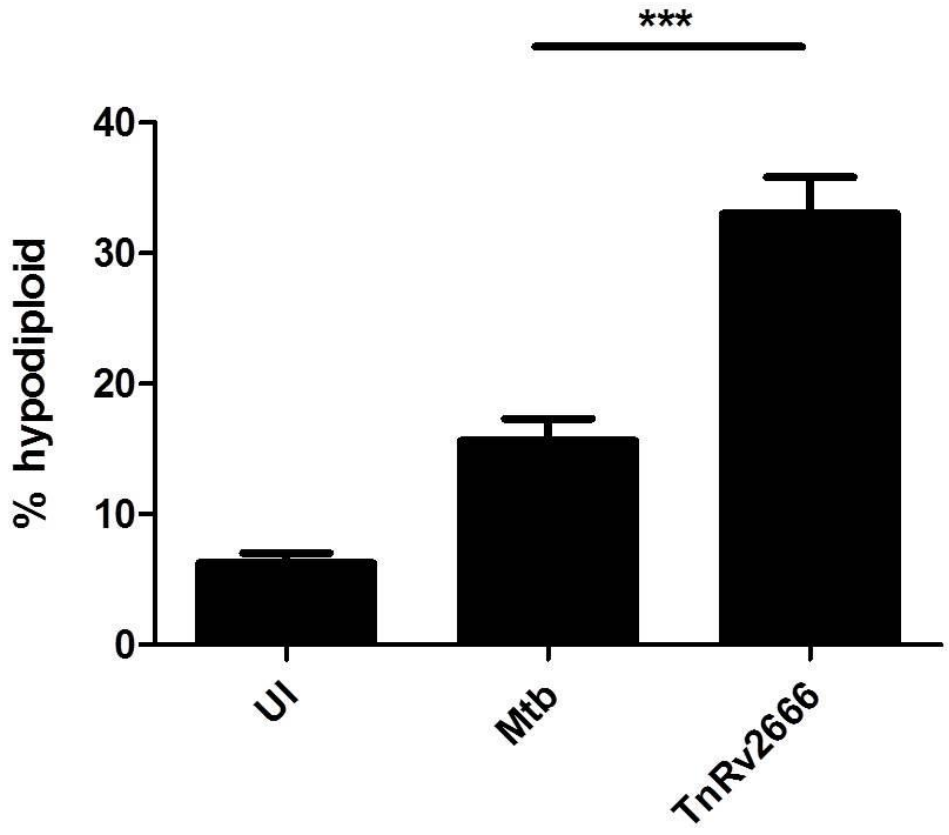


**Figure 12. The *Himar1* transposon mutant of *Rv2666* induces increased host cell apoptosis compared to WT Mtb.**
HMDMs were infected with WT CDC1551 and Tn*Rv2666* at MOI of 5 for 4 hrs followed by a 4 day chase; all experiments include uninfected HMDM wells as a control. HMDMs were collected and hypodiploid labeling was used to assess levels of host apoptosis. Quantification of hypodiploid positives was made by flow cytometry. Data shown are the results of two independent experiments employing HMDMs derived from two unique donors; a minimum of 7 measurements per condition were made in total. Statistical significance bar indicates apoptosis differences between WT Mtb and the Tn*Rv2666* mutant. Error bars indicate ±SD. ***, $p \leq 0.001$. (ANOVA and Tukey post-test).

While WT Mtb and the Tn*Rv2666* mutant both induced levels of host apoptosis greater than the uninfected control (6.3 ± 0.8% of all cells underwent spontaneous apoptosis), the level of host apoptosis in HMDM infected with Tn*Rv2666* induced more than twice as much host-death as WT Mtb- 33.0 ± 2.8% and 15.7 ± 1.7% induced macrophage apoptosis, respectively. The trend of these results was consistent across several experiments in HMDMs, and the phenotype was also seen in the THP-1 cell line as compared to many other transposon mutants in the CDC1551 background (B. Hurley and S. Shah, data not shown). Ultimately, the LoF approach employed to study the potential anti-apoptotic role of *Rv2666* validated results previously observed in $mc^2155$ and Mkan LoGoF screens. All of this evidence, taken together, strongly implicates that the hypothetical transpose-like element *Rv2666* is involved, by a yet-undetermined manner, in suppressing host-apoptosis as part of an Mtb-mediated survival strategy.

### 4.1.4 Complementation of Tn*Rv2666* confirms anti-apoptotic role and identifies *Rv2666* as contributing to the K20 phenotype

Having previously established a potential role for *Rv2666* as a K20, anti-apoptotic gene of interest, our attention turned to confirming this phenotype by genetic complementation of the *Himar1* transposon mutant of *Rv2666*. This was done by transforming the kanamycin-resistant Tn*Rv2666* with a non-constitutive, integrating expression $pDB60^{streptomycin}$ plasmid. This expression plasmid carries the Mtb sequence for *Rv2666*, including the 90 nt region upstream of the gene to attempt inclusion of the native promoter sequence. The $pDB60^{streptomycin}$ vector is specifically

designed for silent integration into the *attB* site within the targeted genome; it also confers a high degree of streptomycin resistance to the transformed bacteria for selection purposes.

In order to validate the anti-apoptotic phenotype of *Rv2666*, the LoF assay previously described was repeated with the inclusion of the complemented Tn*Rv2666* (Figure 13). As before, HMDMs were infected with bacterial strains of interest at MOI 5 for 4 hrs and the infection was followed by a 4-day chase. Analysis and quantification of host apoptosis was once again established by hypodiploid labeling of collected HMDMs and flow cytometry. As in the initial LoF study, Tn*Rv2666* induced significantly more host apoptosis ($p \leq 0.001$) than the WT, 28.1 ± 0.2% and 13.0 ± 0.9%, respectively. The complement-induced 11.8 ± 1.1% host apoptosis, significantly less than the transposon mutant ($p \leq 0.001$); these values have no statistical difference from WT CDC1551. These results establish *Rv2666* as a player in the anti-apoptotic phenotype mediated by Mtb.

Additionally, the successful complementation of Tn*Rv2666* negated the question of a LoGoF-screen phenotype that was the possible result of polar effects in the sg*Rv2667* LoGoF mutant. Polar effects of this nature would have resulted from transposon insertion into *Rv2666*, and would have meant that the sg*Rv2666* LoGoF phenotype was actually a red herring and that *Rv2667* was the true gene of interest in the LoGoF studies.

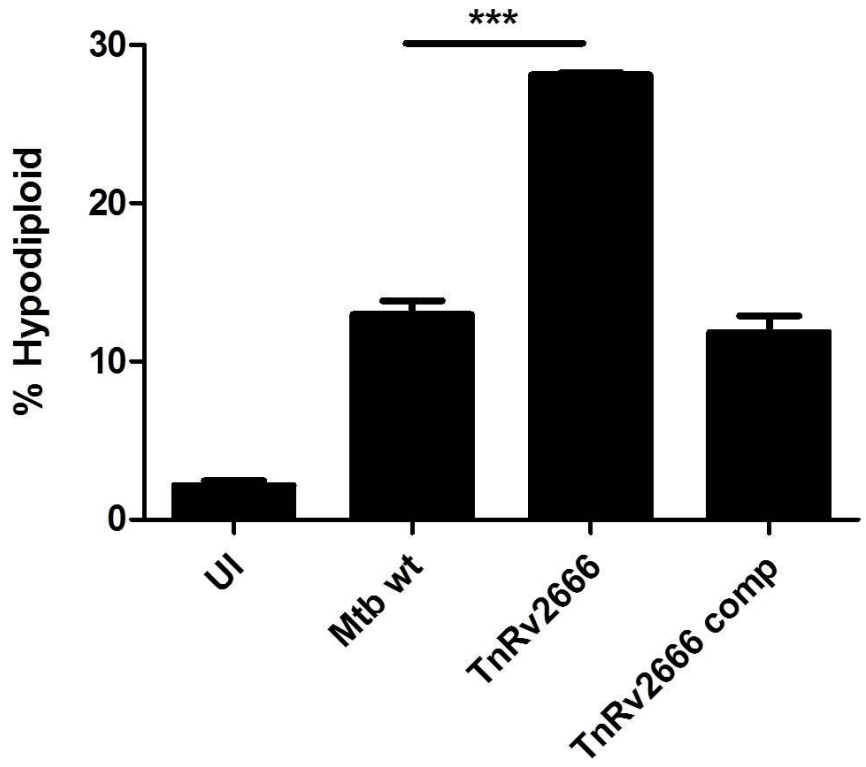


**Figure 13. Complementation of Tn*Rv2666* confirms anti-apoptotic role and identifies *Rv2666* as contributing to K20 phenotype.**
HMDMs were infected with WT CDC1551, Tn*Rv2666*, and *TnRv2666*::complement at MOI of 5 for 4 hrs followed by a 4-day chase; uninfected (UI) HMDM wells were included as controls in all experiments. HMDMs were collected and hypodiploid labeling was used to assess levels of host apoptosis. Quantification of hypodiploid positives was made by flow cytometry. Data shown are the results of HMDMs of a single donor with a minimum of 3 values per group. Significance bar indicates differences between WT Mtb and TnR*v2666*; this level of significance applies to Tn*Rv2666* vs. the complement as well. Error bars indicate ±SD. ***, $p \leq 0.001$. (ANOVA and Tukey post-test).

Figure 13 shows complementation of Tn*Rv2666* and returns host death to WT levels. Similar results were also observed when corresponding experiments were carried out in the THP-1cell line (S. Shah, Figure S1a). Quantification of host cell death by TUNEL staining, as opposed to hypodiploid staining, and the additional host background, THP-1 cell line as opposed to HMDMs, offers added levels of support to our findings. Additionally, adenylate kinase (AK) release assays were employed to establish that Tn*Rv2666*- induced cell death was definitively host-mediated apoptosis, rather than death by uncontrolled necrosis, that would result in substantial loss of cellular membrane integrity and ensuing AK release. Host necrosis has previously been shown to be induced by Mtb in later stages of infection as a probable mechanism of escape and dissemination [162, 163]. This Mtb-mediated necrosis significantly increases AK release due to the great degree of host cell lysis. A dramatic upsurge in host necrosis was not observed in THP-1 infected with Tn*Rv2666* (Supp. Figure S1b), discounting the chance that the observed phenotype involves necrotic host death.

Ultimately, the successful complementation of the Tn*Rv2666* phenotype, that is, the restored ability of the mutant to suppress host apoptosis, confirms the initial findings of the LoGoF and LoF assays. With at least one "K20 anti-apoptosis" gene identified and confirmed, our attention turned to the study of *Rv2667*/*clpC2*, the other gene of interest in the predicted two gene *Rv2666-Rv2667* operon.

### 4.1.5 Creation and confirmation of *clpC2* abrogation mutant

Prior results from a LoGoF screen in two separate mycobacterial species (Figures 9, 10) implicated both *Rv2666* and *Rv2667*/*clpC2* (hereafter denoted *clpC2*) as potentially involved in the K20 anti-apoptosis phenotype. Our work to characterize the *Rv2666* gene in Mtb, previously discussed as the in-operon gene immediately preceding *clpC2*, was tremendously expedited as a transposon mutant of the gene was available through the TARGET research collaboration [155]. As the TARGET library has no corresponding transposon mutants available for *clpC2*, it was necessary to produce a specifically targeted gene abrogation mutant. This was accomplished by employing a system of specialized phage transduction to "knock out" Mtb *clpC2* by way of homologous recombination [159]. This approach was employed in order to vastly increase the relative rate of homologous recombination and generate a strain of Mtb that did not express the *clpC2* gene product. The specialized phage transduction method is frequently used in Mtb genetics work because the rate of obtained recombinant mutants obtained by more traditional electroporation/transformation methods is typically too low to be considered practical [160].

Sequences flanking the *clpC2* gene were amplified using primers that would eliminate the vast majority of the *clpC2* coding sequence upon homologous recombination, but would leave the first and last few nucleotides of *clpC2* intact in order to ideally prevent alteration of the expression of the genes immediately upstream and downstream of the target. The flanking sequences were cut with the restriction enzyme Van91I and ligated into correspondingly cut fragments of p004S

cloning vector, which carries dual multiple-cloning-sites flanking a hygromycin-resistance cassette. Briefly, following the generation of this p004S$^{hygromycin}$ plasmid designed for homologous recombination with *clpC2*, the sequence confirmed plasmid was linearized by PacI restriction enzyme digestion; the vector was then ligated into phage DNA (for the creation of phasmid DNA); phasmid DNA was packaged into viable phage; high titers of this phage were produced; and, ultimately, purified phage was transduced into the WT H37Rv laboratory strain of Mtb (Figure 3), creating recombinant Δc*lpC2* mutant Mtb. The resultant Δ*clpC2* mutants were confirmed as true *clpC2* ablation constructs by PCR analysis of genomic DNA (Figure 14), Southern blotting of genomic DNA (Supp. Figure S2), and RT-PCR analysis (Figure 15). In addition to the *clpC2* mutant, a complementation plasmid was also generated using the kanamycin-resistant, constitutively expressing, episomal mycobacterial vector pMV261 (Figures 14,15). As seen in these figures, the Δ*clpC2* mutant is verified as a true *clpC2* gene abrogation mutant and the complement produces a *clpC2* gene product. These tools enabled a thorough loss-of-function and complementation analysis of *clpC2*.

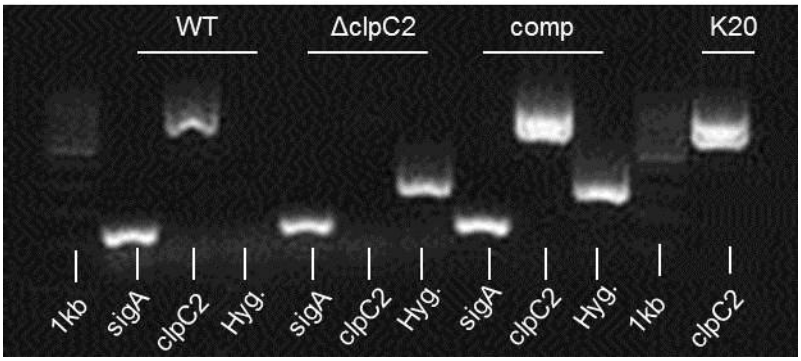


**Figure 14. PCR confirms abrogation and complementation of *clpC2*.**
0.8% agarose gel featuring PCR employing genomic DNA (and plasmid DNA in the case of the complement) and primer sets amplifying gene regions for *sigA* (control), *clpC2* and encoding a hygromycin resistance cassette. Genomic DNA was obtained from bacterial cultures grown under standard *in vitro* growth conditions. Cultures were grown in complete 7H9 media to $OD_{600}$= 0.800. Samples were acquired from WT Mtb H37Rv, Δ*clpC2* and Δ*clpC2* pMV261-based complement; the original K20 GoF control was also included for *clpC2* primer control. Primers amplified small internal regions with the specified genes.

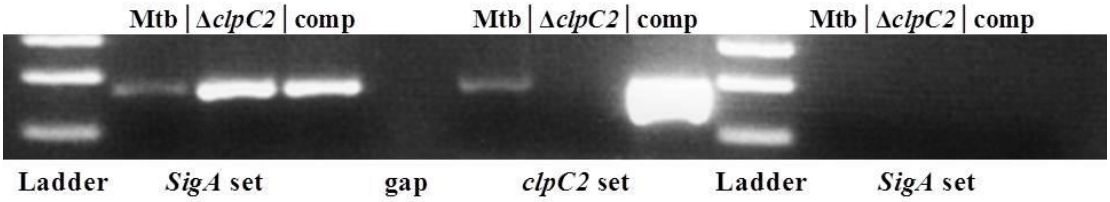


**Figure 15. RT-PCR of purified bacterial RNA from WT Mtb, Δ*clpC2*, and Δ*clpC2*-complement confirms *clpC2* gene expression level.**
0.4% agarose gel featuring RT-PCR generated cDNA synthesized from purified RNA. RNA was obtained from bacterial cultures grown under standard *in vitro* growth conditions. Cultures were grown in complete 7H9 media to $OD_{600}$= 0.800. RNA samples were acquired from WT Mtb, Δ*clpC2* and a Δ*clpC2* pMV261-based complement (expressing *clpC2* with *GroEL2* heat-shock promoter). cDNA was generated from RNA extracted from each culture of interest; RNA samples were free of genomic DNA contamination as determined by the inclusion of a RT control (far right lanes). Primers amplifying small approximately 200nt regions targeted for *SigA* (control) and *clpC2* specific RNA expression assess *clpC2* expression in the three strains.

### 4.1.6 Δ*Rv2667*/*clpC2* is dispensable for a salient role in modulating host anti-apoptosis effects by Mtb

Following validation of Δ*clpC2,* the mutant and the WT H37Rv were employed in infections of HMDMs at MOI of 3. Infections were carried out for 4 hrs and were followed by a chase period of 4 days. HMDMs were then collected. In order to quantify levels of host apoptosis, hypodiploid labeling and flow cytometry were carried out (Figure 16).

Unexpectedly, the results of Δ*clpC2* LoF experiments consistently showed a lack of any significant differences in induced host apoptosis levels between WT H37Rv (12.7 ± 2.3% induced apoptosis) and the Δ*clpC2* mutant (9.8 ± 1.9% induced apoptosis) in HMDMs. These results held true for HMDMs derived from several unique monocyte donors and cannot be dismissed as a donor dependent occurrence.

Additionally, there were no significant differences in host apoptosis when WT (9.5 ± 3.0%) and Δ*clpC2* (4.2 ± 2.3%) Mtb strains were used in the infection of alveolar guinea pig macrophages (Figure 17). Taken together, the results of these LoF experiments suggest that ClpC2 has no obvious role in modulating host apoptosis effects by Mtb. Ultimately, this may indicate that, of the hypothetical *Rv2666*-*Rv2667*/*clpC2* operon, the *Rv2666* gene alone is responsible for the "K20 phenotype" originally identified by the GoF screen of Mtb genomic regions.

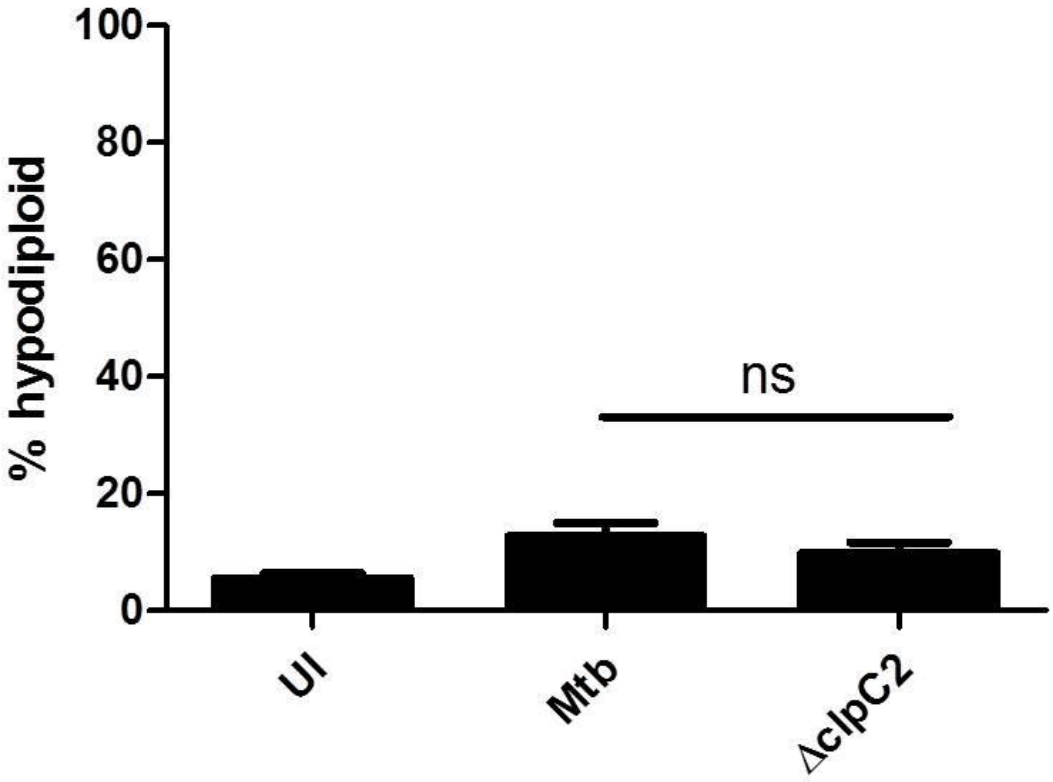


**Figure 16. Infection of HMDMs with WT Mtb and Δ*clpC2* indicates no significant differences in host apoptosis induction.**
No significant differences in apoptosis were observed in HMDMs infected with WT and Δ*clpC2* Mtb. HMDMs were infected at MOI 3 for 4 hrs followed by a 4 day chase; uninfected (UI) controls were included in all experiments. Host apoptosis levels were quantified by hypodiploid staining and flow cytometry. Results shown are the mean from two independent experiments employing unique donors; (n=10). Error bars represent ± SD. Significance bar compares WT Mtb and Δ*clpC2*. Statistical analysis employed ANOVA with Tukey post-test.

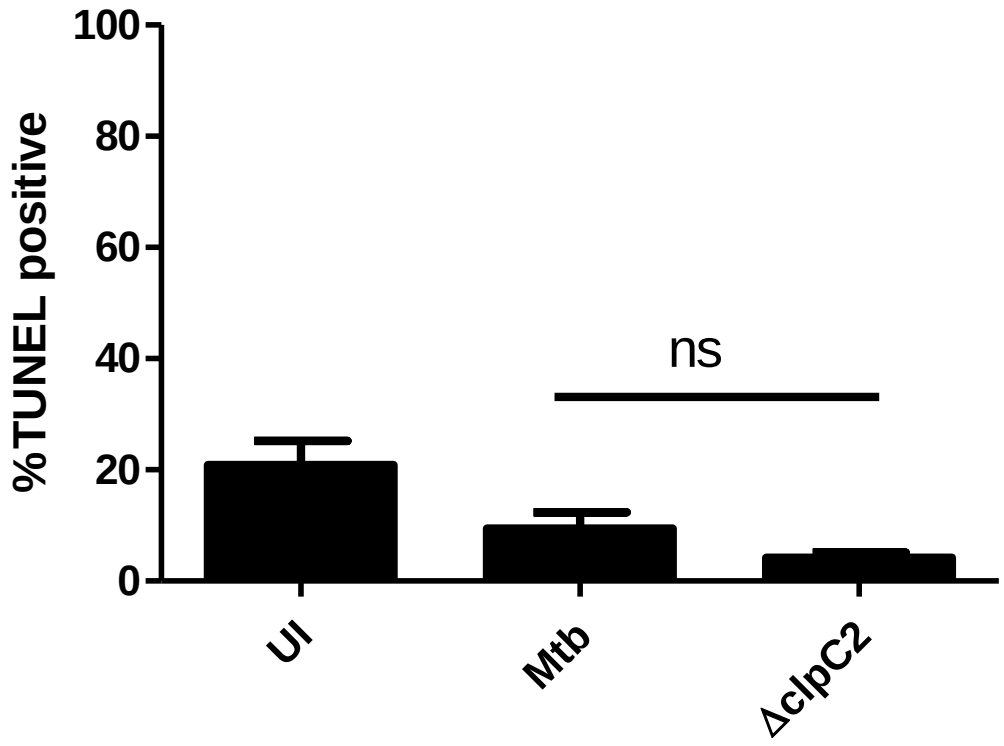


**Figure 17. Infection of alveolar guinea pig macrophages with WT Mtb and Δ*clpC2* indicates no significant differences in host apoptosis.**
No significant differences in apoptosis were observed in alveolar macrophages of outbred Hartley guinea pigs infected with WT and Δ*clpC2* Mtb. Alveolar macrophages were infected 4 hrs at MOI of 3 followed by a 4 day chase; uninfected (UI) controls were included in all experiments. Infections and chase were carried out in triplicate wells on chamber slides for each condition. TUNEL staining and DAPI labeling were employed to quantify percentages of apoptotic host cells against the total number of macrophages present. Values were established by fluorescence microscopy imaging and counting DAPI-TUNEL co-labeled cells against DAPI-only cells; the values were then additionally verified by blinded counting of the same images (former Briken lab member Duc Nguyen). A minimum of 400 cells/well were counted. Results shown are the average of two experiments using alveolar macrophages of two unique animals. Error bars represent ± SD. Significance bar compares WT Mtb and Δ*clpC2*. Statistical analysis employed ANOVA with Tukey post-test.

## 4.2 Discussion: Identification of anti-apoptotic gene(s) for genomic region of Mtb

The apoptosis of a macrophage carrying a bacterial burden is a common form of immune defense employed against a wide variety of pathogens, notably *M. tuberculosis*. Previous work by Dr. K.K. Velmurugan initially established that the K20 genomic region of Mtb as conferring an anti-apoptotic gain-of-function (GoF) phenotype when a vector carrying the region was used to transform *M. smegmatis* $mc^2155$. The subsequent screen used 312 randomized gene segments from the Mtb genome (the average segment size was approximately 40,000 nt; the total size of the clone pool was estimated to be roughly "3X coverage," or (40,000 x 312)/ total Mtb genome nt) and vector-expressed these regions within the aforementioned nonpathogenic, fast-growing, high-apoptosis-inducing relative species *M. smegmatis* $mc^2155$ (Msmeg). The vector-carrying Msmeg were used to infect a human cell line (THP-1). THP-1 cells were infected with individual Msmeg clones, each transformed with a unique genomic region-carrying vector from the GoF library. The THP-1 cells were screened for a reduction in apoptosis relative to the levels of cell death induced by an Msmeg clone transformed with an empty-vector control, and those clones with the strongest anti-apoptotic phenotype were chosen for further rounds of screening at higher stringency. The chosen GoF clones were individually transformed into the slow-growing, high-apoptosis-inducing opportunistic pathogen *M. kansasii* Hauduroy (Mkan) to confirm their apoptosis-suppressing phenotype. The screen was repeated in the Mkan background; the K20 region, along with two other unique genomic regions [53], was confirmed as carrying a gene or genes that conferred a host-apoptosis suppressing phenotype to both the Msmeg and Mkan species.

It is quite possible that the 3x coverage of the Mtb the GoF library did not allow for complete screening of the Mtb genome. The 3x genome coverage is an estimate based on the number of nucleotides generated for the entire GoF library. It is important to note that this determination is distinct from the manner in which "x-values" are assigned in the process of whole genome shotgun sequencing (that is based on the total number of sequence reads). However, if assessed in the "WGS x-coverage manner," the 3x value means that there will be a predicted ~5% gap in the number of nucleotides that are needed, in theory, to cover the entirety of the Mtb genome (the entire GoF library contains roughly 12,480,000 nt while the Mtb genome is 4,411,532 nt, roughly 3x the raw nt value of the genome). Also, it is possible that the GoF clones are not "contiguous regions" or that they cannot be assembled into an approximation of the Mtb genome due to redundancy of some genomic regions and the absence of others within the library. Ultimately, the initial GoF screen may very well have missed several anti-apoptotic genes of Mtb because of these issues. Furthermore, even if all anti-apoptotic genes of Mtb were included in the GoF library, it may be possible that the Mkan and Msmeg species lack the genetic background to successfully implement the gene-products of interest to an anti-apoptotic end. Finally, Mtb may encode anti-apoptotic genes that have a function dependent upon the presence of a distal gene or genes and their respective products; the nature of the GoF screen limits each vector to an average of 40,000 nt, meaning anti-apoptotic effects dependent on distal genes would have been rendered moot and any of the responsible genes will have been overlooked by this particular assay.

### 4.2.1 The K20 genomic region of Mtb displays an anti-apoptotic phenotype in several host models.

The K20 region of Mtb (H37Rv nucleotide region 2,978,367 to 2,990,637, + strand) is 12,271 nt in length, plus an additional distal genomic region (2,945,437 to 2,946,738, + strand) that is 1,302 nt in length. There are a total of 19 complete, predicted Mtb genes [164] included in the K20 vector (Supp. Table ST1).

The initial GoF studies that identified K20 were carried out in the THP-1, monocytic cell that was driven to activation with PMA. As immortalized cell line experimentation results may not always align with primary cell testing outcomes, we repeated the K20 GoF assays in additional host models for further validation of the genetic region's suspected anti-apoptotic phenotype. We were able to confirm our positive GoF findings obtained from the THP-1 host model K20 screen in both primary human monocyte-derived macrophages (HMDMs) and alveolar guinea pig macrophages (Figure 6).

These results alleviated our concerns that the observed anti-apoptotic phenotype conferred by the K20 gene region was potentially an artifact of cell-line experimentation that was not indicative of *in vivo* host-pathogen interactions. Confirming immortalized cell-line phenotypes in primary cell lines is quite important, especially considering our particular GoF phenotype of interest (host cell suicide) could be adversely affected by the mechanisms causing cell-lines to indefinitely propagate.

Also, in the course of our preliminary experimentation and optimization of potential model systems, we attempted several infections of the murine alveolar macrophage (MH-S) cell line. The MH-S cell line was initially created in a

laboratory by immortalizing Balb/cJ alveolar macrophages with simian virus 40 (SV40) [165]; MH-S are commonly employed to model alveolar macrophages under *in vitro* conditions [177, 178]. Although this cell-line seems like a promising model given that alveolar macrophages are the native habitat of Mtb, our experiments determined MH-S were far too resistant to pathogen-induced apoptosis to operate as a feasible model for our work (Figure 18). The SV40 immortalization that created the MH-S line likely interferes with pathways important for host apoptosis following infection with mycobacteria.

With further regards to infeasible model systems, our studies also revealed that resident peritoneal macrophages of Hartley guinea pigs were not a practical model for studying host-pathogen apoptosis events (Figure 7), although peritoneal macrophages were far more plentiful than alveolar macrophages from the very same animal. It may be that these peritoneal macrophages, generally sheltered from antigenic insult due to their location in the peritoneal cavity, are extremely sensitive to encounters with foreign particulates and respond far more robustly than alveolar macrophages, which are continuously exposed to foreign particulates due to their *in situ* locale in the alveoli of the lung. The David McMurray research group published a 2008 report that supports our interpretation [77]. The McMurray paper suggests that alveolar macrophages, being constitutively activated by environmental artifacts, will exhibit an innately diminished inflammatory cytokine response to minimize damage to surrounding lung tissue. This may explain why Hartley alveolar macrophages were a superior model system in our experimentations (Figure 6).

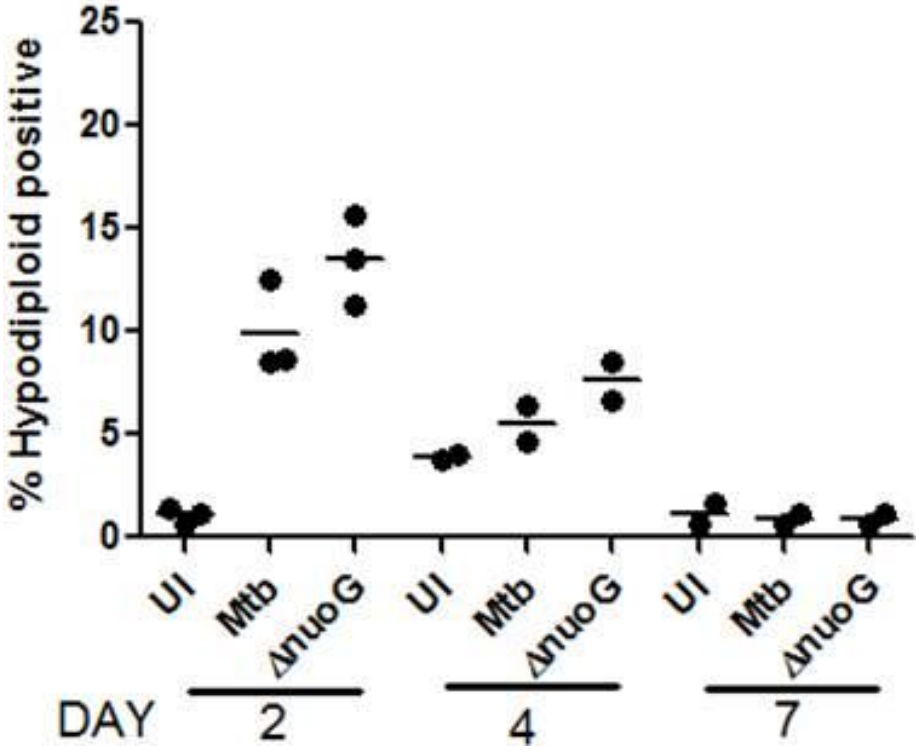


**Figure 18. Murine alveolar macrophage cell line (MH-S) is not a viable option for the study of Mtb-mediated suppression of host apoptosis.**
MH-S cells were infected with WT Mtb or Δ*nuoG* Mtb (a positive control for apoptosis induction) at an MOI of 5 for 4 hrs; uninfected (UI) control wells were included in all experiments. A chase of 2, 4 or 7 days followed. Cells were analyzed for percentage of apoptosis induction by hypodiploid labeling and flow cytometry. Individual values were obtained for each well and are graphed with the mean value indicated by a horizontal bar. Figure is representative of several experiments.

### 4.2.2 *Loss-of*-Gain-of-Function (LoGoF) screening approach to identify possible K20 GoF phenotype genes of Mtb

The *loss-of*-gain-of-function (LoGoF) genetic screen to identify anti-apoptotic genes of Mtb (see sections *Materials and Methods*-3.3 and *Results*-4.1.2) is a relatively novel approach; this screening technique was used for efficiency, and was employed due to the extensive growing time required for Mtb knockout generation and confirmation [160]. Understandably, the LoGoF screening approach is by no means the only secondary screening approach that could have been used to identity genes of interest in the K20 Mtb genomic region and corresponding GoF vector. However, former Briken lab member Dr. Serdar Gurses had previously generated and sequenced a sizable pool of LoGoF mutant clones (Figures 4 and 8; Supp. Table ST2), and it was assumed that employing these pre-assembled constructs to identify specific K20 genes of interest would have greater cost efficiency (from both time-invested and financial perspectives) than other secondary screening approaches. Additionally, we felt that the LoGoF screen would better identify *individual* genes critical to the K20 GoF phenotype. We believed LoGoF screening was ultimately a more efficient approach than alternative methods (such as a repetition of the K20 GoF screen with smaller, genetic subunits of the K20 region) in terms of our ultimate goal of specific-anti-apoptotic gene identification. Alternative GoF approaches may result in the same problems inherent to the initial GoF screen that identified the K20 region; namely, screening individual K20 genes in a second, "subunits of K20" GoF approach may have provided erroneous results as more than one of the K20 genes may have been responsible and/or required for the anti-apoptotic phenotype. LoGoF screening theoretically bypasses this issue and, assuming a lack of polar effects

resultant from transposon mutation, detects those individual K20 genes critical for the anti-apoptotic phenotype of interest.

#### 4.2.2.1 *Loss-of*-Gain-of-Function (LoGoF) screen in mc$^2$-155 background identifies possible K20 GoF phenotype genes of Mtb

The initial LoGoF screening was carried out in the Msmeg mc$^2$-155 background (Figure 9). The results were reproducible in four different large-scale screening rounds using the Msmeg model species and ultimately two LoGoF clones, sg*Rv2666* and sg*Rv2667*, were the highest inducers of host cell death. However, there was very little variation of differences between the highest and lowest inducers of cell death. This is clearly demonstrated in total difference of THP-1 death induced by the K20 positive control and the null-vector control, which amounts to a roughly 10% decrement (Figure 9). One of the primary reasons for these unimpressive differences may be the enormous intensity with which Msmeg induces apoptosis in host macrophages [168].

The Msmeg-THP-1 host-pathogen modeling system is a severely limited model, as the conditions to which Msmeg is subjected in an experiment such as this are far outside the normal life cycle of the nonpathogenic Msmeg; the bacteria's native environment is topsoil [51], a habitat far-removed from the caustic phagosomes of alveolar macrophages. The relative contribution of GoF vectors to Msmeg's suppression of host-apoptosis is likely insubstantial due to masking of the GoF phenotype by the bacteria's innate tendency to generate extreme host-apoptotic responses. Additionally, though PI staining (which is interpreted in a manner similar

to trypan blue exclusion) is a rapid readout for "cell death," it may not be the most accurate indicator of true apoptosis, and the statistical differences in any GoF or LoGoF phenotype may be masked by necrotic death as well. Though Msmeg LoGoF screening results were reproducible, the lack of strong statistical correlations and distinctions compelled us to repeat our LoGoF study in a second species, *M. kansasii*.

#### 4.2.2.2 LoGoF screen in *M. kansasii* identifies two possible anti-apoptotic genes of Mtb

The second round of LoGoF screening was carried out in the Mkan model species in order to validate the findings of the Msmeg study and to take advantage of the species' "cleaner phenotype" in terms of host apoptosis-induction. While anti-apoptotic GoF/LoGoF screening in the Msmeg background resulted in slight differences in host death induction between the highest and lowest inducers, screening for this phenotype in the Mkan background provided much cleaner resolution and a clearer picture of what K20 genes are, and are not, contributing to the suppression of host cell death. In terms of experimental efficiency, the robust statistical significance of results gained by studying the K20 anti-apoptotic phenotype in the Mkan background greatly compensated for the enormous speed but weaker statistical correlation of findings generated by our work employing Msmeg as a model.

The four LoGoF clones used for screening in Mkan (Figure 11), sg*Rv2665*, sg*Rv2666*, sg*Rv2667* and sg*Rv2668*, were chosen based on the initial findings of four repetitions of the Msmeg screen. As previously mentioned, the LoGoF clones

sg*Rv2666* and sg*Rv2667* (encoding transposon mutants of *Rv2666* and *Rv2667*/*clpC2*/*clpX'*) were consistently the strongest inducers of host cell death in all Msmeg LoGoF repetitions (sg*Rv2665* and sg*Rv2668* were included in the Mkan screen as border-gene controls for the gene-pair of interest), suggesting these genes were possibly responsible for conferring the K20 anti-apoptotic phenotype.

We found clear differences in the LoGoF-clone host-apoptosis induction with our Mkan experiments. TUNEL staining and flow cytometry indicated a statistically significant 30% or more increase ($p \leq 0.01$) in host-apoptosis in both of our LoGoF clones of interest, sg*Rv2666* and sg*Rv2667*, compared to the levels of host death induced by the original K20 GoF vector (Figure 10). At this point, we felt that the functional ablation of at least one of these genes (or possibly both genes if polar effects created by transposon disruption were not a factor) from K20 GoF vector eliminated the ability of the GoF vector to confer a protective anti-apoptotic response to typically high apoptosis-inducing species of mycobacteria. Furthermore, the control LoGoF clones, sg*Rv2665* and sg*Rv2668* did not induce significantly more host apoptosis than the K20 parent vector (Figure 10), further suggesting the validity of our results implicating *Rv2666* and/or *Rv2667*. The sum of these findings (looking at data generated by modeling in both Mkan and Msmeg) suggests that the LoGoF screening method is valid as an approach for the study and identification of anti-apoptotic genes of mycobacteria.

At the time of these findings, major Mtb annotation and investigative databases using *in silico* analysis and statistical correlations to study mycobacterial genomes suggested that the *Rv2666-67* gene-pair in question was quite likely a two-

gene operon and was co-regulated as such [175, 180]. This raised the question of whether the LoGoF phenotypes observed were due to one or both of these genes. It is possible that if these two genes truly lay in a co-regulated operon, then the insertion of a transposon into one of the genes may have resulted in polar effects, negatively affecting the expression of the partner gene. Though both the sg*Rv2666* and sg*Rv2667* LoGoF clones had a transposon interruption in a point that could significantly affect the functionality of the gene product (Figure 11, insertions at nucleotides 561 of 803 nt and 161 of 758 nt, respectively), it was fair to assume polar effects may be occurring due to the nature of transposon insertion and mutations [181, 182]. It was therefore necessary to employ a separate approach in order to conclusively establish which of these genes is ultimately responsible for the anti-apoptotic effects of the K20 genomic region.

### 4.2.3 *Rv2666* is an Mtb gene contributing to the K20 anti-apoptotic GoF phenotype

In an effort to identify the specific gene(s) responsible for the K20 phenotype, we moved forward with the characterization of possible anti-apoptotic roles for Rv2666 and Rv2667/ClpC2 separately. Simultaneously, it was important to validate our findings within Mtb itself. Our attention turned first to *Rv2666* (H37Rv nucleotide region 2,983,071-2,983,874, + strand), a hypothetical truncated transposase-like gene [161] of Mtb and the "upstream" gene of the hypothetical *Rv2666-67* operon. (It is important to note that at the time of initial experimentation with the LoGoF screens, these two genes were believed to lie together within a

hypothetical two gene operon [164]; however, more recent analyses, employing alternative analytical tools, have lowered the confidence of those initial predictions [171] and cast doubt on the validity of assigning of these genes to a shared operon.)

No literature of note has been published explicitly examining *Rv2666* at this time; very little literature has been published with regards to the transposases of Mtb beyond their use in clinical detection of the pathogen or phylogenetic analysis/genotyping of the Mtb complex [130, 131, 184, 185]. No currently circulated report has discussed Mtb transposases as contributing a possible role in virulence to the pathogen, and data linking bacterial transposases or insertion elements to anti-apoptotic phenotypes have not been published as of this writing.

#### 4.2.3.1 The *Rv2666* gene of Mtb and the Tn*Rv2666* transposon mutant: overview

It is accepted that it requires a substantial amount of time to generate a gene-deletion within Mtb [159, 160]. Compared to fast-growing mycobacteria like Msmeg [159, 160], it can take approximately 2 to 3 months to create and confirm a Mtb knock-out. As previously described, we obtained Tn*Rv2666*, a *Himar1* based transposon mutant of *Rv2666* in the CDC1551 genetic background of Mtb [158]. Transposon mutants from the TARGET project have been employed in genetic screens and characterization studies by other Mtb research groups [185, 187, 188] to an experimentally satisfactory end, generating consistent and reproducible results for investigators.

The TARGET project provided Tn*Rv2666* mutant has an insertion point that begins at nucleotide position 322 of 804 nt total (Supp. Figure S3); this disruption should, at the very minimum, prevent the final 60% of the gene product from being transcribed and translated into functional product. Incidentally, this final 60% of the *Rv2666* encodes a region possessing MULE (Mutator-like element) transposase-like homology [177]; MULE homology may indicate possible metal chelation and DNA-binding properties for the gene product [178]. The entirety of *Rv2666* seems to encode a truncated IS*1081* transposase insertion; IS*1081* is a 1,324 nt length insertion element that is exclusive to the Mtb complex (Mtb, *M. bovis*, *M. africanum* and *M. microti*, but not *M. bovis* BCG) and has been used to distinguish Mtb and *M. bovis* BCG in various clinical isolates from HIV patients in years past [184, 185]. The IS*1081* class element is also extremely stable relative to IS*986*, another major class of transposase insertion element found in Mtb. In fact, the 267-amino acid sequence of Rv2666 is completely conserved across all sequenced strains of Mtb, including both laboratory and clinical isolates [161]; five of these strains contain a synonymous SNP mutation for a single nucleotide position (H37Rv genome nucleotide position 2,983,873 + strand, an adenine to guanine substitution), and no other Mtb SNPs are presently known to exist for this gene [179].

Furthermore, *Rv2666* expression has been shown to be greatly upregulated following infection of macrophages [179]. This evidence, taken with the absolutely conserved peptide sequence of Rv2666 across all sequenced strains of Mtb, leads us to expect Rv2666 plays a major role in the survival of pathogenic Mtb. Whether this

role is directly or indirectly implemented by the pathogen remains to be seen, offering a potentially interesting avenue of research for future investigations.

#### 4.2.3.2 Loss-of-function (LoF) study confirms anti-apoptotic role for the *Rv2666* gene

Using the Tn*Rv2666* TARGET-mutant previously described, a loss-of-function (LoF) study was undertaken. The study used a low MOI infection of HMDMs with the Tn*Rv2666* mutant and a WT Mtb control; results from this experiment indicated that the presence of Rv2666 may be important for the suppression of host-apoptosis. These Tn*Rv2666* results corroborated the previous LoGoF data generated in the Msmeg and Mkan backgrounds.

Infecting M-CSF differentiated human macrophages with the Tn*Rv2666* mutant resulted in more than twice the level of induced host-apoptosis generated by infection with the corresponding WT strain (Figure 12). The trend of these findings was similar across several experiments that employed HMDMs cultured from unique donor monocytes, providing an additional level of genetic diversity and greater validation of these results. The evidence implicating *Rv2666* as an anti-apoptotic gene of the K20 region was thus far quite compelling. We were able to confirm these initial results via complete complementation of the mutant phenotype. This was accomplished by transforming Tn*Rv2666* with an episomal plasmid expressing *Rv2666* (cloned behind the gene's expected native promoter region) and repeating the HMDM infection (Figure 13).

We can ultimately conclude that Rv2666 plays a role in the suppression of host macrophage apoptosis and that this gene is at least partially responsible for the K20 gain-of-function phenotype. As an additional measure of validation, a clean *Rv2666* gene deletion mutant could be created in the H37Rv background, fulfilling the gold standard of Mtb genetic analysis [180]. H37Rv is the most commonly used laboratory strain of Mtb, while CDC1551, our Tn*Rv2666* background strain, comes from a clinical isolate [41] and is less prevalently employed in Mtb research.

Though both strains are employed for Mtb investigation, studies have suggested that CDC1551 induces an increased host inflammatory response relative to H37Rv as determined by secretion of pro-inflammatory cytokines [42] under both *in vitro* and *in vivo* infectious conditions. However, the inflammatory robustness of the CDC1551 isolate strain does not translate into more virulent colonization or amplified rate of growth relative to other strains of Mtb. Moreover, recent experimentation has revealed distinct differences in host transcription of immuno-linked genes and nitric oxide production when macrophages are infected with CDC1551 or HN878, another clinical isolate [181].

While the data of the aforementioned studies do not contradict our findings in any appreciable manner, subtle differences in host immune response to distinct strains of Mtb may affect the outcome of our experiments. These studies reiterate the importance of confirming our Tn*Rv2666* CDC1551 results with a clean deletion mutant of *Rv2666* in the H37Rv genetic background.

### 4.2.4 Relevant experimental design and controls for the identification of K20 anti-apoptotic genes

#### 4.2.4.1 Experimental design: differentiating host apoptosis vs. necrosis outcomes

More extensively on the issue of experimental design and controls employed in this dissertation, HMDM infections with Mtb described in this study were carried out for 4 hrs at an MOI of 5 (unless otherwise stated); this can be considered a relatively low MOI format [182]. Importantly, HMDM infections at "high" Mtb MOI of $\geq 10$ have consistently shown an induction of caspase-independent host macrophage death [101, 194, 195, 196] which closely resembles a necrotic host death outcome rather than the definitively apoptotic host-death of interest to our research. Specifically, Welin *et al.* demonstrated caspase-independent host death of HMDMs infected at MOI $\geq 8$ in a 2011 publication [101]; around the same time, Lee *et al.* published a report detailing atypical macrophage death at high MOI numbers [184].

To that end, we took several measures attempting to ensure observed host death was conclusively apoptotic in our studies. Beyond undertaking infections at a low MOI of 5, we employed apoptosis-specific cell death assays such as hypodiploid staining [185] and TUNEL labeling [186] throughout our anti-apoptotic gene investigation. Moreover, AK release in THP-1 cells (Supp. Figure S1b) revealed no significant differences between macrophages infected with WT CDC1551 and those infected with Tn*Rv2666*; this further validates our finding that Mtb lacking the *Rv2666* gene, as well as K20 transposon LoGoF mutants of *Rv2666* in the Mkan background, are specifically defective in the ability to inhibit host apoptosis.

#### 4.2.4.2 Experimental design: cytokine differentiation of HMDMs and host apoptosis outcomes

Much of our reported findings depend on the behavior of HMDMs following infection by Mtb. The manner of monocyte to macrophage differentiation has a bearing on the reported findings [59, 199]. For our work, initial optimization studies were carried out to determine a method of HMDM differentiation that would produce mature macrophages that could be used to accurately assess the ability of Mtb to suppress host apoptosis. It was important that the differentiated macrophages undergo Mtb-mediated cell death in a quantifiable and discernible manner, and that the model macrophages were sensitive to controllable variations in the MOI, strain and/or clone of Mtb employed as well as the duration of infection. Optimization studies with the K20 GoF vector and Mkan-null vector in both recombinant human M-CSF differentiated monocytes and recombinant human GM-CSF differentiated monocytes (Figure 19) suggested both cytokines would generate macrophages possessing the desired traits for studies involving host-pathogen interaction and apoptotic outcomes. However, for a yet-undetermined reason, monocytes differentiated with M-CSF consistently produced mature, $CD14^{+}$ macrophages more frequently than GM-CSF; thus M-CSF was employed as the preferred cytokine of monocyte differentiation in all subsequent work.

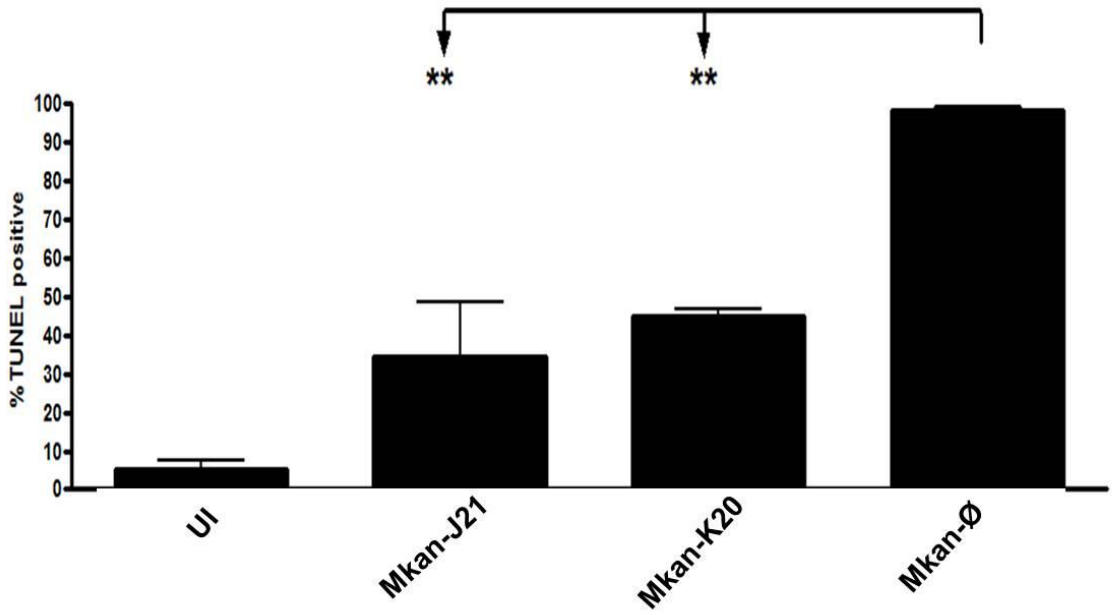


**Figure 19. GM-CSF differentiated HMDMs infected with GoF vector transformed *M. kansasii* exhibit K20 GoF phenotype.**
Human monocytes were differentiated to $CD14^{+}$ macrophage maturation by culturing the recombinant human GM-CSF (Peprotech) and off-the-clot human AB serum for 7 days. HMDMs were infected with Mkan-K20, Mkan-empty vector and Mkan-J21 [53, 109] as a positive control. A 4 hour infection was followed by a 2 day chase; unifected (UI) wells were included as controls. TUNEL staining and flow cytometry quantified total percentage of apoptotic HMDMs. (n=3). Error bars show ±SD. **p<0.01 (ANOVA and Tukey post-test).

Reports published by other research groups have suggested the particular method of cytokine differentiation used in the monocyte-to-macrophage differentiation process affects the outcome of subsequent bacterial infections [59, [187]. Furthermore, it has been reported [59, 66] that in many respects (surface markers, morphology, catalase production, etc.), human monocytes cultured with human GM-CSF generate a mature macrophage with properties similar to resident, human alveolar macrophages (the primary, hallmark host of Mtb), while co-culturing monocytes with human M-CSF produces a peritoneal-like macrophage. As with all *in vitro* host-pathogen modeling systems, a close approximation of clinical disease is the most for which a researcher can hope.

Additionally, several experiments were carried out in human THP-1 cell line and produced similar results when validated by visual inspection. An example of a TUNEL stained experiment can be seen in Figure S1a (Figure S1a courtesy S. Shah). These results suggest the Tn*Rv2666* pro-apoptotic phenotype may be consistently seen in multiple models of Mtb infection.

While repeating these experiments within a GM-CSF differentiated macrophage model system, as well as human alveolar macrophages, would seem to be an enticing proposition, a characterization of the anti-apoptotic role of Rv2666 under *in vivo* conditions would also be beneficial. Our work establishing a GoF phenotype for Mkan-K20 in guinea pig alveolar macrophages (Figure 6) suggests a viable and sensitive animal model may already exist [200, 201].

### 4.2.5 Potential role of a hypothetical transposase, *Rv2666*, in Mtb virulence pathways

To date, it has been noted that some transposase genes seem to play a beneficial role in certain bacterial organisms [190], with the general assumption that the transposase genes are functioning as promoters of genetic diversity and mutation in times of great environmental stress [122, 203]; this benefit generally seems to stem from stress induced promotion of well conserved, functional transposases. Also, transposase activity may create genetic diversity by insertion of the transposase into a novel location within the genome, ablating gene function or repressors/promoters of a gene, or having other modulating/regulatory effects upon an environmentally stressed bacterium.

More specifically, the hypothesis put forth most by transposase researchers is that organisms will continue to maintain "selfish" transposase genes that confer a benefit to the host; it is believed that these benefits are often a result of *indirect* regulatory effects. These transposase-resultant effects upon "host" genomes, though indirect, contribute to the survival of the organism thus fulfilling the mandates of selective pressure. In one example, a group working at Trinity College Dublin, recently noted that *E. coli* strains lacking the sigma factor RpoS are nonetheless able to adapt to a high-osmolarity environment by IS*10* insertion into the promoter for the otsBA operon, which alters the operon's expression from RpoS-dependent to RpoS-independent [191]. It seems that the transposase element ultimately grants its beneficial phenotype by allowing for (and increasing the rate of) successful adaptive mutations rather than directly creating this phenotype by its own devices. In another scenario, Rv2666 may be interacting with another gene product, perhaps even ClpC2

which seems to have some effect on the Il-1β secretion of host macrophages (see section 5.2.4), though our experiments show ClpC2 to be dispensable for Mtb-mediated suppression of host apoptosis.

Alternatively, Rv2666 may modulate the expression or function of another factor important in the Mtb suppression of host-apoptosis, perhaps acting as a transcription factor. The *Rv2666* gene encodes a region [179] possessing MULE (mutator-like element) transposase homology [178]. It has been suggested that these MULE transpose elements have a zinc finger homology and may indicate possible metal chelation and DNA-binding properties [178]. Furthermore, some functional gene products or transcriptional regulators may have evolved from MULE transpose precursors. While this phenomenon would likely be considered a novel finding in Mtb, the FAR1 protein, FHY3 protein and FAR1 related sequence (FRS) transcription factors have been well-established as regulators of gene transcription in *Arabidopsis* [205, 206] and several other plants, providing a biological precedent for transposase-to-transcription factor evolution.

### 4.2.6 *clpC2*/*Rv2667* is not an anti-apoptosis gene of Mtb

After confirming *Rv2666* as an anti-apoptosis gene of the K20 genomic region, our attention turned to characterization of the second gene identified by our LoGoF screens, *Rv2667*/*clpC2*/*clpX'* (Figures 9, 10). The *clpC2* gene of Mtb (H37Rv nucleotide region 2,983,896 to 2,984,654, + strand) is a hypothetical ATPase member of the Clp family of proteases [194]. The essentiality of the bulk of the Mtb Clp protease family for *in vitro* growth is well-established [137, 138]. Investigators

screening transposon mutant libraries have shown that Clp protease subunits ClpP1/Rv2561c and ClpP2/Rv2460c, ATPase subunits ClpX/Rv2457c and ClpC1/Rv3596c, and the chaperone ClpB/Rv0384c are all requisite for *in vitro* growth of Mtb. In the latter report [138], ClpC2 was found to be nonessential for *in vitro* culturing as several transposon-generated mutants of *clpC2* were able to proliferate under normal culturing conditions. We have been able to confirm those initial findings by the generation and confirmation (through genomic DNA and cDNA analysis) of a deletion mutant of *clpC2* in the H37Rv genetic background (Figures 14, 15 and Supp. Figure S2).

The *clpC2* gene sequence bears homology to the established Clp ATPases *clpC1* and *clpX*; *clpC2* has been alternatively annotated as a truncated version of both of these genes at various times past [175, 207]. While several reports regarding ClpX and ClpC1 and their expression regulation have been published in recent years [139, 140, 145], there is no literature explicitly characterizing *clpC2* or its gene product. However, some of the aforementioned studies have suggested that ClpC2 expression is not regulated as part of the ClgR (Rv2745c) operon. Several reports [151, 152, 153] have established the ClgR operon as a key factor in the Mtb stress induced response. In high-stress conditions, such as a bacterium being phagocytosed by an alveolar macrophage, the Clp protease activity of the intracellular pathogen is critical to the rapid elimination of aberrant and misfolded proteins in an ATP-dependent manner and thus essential for the survival of the bacterium. The lack of co-regulation with the other Clp family members suggested to us that ClpC2 may be an outlier of the

ClgR-linked stress response, and may play an alternative role in the well-being of Mtb.

In terms of our study, the *clpC2* LoGoF transposon mutant was repeatedly a "positive hit" in several rounds of both Msmeg and Mkan LoGoF screening (Figures 9 and 10, respectively). We felt that, rather than a direct link with the ClgR stress-response, ClpC2 may play a role in virulence by supporting the Mtb-mediated suppression of host-apoptosis. Additionally, *clpC2* was shown to be one of about 100 genes upregulated *in vitro* following a long period of anaerobic maintenance with sudden reaeration [152]. This study mimicked conditions very similar to what one would expect following transmission of Mtb into a new host, or transitioning from a latent to an active state of pulmonary TB, precisely when an anti-apoptotic response would be most desired by the pathogen.

#### 4.2.6.1 Generation of a *clpC2* deficient strain of Mtb, details and relevant issues

A *clpC2* deficient strain of Mtb was generated by homologous recombination in order to study the function of the gene. Specialized phage transduction was used to increase efficiency of the method [159]. Homologous recombination was specifically targeted to leave the first 58 and final 5 nucleotides of the gene intact within the chromosome to avoid disruption of the neighboring genes. The *clpC2* gene is coded for on the + chromosomal strand and there is no known or predicted overlapping gene or promoter regions that could be affected by the recombination event on the corresponding - strand.

Preliminary observations of WT H37Rv and Δ*clpC2* colony formation and morphology on 7H10 media plates revealed no noticeable differences. Deletion of the *clpC2* gene was confirmed by analysis of genomic DNA (Figure 14; Supp. Figure S2); this was further validated by RT-PCR to validate lack of gene expression (Figure 15).

Genomic DNA was used to confirm the successful deletion of *clpC2* in two ways; PCR amplification of small internal sections of genes of interest to determine the presence or absence of these genes, and Southern blotting which used a labeled probe to identify alterations to restriction enzyme patterns that would result from this targeted homologous recombination event. First, PCR of genomic DNA (plus episomal DNA in the case of the pMV261-based complement) was carried out using small primers that would amplify short, internal regions of *sigA* (as a PCR control), *clpC2* and the hygromycin resistance gene. Once the PCR products were visualized by agarose gel electrophoresis, the presence or absence of an amplification band can be correlated by the respective presence or absence of the gene in question. As seen in Figure 14, bands suggesting the absence of the *clpC2* gene but the presence of a hygromycin resistance gene could be seen in the Δ*clpC2* PCR product lanes; conversely, WT H37Rv genomic showed the presence of *clpC2* but no hygromycin resistance gene. Moreover, the complemented mutant strain demonstrated amplification banding that verified the presence of both the *clpC2* gene (the episomally provided complement copy) and a hygromycin resistance gene as expected. Due to the high G/C content of the Mtb genome and the relatively large

size of the hygromycin resistance insert cassette (3,672 nt), we were unable to amplify across the entirety of the insert.

As a second measure of DNA based confirmation of *clpC2* abrogation, Southern blotting was employed. A probe was created from the upstream portion (H37Rv nucleotide region 2,983,896 to 2,984,654, + strand) of the original allelic-exchange substrate vector used for the targeted homologous recombination event. The labeled probe was used to identify expected shifts in Van91I restriction enzyme patterns that would have resulted from recombination of the *clpC2* and the hygromycin cassette (Supp. Figure S2). The resultant Southern blot image confirmed the WT H37Rv and K20 control vector having an identical band indicating probe hybridization with a fragment roughly 6.3kb in size, while Δ*clpC2* demonstrated an expected absence of the 6.3kb band and presence of a heavy band approximately 3.5kb in size. However, unexpected smaller bands can also be seen in the image; this is likely the result of nonspecific binding of the probe, as this particular probe shares a portion of its nucleotide sequence with IS*1081* sequences, of which five independent regions exist in the Mtb genome. Redesigning this probe to avoid the transpose region would likely eliminate this background banding pattern.

Finally, RT-PCR was employed to suggest that RNA expression of *clpC2* had been completely ablated by the mutation. RNA was obtained from WT H37Rv, *ΔclpC2* and the pMV261-based complement. The purified RNA samples were used to generate cDNA and "reverse transcriptase null" controls were included for each sample to ensure purity. Primers targeted to *sigA* (a reaction control) and *clpC2* were

employed in the RT-PCR; the generated cDNA and purity-controls for each respective strain were used as templates. Figure 15 shows the results.

WT H37Rv and the episomally complemented Δ*clpC2* demonstrate transcription of *clpC2*, while the mutant, as expected, does not. Interestingly, the RT-PCR revealed that the complemented mutant seemed to express *clpC2* RNA at a much greater rate than WT Mtb; this is to be somewhat expected as the complementation plasmid employed (pMV261) includes a constitutive promoter and there may also be multiple copies of this plasmid in each Mtb bacterium. Taken with the previously discussed genomic validation of *ΔclpC2*, we can confidently assume that we generated a homologous recombinant mutant of *clpC2* in the H37Rv genetic background of Mtb.

### 5.1.6.2 LoF study of a *clpC2* deficient strain of Mtb

To our surprise, the infection of HMDMs with WT H37Rv and Δ*clpC2* consistently demonstrated no significant differences in host apoptosis between the strains (Figure 16); this lack of the expected Δ*clpC2* pro-apoptotic phenotype was also observed when infections were carried out in alveolar macrophages of Hartley guinea pigs (Figure 17), the guinea pig being the gold-standard of TB animal models [189]. These results imply that ClpC2 plays no striking role in the Mtb-mediated inhibition of host apoptosis. If this were true, it would contradict our initial hypothesis that there was an anti-apoptotic role for the gene based on the Msmeg and Mkan LoGoF data we generated. However, there are many plausible possibilities that may explain the discrepancy in our LoGoF and Δ*clpC2*-Mtb results.

### 4.2.7 Alternative hypotheses explaining *clpC2* LoGoF and LoF discrepancy

This subsection highlights possible reasons for the incongruous results between the our LoGoF screening results for *clpC2* that implicate the gene as playing a role in anti-apoptotic mediation by Mtb, and our LoF study results that suggest no apparent part for *clpC2* in this particular virulence tactic.

#### 4.2.7.1 Alternative hypotheses: Genetic redundancy

The evolutionary redundancy of mechanisms and pathways critical to the pathogen's survival may explain why we can attribute an anti-apoptotic effect in the LoGoF screens but the phenotype fails to appear in a LoF Δ*clpC2*-Mtb study. For more than a decade, numerous research groups have reported on and dissected the Mtb-mediated suppression of host-apoptosis [90, 161] with many unique mechanisms reported; there are two other known Clp ATPases encoded by the Mtb genome. A complex interplay of factors from both the host and the pathogen are clearly involved in a balancing act [117] not only in the host-pathogen host-cell death outcome, but in the formation of TB granulomas as well [208, 209].

In terms of the process of natural selection, it stands to reason that inhibition or interference of a single, specific point in one of these pathways (of pathogen or host) critical to survival, and subsequently the replication/reproduction of the organism, will likely have several redundant mechanisms that will counter this loss, especially where an ancient pathogen such as Mtb, which has evolved as a human-specific pathogen with countless generations of selection, is concerned. The genomic sequencing of several clinical isolates of Mtb has revealed at least five points of

mutations in the respective *clpC2* gene of various strains, leading to non-synonymous amino acid substations between strains [194]; the occurrence of non-synonymous substitutions that may affect protein function or efficiency (i.e., S120G, polar side-chain to nonpolar side-chain substitution) suggest that a fixed ClpC2 amino acid sequence is not a requisite for Mtb virulence and the protein may be expendable in its importance to the survival of Mtb in a clinical setting.

#### 4.2.7.2 Alternative hypotheses: *clpC2* is a marginal player in Mtb virulence

It is also possible that ClpC2 does, in fact, contribute to an anti-apoptotic effect in Mtb, but its effect exists as a marginal "downstream player" in its respective pathway and the ablation of *clpC2* affects no striking phenotypic shift in host-apoptosis outcome. This could explain why we can confer an anti-apoptotic GoF to nonpathogenic Msmeg and the opportunistic pathogen Mkan when the bacteria are transformed with the K20 genomic region of Mtb, a phenotype that is lost by the LoGoF transposon interruption of *clpC2*. We know from DNA sequence analysis that the *clpC2*-LoGoF clone (sg*Rv2667*) should disrupt functional gene product from being expressed; likewise, RT-PCR (Figure 15) confirms the lack of *clpC2* transcription in the Δ*clpC2*-Mtb strain. The incongruity of our observed host-apoptotic outcomes may be the result of a novel ability conferred to Msmeg and Mkan by transformation with the K20 GoF vector, an ability that is simply a downstream effector in Mtb. The differences in the evolutionary specialization and environmental niche [55, 210, 211, 212] of each of the mycobacterial species may be responsible for a novel phenotype.

#### 4.2.7.3 Alternative hypotheses: *clpC2* may be important in another virulence capacity

Finally, it is possible that ClpC2 has no direct effect on host-apoptosis outcomes whatsoever. The phenotype observed in our LoGoF screens could be simply an experimental artifact specific to that particular transposon mutant clone, however, we feel this is unlikely. A second LoGoF clone of *clpC2* (sg*Rv2667*.b) was also screened in the Mkan background (data not shown); the findings suggested an inability to suppress host-apoptosis in this *clpC2* transposon mutant as well. It is plausible that ClpC2 may be acting in another capacity (see section 5.1.4 and 5.2.4), possibly affecting a LoGoF resultant phenotype as a byproduct of its action. This potential for an alternative ClpC2 mechanism of virulence is further examined and discussed in the second portion of these reported findings.

# Chapter 5: Characterization of pathogenicity of *clpC2* abrogation mutant

The second portion of this dissertation details the characterization of a Δ*clpC2* mutant generated in H37Rv genetic background of Mtb. A focus is placed on identification of possible roles affecting Mtb virulence. As previously described, our characterization of Δ*clpC2* began as the result of an attempt to identify anti-apoptotic genes of the K20 genomic region of Mtb. Preliminary results from a LoGoF screen in Msmeg and Mkan suggested a potential role for ClpC2/Rv2667 in the mediation of an anti-apoptotic phenotype. However, further testing with a Δ*clpC2* mutant revealed no apparent role for ClpC2 in the suppression of host apoptosis.

Very little is known or published about this particular hypothetical Clp family ATPase gene. In order to further understand ClpC2, we wished to characterize the mutant previously generated in terms of basic fitness as well as virulence. We approached this goal by comparing WT Mtb to the mutant with several assays chosen to reveal these differences between the two strains. Additionally, we hoped our characterization of the *clpC2* gene might reveal the reason for discrepancy between our LoGoF and LoF results. Our hypothesis was that the Mtb *clpC2* gene plays a role in the virulence of Mtb; our findings are as follows.

## 5.1 Results: Characterization of pathogenicity of *clpC2* abrogation mutant

### 5.1.1 Altering *clpC2* expression has no effect on *in vitro* growth of Mtb in complete media, overexpression of *clpC2* in minimal media results in defective replication

Mutations of ATPase function in other bacteria have been shown to alter the ability of the organism to function properly in terms of growth defects *in vitro* [200]. The Mtb Clp protease proteolytic subunits ClpP1/P2, ATPase subunits ClpX and ClpC1, and a predicted chaperone (ClpB) are all known to be essential for *in vitro* growth of the pathogen [137, 138]. Additionally, the alteration of expression of the ATPase *clpX* was shown to effect a delayed rate of bacterial growth when strains expressing both decreased and elevated levels of ClpX were grown *in vitro* and compared to a H37Rv control [140]. Although the ATPase encoding *clpX* gene of Mtb has been found to be essential for *in vitro* growth, we were able to generate and confirm a *clpC2* (previously annotated as *clpX'* ) deletion mutant of H37Rv in complete 7H9 media. Thus, we have established that ClpC2 is not a requisite for the *in vitro* viability of Mtb. However, we did not yet know if altering the expression of the *clpC2* gene would affect the rate of Mtb *in vitro* replication.

In order to assess the importance of ClpC2 expression levels for the *in vitro* replication of Mtb, WT H37Rv, Δ*clpC2* and two versions of the complemented mutant (integrating pMV361-based complement and plasmid-based pMV261) were used to inoculate complete 7H9 media and Sauton's minimal media at bacterial concentrations equivalent to [$OD_{600}$ = 0.010], or 3.0 x $10^6$ bacteria/mL.

Results were graphed log-scale (semi-log scale) rather than a linear $OD_{600}$ format which is often employed in Mtb-publications. We noted no obvious

differences between the relative growth rates of WT Mtb and Δ*clpC2* mutant in the complete or minimal medias (Figure 20), suggesting the absence of ClpC2 does not play a substantial role affecting bacterial growth under these conditions.

Significant differences in the rate of bacterial replication were noted in one of the constitutively expressing *clpC2* complement strains in our initial results (Figure 20). The pMV261-based extrachromosomal plasmid complement demonstrated a slight lagging rate of growth during the experimental growth phase compared to WT, mutant and pMV361-based *attB* integrating complement in the complete media study. This lagging phenotype was amplified in the minimal media study (Figure 20b); additionally, the WT and Δ*clpC2* mutant had nearly identical growth curves in the same experiment.

Further testing of this phenotype (Figure 21) was employed to determine if the defect in replication was an artifact or due to the presence of the kanamycin antibiotic, included to maintain expression of the episomal plasmid. The initial experiment was repeated in complete 7H9 media, with additional controls chosen to establish whether the pMV261-complement was defective due to the added kanamycin antibiotic or if the phenotype could be attributed to the nature of this particular strain.

Figure 21 suggests all strains grew in a similar manner, regardless of the presence of kanamycin in the media. These results suggest that the observed rate of growth decrement was likely not due to the 40 µg/mL of kanamycin antibiotic in the media, included with the pMV261-based complement strain to maintain the extrachromosomal plasmid expressing *clpC2*, but rather the result of a defective

replication phenotype similar to the one observed following overexpression of Mtb ClpX [140]. From these studies, we conclude that ClpC2 abrogation has no obvious effect on the *in vitro* growth of Mtb in complete 7H9 or Sauton's minimal defined media, however, overexpression of the *clpC2* gene by an episomal plasmid with a *groEL2* constitutive promoter results in an clear replication defect when grown in Sauton's minimal media.

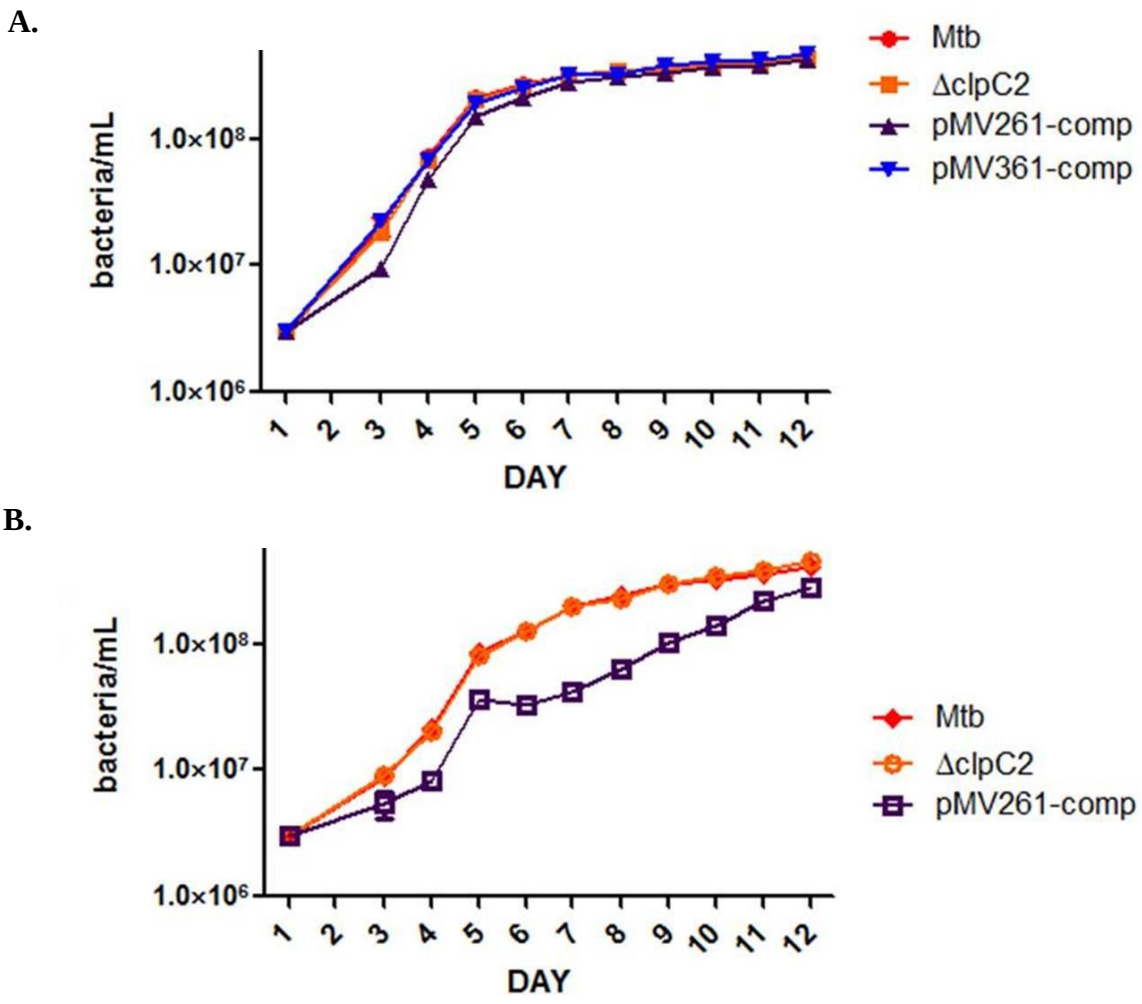


**Figure 20.** ***In vitro*** **growth curves of WT Mtb, Δ*clpC2* and two complements of Δ*clpC2* in complete and Sauton's minimal media.**
Triplicate inoculations of WT Mtb, Δ*clpC2*, and pMV261 (extrachromosomal plasmid, *media contains 40µg/mL kanamycin antibiotic to retain the plasmid) and pMV361 (*attB* integrating) complements of the mutant were made in **A**.) 7H9 and **B**.) Sauton's minimal medias at a concentration of [$OD_{600}$=0.010], or [3.0 x $10^6$ / mL]. Duplicate optical density readings at 600nm were taken every day for 12 days. Data is presented as means ± SD from duplicate readings of triplicate cultures (n=6).

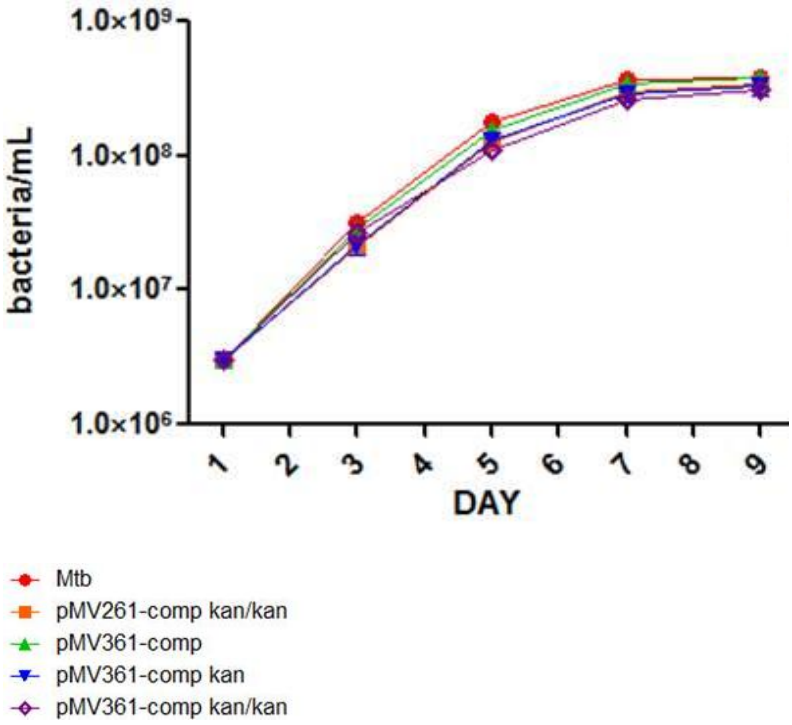


**Figure 21.** ***In vitro*** **growth curves of WT Mtb and complements of Δ*clpC2* in complete media for study of kanamycin inclusion effect.** Triplicate inoculations of WT Mtb and pMV261 (extrachromosomal plasmid) and pMV361 (*attB* integrating) complements of the Δ*clpC2* mutant were made in media at a concentration of [$OD_{600}$=0.010], or [3.0 x$10^6$/mL. *NOTE: "kan" annotation indicates a culture initially maintained in the presence of 40µg/mL of kanamycin then transferred into plain media lacking the antibiotic to study growth rates as a control; "kan/kan" annotation denotes a culture maintained in the presence of 40µg/mL of kanamycin then also grown in kanamycin containing media lacking the antibiotic to study comparative growth rates as a control; both "Mtb" and "pMV361-comp" cultures were initially maintained and used for this study in plain media with no antibiotic. Duplicate optical density readings at 600nm were taken every other day for 9 days. Data is presented as means ± SD from duplicate readings of triplicate cultures (n=6).

### 5.1.2 ClpC2 plays no salient role in mediating late-stage *in vivo* host necrosis

Having established that Δ*clpC2* plays no essential role in host apoptosis suppression by Mtb (see section 4.1.7), we sought to determine if the gene could possibly be contributing to other forms of cell death manipulation.

To that end, HMDMs were infected at MOI of 3 with WT Mtb and the Δ*clpC2* mutant strain. Infections proceeded for 4 hrs; then the HMDMs were washed twice with sterile PBS to remove extracellular bacteria, and chase media was added. Infections were allowed to progress for 3 or 10 days; experimental endpoints were specifically chosen to model late-stage *in vivo* infections of cultured macrophages. At days 3 or 10 post-infection, cell-free infection media supernatants were collected and examined for Mtb-induced necrosis of HMDMs. Toxilight™ assays were employed to quantify levels of adenylate kinase (AK) release. Levels of host cell necrosis in the infections were assessed by comparison of fold change relative to AK release in uninfected macrophages and total lysis controls. Data pooled from multiple experiments is shown in Figure 22. Lysis controls demonstrated similar levels of AK release at both time points (indicating little background atrophy of host cells) and AK release by uninfected macrophages was only slightly greater at the later time point.

These controls suggest that observation of infected HMDM-AK release is a feasible measure of Mtb-mediated host-necrosis at these time points. WT Mtb and Δ*clpC2* infected HMDMs had no significant differences in terms of AK release at either day 3 or day 10 post-infection. All infected macrophages were significantly lower in AK release than the total cell lysis controls at both time points as well. However, at both day 3 and day 10 time points the level of necrotic induction was

slightly higher in the mutant infected HMDMs. Compared to the uninfected cells, H37Rv WT infected an approximately 2-fold difference in AK release, while Δ*clpC2* infected macrophages saw a roughly 3-fold difference, though these variations had no statistically significant difference when compared directly to each other (1290 ± 110 versus 1930 ± 254 relative light units (RLUs), respectively).

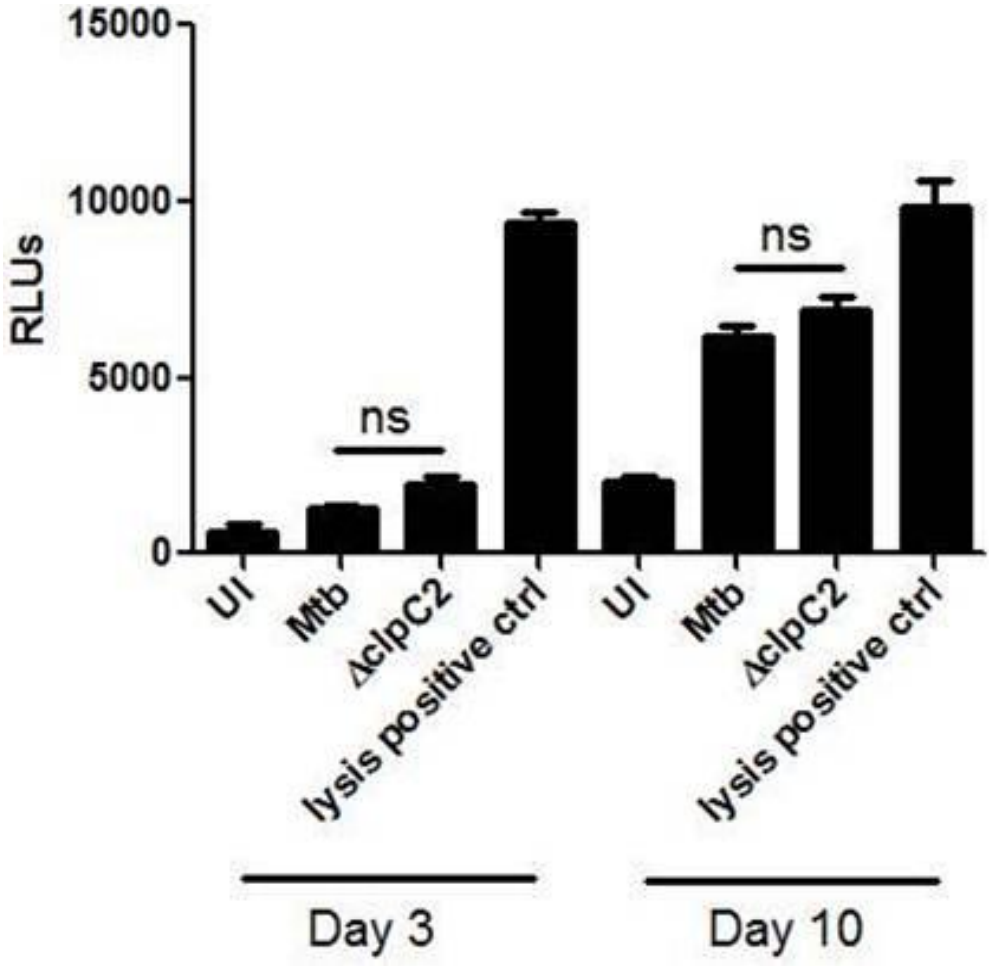


**Figure 22. No significant differences in necrosis of HMDMs infected with WT Mtb or Δ*clpC2* at days 3 and 10 post-infection.**

HMDMs were infected with WT or Δ*clpC2* Mtb at MOI of 3 for 4 hrs; uninfected (UI) HMDM wells were included for all experiments. Values are given in relative light units (RLUs). Triplicate wells are shown; duplicate measures were collected from each well; triplicate measures were taken for a single lysis control well for each day (n=6 for samples; n=3 for lysis control). Error bars represent ± SD. Statistical analysis employed ANOVA with Tukey post-test. Significance bars compare Mtb to Δ*clpC2* at days 3 and 10, respectively. Data is pooled from separate experiments employing macrophages derived from the monocytes of two unique donors per time point.

WT infection induced 6164 ± 263 RLUs and HMDMs infected with Δ*clpC2* saw a generation of 6882 ± 401 RLUs at day 10. Meaning that by day 10 post-infection, overall necrotic induction had significantly increased in both strain-sample sets; however, the slight difference in the degree of AK release observed at the day 3 time point was further diminished.

Taken as a whole, the data suggests indicates that both strains induced HMDM necrosis similarly at late-stages of Mtb infection; should a difference in necrosis induction exist between the strains, it is found earlier in the course of infection. The described day 3 differences in WT and mutant RLU values are not statistically significant; however, the marginal differences indicated to us that ClpC2 may play a role in other virulence mechanisms at earlier time points. These alternative roles suggested that mechanisms that might have an effect upon less regulated forms of host cell death, such as manipulation of cytokines affecting the host inflammasome response, thus having an indirect and slight effect upon AK release by the Δ*clpC2* mutant. Ultimately, these experiments suggest that ClpC2 does not play any overwhelming role in the manipulation of host necrosis by Mtb.

### 5.1.3 ClpC2 has no noticeable effect on *in vivo* replication of Mtb

While we have shown *clpC2* is not essential for *in vitro* growth (but overexpression may cause a growth defect in Sauton's minimal media), we wished to see if altering the expression of this particular Clp family member would adversely affect *in vivo* survival and replication of Mtb due to the greatly added stress of the intracellular environment.

It is well-established that many of the Mtb Clp family of proteins (including both ClpX and ClpC1 ATPases), ClpP1,P2 protease subunits and the chaperone/endopeptidase ClpB are required for *in vitro* growth of Mtb [137, 141, 139]; moreover ClgR, which controls a Clp stress response regulon, has been shown to be critical for a mediating an infection desirable for the pathogen following phagocytosis [151]. While *clpC2* does not seem to be a member of the ClgR-regulon [153], its strong homology to *clpX* and *clpC1* warranted investigation of whether it might be important for *in vivo* survival and replication following macrophage phagocytosis. Likewise, observation of colony forming units (CFUs), produced by infection of HMDMs and collected at days 3 and 10 post-infection, revealed a statistically insignificant CFU variation between the WT Mtb, Δ*clpC2* and the pMV261-based complement of the mutant at these days. At day 3 post-infection CFU values were $1.5 \times 10^6 \pm 0.4$ bacteria/mL for the WT, $1.31 \times 10^6 \pm 0.2$ bacteria/mL for Δ*clpC2* and $1.6 \times 10^6 \pm 0.1$ bacteria/mL for the complemented mutant; all CFU values at day 3 post-infection have no significant differences. At day 10 post-infection, CFU values were $9.49 \times 10^6 \pm 2.86$ bacteria/mL for the WT, $7.6 \times 10^6 \pm 0.7$ bacteria/mL for Δ*clpC2* and $7.7 \times 10^6 \pm 0.6$ bacteria/mL for the complemented mutant; all CFU values at day 3 post-infection have no significant differences. Furthermore, CFU counts revealed all HMDMs were similarly infected with the three strains at day 0; this control established that any future observed CFU variances between strains would not be due to unexpected MOI differences.

Figure 23 ultimately indicates the functional deletion of *clpC2* has no conspicuous effect upon *in vivo* bacterial survival or replication. Taken together, the

data generated by these experiments suggest ClpC2 does not play a significant role in Mtb-coordinated necrotic host cell death induction and subsequently, its ablation has no obvious effects on survival and/or replication of the pathogen.

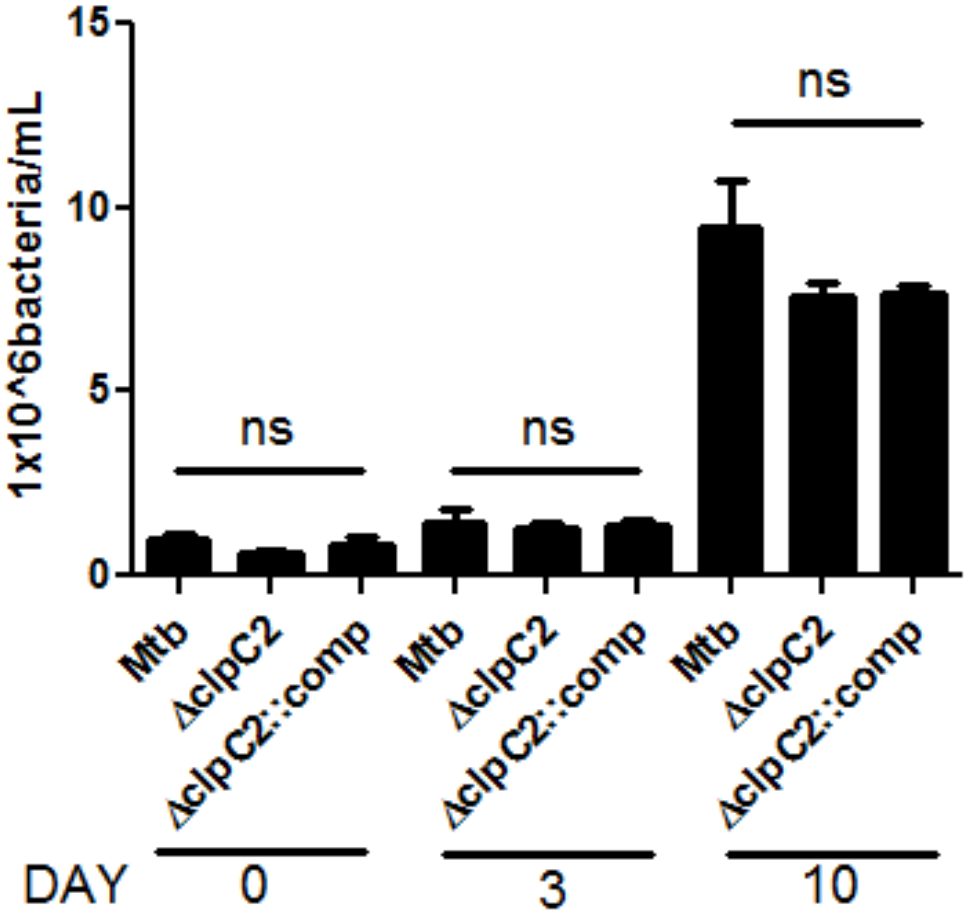


**Figure 23. No significant differences in CFU counts during early and late-stage HMDM infection with WT Mtb, Δ*clpC2* and complement.**

HMDMs were infected with the three listed strains of Mtb for 4 hrs at an MOI of 3. Macrophages were lysed and colony forming unit (CFU) dilutions were made and plated on 7H10 media plates. Error bars represent ± SD. Statistical analysis employed ANOVA with Tukey post-test. Data is pooled from separate experiments employing macrophages derived from the monocytes of two unique donors (n=4).

### 5.1.4 ClpC2 has no role in altering TNFα secretion by HMDMs, but *clpC2* deletion elicits a significant increase in host Il-1β release

Inflammatory cytokines are known to be a critical factor modulating host response to infection by Mtb. Tumor necrosis factor-α (TNFα) has previously been shown to be important for granuloma formation [165, 166]. TNFα-defective mice are exceptionally sensitive to Mtb infection and experience a high degree of extra-pulmonary dissemination of the pathogen that is not seen in immunocompetent mice [203]; a similar phenotype can been reported by investigators who manipulate *in vivo* concentrations of TNFα [166, 168, 169]. Also, recent reports have indicated an important role for TNFα in preventing active TB outbreak in immunocomprised patients and those treated with anti-inflammatory compounds [19, 170, 171]. Mtb mutants such as Δ*oppD* have all been shown to have altered inductions of TNFα by infected macrophages [208]. Another inflammatory cytokine, interleukin-1β (IL-1β) also plays a critical role in the mediation of host response to Mtb infection [173, 174]. IL-1β receptor (r) null mice infected with Mtb demonstrate a greater susceptibility to the pathogen; relative to a WT mouse, this IL-1r mutant mouse will be unable to efficiently contain the bacteria and experience diminished survival [210].

Given the importance of Clp protease family members in high-stress conditions as Mtb experiences during host infection and colonization, we wished to see if altering ClpC2 expression levels alters host inflammation response. To study this, HMDMs were infected with relevant strains of Mtb; the hallmark pro-inflammatory cytokines TNFα and IL-1β secreted into the infection supernatant were subsequently quantified by ELISA.

In order to examine this potential effect, HMDMs were infected with H37Rv,

Δ*clpC2* and the complemented Δ*clpC2* at MOI of 3 for 4 hrs; this was followed by a 24-hour chase period, after which the infection supernatants were collected for analysis by ELISA. The results of two independent experiments can be seen in Figure 24.

Host TNFα release had mean values of 263.6 ± 21.1 pg/mL, 309.9 ± 22.5 pg/mL and 293.9 ± 24.8 pg/mL for WT Mtb, Δ*clpC2* and complement, respectively. HMDMs infected with the Δ*clpC2* strain secreted significantly more TNFα than was produced by the uninfected controls (207.9 ± 12.3 pg/mL), while there were no significant differences in WT Mtb and uninfected macrophage TNFα release. There were no significant differences in host-TNFα secretion among any of the three strains used in the infections, leading us to conclude that ClpC2 has no obvious role in the Mtb modulation of host-TNFα secretion.

Yet, a statistically significant difference ($p \leq 0.001$) in host IL-1β secretion by infection with WT Mtb or Δ*clpC2* was observed. HMDMs infected with WT Mtb, Δ*clpC2* and the complemented mutant induced 4.7 ± 2.7 pg/mL, 61.1 ± 6.4 pg/mL and 19.9 ± 4.7 pg/mL, respectively. Uninfected HMDMs did not release IL-1β at a detectable concentration by our assay methods. Mtb incapable of expressing ClpC2 generated a 13-fold greater induction of host IL-1β release than WT Mtb. We were also able to partially restore the mutant phenotype to WT Mtb induction levels by complementation of the mutant with a pMV261 plasmid expressing ClpC2. Our results suggest *clpC2* plays a noticeable role in modulating secretion of host IL-1β, but not TNFα.

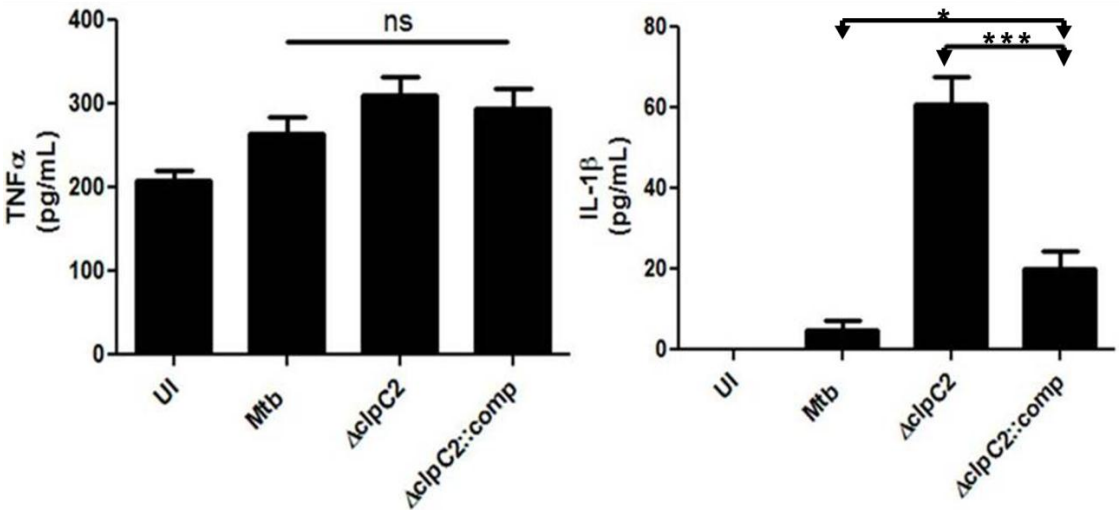


**Figure 24. Host secretion of cytokines TNFα and IL-1β is differentially affected by infection with WT Mtb, Δ*clpC2* and complemented mutant.**
HMDMs were infected with WT H37Rv Mtb, Δ*clpC2*, and the pMV261-based complemented mutant at MOI of 3 for 4 hrs; uninfected (UI) wells were included in all experiments. Supernatants were collected at 24 hrs post-infection and the amount of secreted TNFα and IL-1β was simultaneously assessed by ELISA. Values represent 3 wells per condition, with 3 replicates per well measured. Data is pooled from two experiments, with macrophages from a unique donor for each experiment (n=18). Error bars represent ± SD. Statistical analysis employed ANOVA with Tukey post-test. Significance bars compare (A) induction of TNFα release by all three mycobacterial strains and (B) Mtb vs. Δ*clpC2*:: complement (*, $p < 0.05$) AND Δ*clpC2* vs. Δ*clpC2*::complement (***, $p \leq 0.001$).

## 5.2 Discussion: Characterization of pathogenicity of an Mtb *clpC2* abrogation mutant

The intracellular regulation and recycling of aberrant and misshapen proteins by protease activity is absolutely essential for the survival of all organisms. Protease importance is even more readily apparent in pathogens, such as Mtb, that spend a significant portion of their life cycle dealing with the ramifications of phagocytosis by alveolar macrophages and subsequent acidification of the host phagosome. The activity of the Clp proteases of Mtb is an essential part of the organism's arsenal for dealing with the relatively high-stress conditions of the intraphagosomal space [153].

Investigators employing transposon site hybridization (TraSH) to study Mtb have previously shown that the Clp protease subunits ClpP1/Rv2561c and ClpP2/Rv2460c, ATPase subunits ClpX/Rv2457c and ClpC1/Rv3596c, and ClpB/Rv0384c are all essential for the *in vitro* growth of Mtb [137]. Additionally, studies examining the Clp ATPase subunits ClpX [140] and ClpC1 [139, 145], and the Clp proteolytic subunits [141, 142] clpP1and clpP2 have all provided additional evidence supporting the essentiality of these genes in Mtb. Incidentally, the Mtb genome encodes three hypothetical ATPase subunits: the aforementioned *clpC1* and *clpX* which are both required for *in vitro* growth of the bacteria, and *clpC2*/*clpX'*/*Rv2667* (H37Rv nucleotide region 2,983,896 to 2,984,654, + strand; 252 amino acids), a hypothetical ATPase which prior studies have deemed likely dispensable for *in vitro* bacterial replication [138]. Our generation and confirmation of a *clpC2* deletion mutant of H37Rv has confirmed the dispensability of the gene for *in vitro* growth of Mtb within complete 7H9 media; however, this does not preclude ClpC2 from contributing to a survival or virulence benefit in Mtb.

To create a *clpC2*-specific deletion mutant, a targeted homologous recombination was employed with a crossing-over event that replaced the gene with a hygromycin resistance cassette (previously described in section 3.2.1and Figure 3).

### 5.2.1 Abrogation of *clpC2* has no effect on *in vitro* growth in complete or defined media; overexpression of the gene in minimal media generates an observable growth defect

Reverse genetic characterization of bacterial mutants will often begin with an examination of potential *in vitro* growth defects. This establishes a working baseline of understanding for any phenotypes that may arise with future characterization studies. In that respect, we examined *in vitro* growth rates of Mtb with regards to altered expression of the *clpC2* gene in both complete 7H9 media and Sauton's minimal media. Incidentally, the Mtb gene *clpX* has been shown to affect the rate of bacterial division when expression of this gene is significantly altered [140], especially when it is overexpressed. The authors of the study suggest the growth decrement is due to varied levels of ClpX expression giving rise to an alteration of a precise stoichiometric relationship between ClpX and FtsZ, ultimately leading to irregular cell division. Additionally, it is known that manipulations of other Mtb Clp family members demonstrate growth defects in their respective strains when the expression of the Clp-gene was significantly altered [140, 141, 142]. We wondered if altering the expression of the *clpC2* gene (formerly annotated as *clpX'*) would produce a similar phenotype.

Our studies initially found a distinct difference in the growth rates of Mtb (Figure 20) when the gene was overexpressed by a pMV261 plasmid. The

overexpression of the *clpC2* gene results from being carried on a cytosolic plasmid, with expression driven by a constitutive *groEL2* promoter (see RT-PCR comparison in Figure 15). A follow-up study designed to verify these initial results and control against possible bacterial growth defects attributable to inclusion of the kanamycin antibiotic in the growth media was implemented (Figure 21). This experiment employed the *attB* site-integrated *clpC2* complement (the pMV361-based complement) and the plasmid-based pMV261 complement in a series of controls to demonstrate whether the observed *clpC2* "overexpression phenotype" was attributable to inclusion of antibiotic, but rather was likely an artifact of the pMV261 grown in minimal media; further study (preferably in Sauton's defined media) will better establish the true reason for this defect. Finally, RT-PCR confirms that the Δ*clpC2* mutant is not expressing RNA to generate functional product (Figure 15), thus this abrogation mutant is "clean" and the lack of phenotype may be accepted at face-value. From the data taken as a whole, we may assume that the total absence of ClpC2 expression has little bearing on *in vitro* replication of Mtb in 7H9 or minimal media; however, as in the case of ClpX, overexpression of the hypothetical ATPase can result in a substantial growth defect.

Dziedzic *et al*. suggest that the overexpression of ClpX leads to a growth defect in Mtb due to an alteration in the precise stoichiometric relationship (1 ClpX : 2 FtsZ) that exists between the ATPase and FtsZ, limiting the ability of FtsZ to properly assemble and form the Z-ring essential for cell division [140]. It is possible that ClpC2 also interacts with FtsZ in a stoichiometric manner and expression leads to a phenotype similar to the one observed by Dziedzic and colleagues. However, the

Dziedzic publication suggested the N-terminal region of ClpX was important for interaction with FtsZ [140]; vtBLAST comparison of Mtb ClpX and ClpC2 suggests no obvious homology between the two proteins.

Alternatively, overexpression of a possible ATPase such as ClpC2 is quite likely an energetic drain on Mtb; when this particular strain of Mtb is further taxed by growth in Sauton's minimal media, the burden of the overexpressing ClpC2 plasmid is detrimental to normal bacterial replication. This may be why a *clpC2*-pMV261 complement demonstrates an observable defect in minimal defined media, but is not seen when the strain is cultured in complete 7H9 media. Further studies are needed to conclusively establish if one of these hypotheses is correct. However, we can say that ClpC2 is entirely dispensable for *in vitro* growth of Mtb in both complete and minimal medias; it may be that ClpC2 is made redundant by the presence of ClpX or other factors.

### 5.2.2 ClpC2 plays no salient role in mediating late-stage *in vivo* host necrosis manipulation

Aside from a role in suppressing host apoptosis, studies have shown that virulent mycobacteria will actively promote an non-apoptotic, necrosis-like death of host macrophages [100] and dendritic cells [211]. It is believed that this Mtb-mediated host death is akin to necrosis in that it lacks the bactericidal effect of host apoptosis and allows the pathogen to migrate to surrounding tissues, immensely benefiting the bacteria [162].

One such mechanism employed involves Mtb disruption of the host's plasma membrane. Host repair of this damage is prevented by Mtb stimulated production of $LXA_4$. $LXA_4$ then blocks host production of $PGE_2$, a requisite compound for initiating the lysosome-mediated repair of the cellular membrane [100]; this quickly leads to host necrosis and pathogen dissemination. Additionally, ESAT-6 is an Mtb secretion that has been shown to be critical in the induction of host necrosis by way of inflammasome activation [99, 214, 215]. ESAT-6 is an early infection product of Mtb, likely secreted during times of high bacterial stress and has been linked to dose-dependent lysis of pneumocytes [214]. Concordantly, Mtb will greatly upregulate transcription of Clp proteases by way of a ClgR-mediated response in times of high stress [108, 151, 152]. Expression of *clpC2* RNA seems to be largely unaffected by this putative regulon [153]. However, *clpC2* expression is upregulated in times of starvation (5-fold [215] and 8-fold [216] ) induced stress and was shown as one of about 100 genes upregulated following reaeration from a hypoxic state [152]. These are conditions one might expect after a long period of latency and sudden reaeration; such events will immediately precede the spread of Mtb from a maintained granuloma to new tissues in the host or may result in the aerosolized infection of an entirely new host upon cavitation of a granuloma. Upon stable infection of new macrophages, the pathogen will likely seize the initiative and quickly attempt to induce host necrosis upon infection by the aforementioned methods, propagating itself even further. We wondered if there existed a yet undetermined role for ClpC2 in modulating host necrosis, and subsequent survival and/or replication outcomes.

A low MOI infection of HMDMs was carried out to identify any significant differences between Mtb-mediated necrosis (as measured by AK release) at 2 separate time points. The chosen time points represent early (3 days post-infection) and later (10 days post-infection) *in vivo* infection models, approximating similar mycobacteria-mediated host-necrosis [217]. Furthermore, in our experience, culturing HMDMs for time periods beyond 10 days following infection will result significant death of uninfected macrophages and a lack of observable differences in infected HMDMs relative to lysis controls (data not shown). Also, the MOI of 3 was employed in this study to avoid any potential for high-MOI induced necrosis [101, 195, 196] an oft-observed phenomenon that would potentially mask any ClpC2 necrosis-mediating phenotype of interest.

As seen in Figure 22, there were no statistically significant differences for WT Mtb or Δ*clpC2* in terms of induced host necrosis at either time point. However, relative to WT a slight elevation in the degree of AK release in was seen in the Δ*clpC2* infected macrophages at 3 days following infection (compared to uninfected wells, 2-fold and 3-fold higher necrosis inductions, respectively). This effect was almost entirely diminished by 10 days out, and even at its third day peak the phenotypic differences in WT and Δ*clpC2* are not statistically significant. We conclude that there is no obvious or overwhelming role for ClpC2 in promoting host necrosis. The minimal difference in AK release at day 3 post-infection may indicate a slight discrepancy in the MOI for the respective bacteria. Alternatively *clpC2*, often annotated as a hypothetical gene with possible roles as an Mtb ATPase or chaperone [180, 207] acting in any number of metabolic pathways, may have a marginal,

possibly indirect, effect on the bacteria's ability to mobilize a pro-host necrosis response at maximum efficiency during early infection.

### 5.2.3 Δ*clpC2* shows no difference in intracellular survival compared to WT Mtb or complemented mutant

As another measure of potential virulence, a role for ClpC2 in promoting survival or replication of the pathogen was studied. Several experimental infections of HMDMs with relevant Mtb strains were carried out; infection supernatants macrophage lysates were collected at days 3 and 10 post-infection. CFUs were subsequently calculated for each sample; pooled results are shown in Figure 23. All zero-hour CFU controls taken to establish initial infection consistency were statistically similar, indicating that the bacterial load was equitable in for all 3 strains used in the infection.

The lack of significant differences in CFUs between WT, Δ*clpC2* and the complemented mutant at both early (day 3) and late (day 10) post-infection time points studied suggests that there is no essential role for ClpC2 survival or replication under these particular *in vivo* conditions. These results indicate that in the *clpC2* gene is dispensable for not only *in vitro* growth of the pathogen, but is also non-requisite for Mtb replication within the much greater *in vivo* stresses of intra-macrophage phagosomes.

### 5.2.4 Mtb *clpC2* has no apparent role in altering host TNFα secretion, but deletion elicits a significant increase in host Il-1β release

ClpC2 was recently identified as one of roughly 100 Mtb genes upregulated by reaeration following an extended period of hypoxia [152]. These conditions approximate what an Mtb bacterium might encounter upon a sudden shift from a latent to an active TB disease state, perhaps following the cavitation of a granuloma. The link between the hallmark inflammatory cytokines, TNFα and IL-1β, and formation and maintenance of a granuloma is well-established [166, 174, 220]. Given the clear link between granulomatous containment and hypoxia [219], we wished to study a potential role for Mtb ClpC2 in effecting a change in host inflammatory cytokine secretion.

Our results suggested that Mtb ClpC2 may play some role in the Mtb response to inflammatory cytokines (Figure 24). We saw statistically significant differences ($p \leq 0.001$) in IL-1β secretion by HMDMs infected with either WT Mtb or Δ*clpC2* Mtb, but observed no significant differences in host-induced TNFα secretion between the strains. The HMDMs employed in these experiments originated from the monocytes of unique donors, and the collected infection supernatants were split to analyze TNFα and IL-1β release separately; the TNFα and IL-1β ELISAs were run in tandem. Also, the cytokine standards worked quite well for all experiments. Linear correlation values of $R^2 = 0.99$ were obtained for each set of standards, suggesting variation due to technical issues were likely inconsequential for the data readout, and these reproducible discrepancies in host cytokine induction were not produced in error.

Moreover, the IL-1β we observed was the mature, cleaved and secreted form, rather than the constitutively present and intracellularly maintained pro- IL-1β form

of the cytokine that may have escaped from the host by way of necrosis [61]; Figure 25 presents a representative sample of our infected macrophages and establishes that there are no significant differences in necrosis, as measured by AK release, generated by any of our three strains of Mtb. Finally, though the reported concentration of IL-1β may appear low relative to the TNFα concentration from the same supernatant, the values obtained are in complete agreement with a very similar study published in *PLoS One* of 2011 [101]. We therefore feel that our results are valid and interpreted them as such.

In the HMDM-Mtb host-pathogen model, the deletion of the Mtb *clpC2* gene leads to an approximately 13-fold increase in host IL-1β secretion relative to WT Mtb infected macrophages; additionally, we achieved partial, but statistically significant, complementation of the mutant back to WT induction levels ($p \leq 0.05$; WT versus complement) (Figure 24). The levels of host TNFα induction were statistically similar for all three strains of Mtb (Figure 24). Perhaps the most intriguing interpretation of this difference in inflammatory cytokine secretion is that ClpC2 may affect Mtb virulence or survival pathways that are specifically tailored to manipulate host IL-1β secretion; alternatively, Δ*clpC2* may act as a broad-range mechanism altering numerous pathways and ultimately producing a largely defective Mtb strain which induces host IL-1β due to a general lack of fitness. However, in terms of *in vitro* growth in both complete and minimal media, *in vivo* survival and replication, host apoptosis suppression and Mtb-mediated necrotic induction, we have established that Δ*clpC2* behaves quite similarly to WT Mtb, suggesting a mutation that may act in a specific, limited capacity.

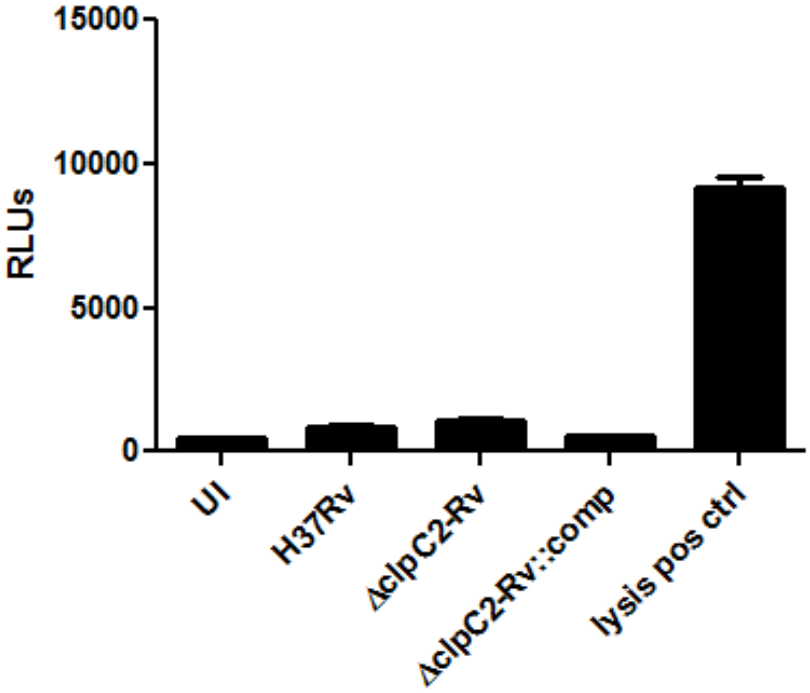


**Figure 25. Necrosis of HMDMs at 24 hours post-infection: a quality control experiment for IL-1β ELISA results.**

Necrosis was not observed and no significant differences were detected between any of the experimental groups, thus providing assurance to the quality of the observed IL-1β results (Figure 2). HMDMs were infected with WT, Δ*clpC2* or complement mutant strains of Mtb at MOI of 3 for 4 hrs; uninfected (UI) control wells were included in all experiments. Values are given in relative light units (RLUs). Triplicate wells shown; triplicate measures from each well; triplicate measures were taken for a single lysis control well for each day (n=9 for samples; n=3 for lysis control). Error bars represent ± SD. Statistical analysis employed ANOVA with Tukey post-test. Data is a representative experiment employing macrophages derived from the monocytes of a single unique donor.

#### 5.2.4.1 Potential for a ClpC2 role in affecting host IL-1β secretion

If ClpC2 is truly specific to pathways involving Mtb-mediated manipulation of host IL-1β activation, Δ*clpC2* will be quite useful in the characterization of these virulence mechanisms. Few Mtb mutants affecting host IL-1β secretion have been reported to date. A 2011 paper published in *The Journal of Immunology* showed that ESX-1 and ESX-5 virulence factor mutants of Mtb do not induce IL-1β release, and this phenotype could be complemented so that host IL-1β secretion was restored [220]. The same paper demonstrated that this secretion defect was limited to ESX-1 in *M. marinum*, which suggests Mtb has multiple IL-1β modulating systems to influence host inflammasome activity. Furthermore, ESAT6 of Mtb has been identified as a powerful generator of host inflammasome, and IL-1β release, response [212]. However, these are all virulence mechanisms with broad, large-scale effects. In terms of genetic analysis and the characterization of complex pathogen-host-cytokine induction interactions, employing these mutants as one's tools may be like using a using a hammer where a scalpel is preferred. Additionally, all of these reported mutants suppress host IL-1β induction. If the observed Δ*clpC2* phenotype, which induced IL-1β secretion in HMDMs, is indeed valid (and the results we describe are reproduced by others) then *clpC2* may be the very first gene of Mtb encoding a product verified to suppress host IL-1β release.

Any virulence mechanisms that actively promote a reduced host inflammatory response would likely be advantageous to a pathogen. From a clinical perspective, an inverse relationship between induction of inflammatory cytokines and the virulence of various clinical isolates has been reported in several publications [223, 224, 225].

It can be argued that the increased pathogenicity of these isolates stems from a diminished host inflammatory response, which results in a delayed adaptive immune response, thus providing the bacteria with a head start during the earliest moments of infection, such as the 24-hour chase employed in our ELISA studies. Furthermore, an infection of SCID mice found the Δ*clpC2* mutant to be slightly, but significantly, more virulent than WT Mtb in terms of morbidity induction (Figure 26). Though this was only an initial experiment that needs to be replicated, these results suggest that the Δ*clpC2* induced 13-fold increase in IL-1β secretion observed in HMDMs may be at least partially conserved in the SCID mouse model, and may be biologically relevant *in vivo*.

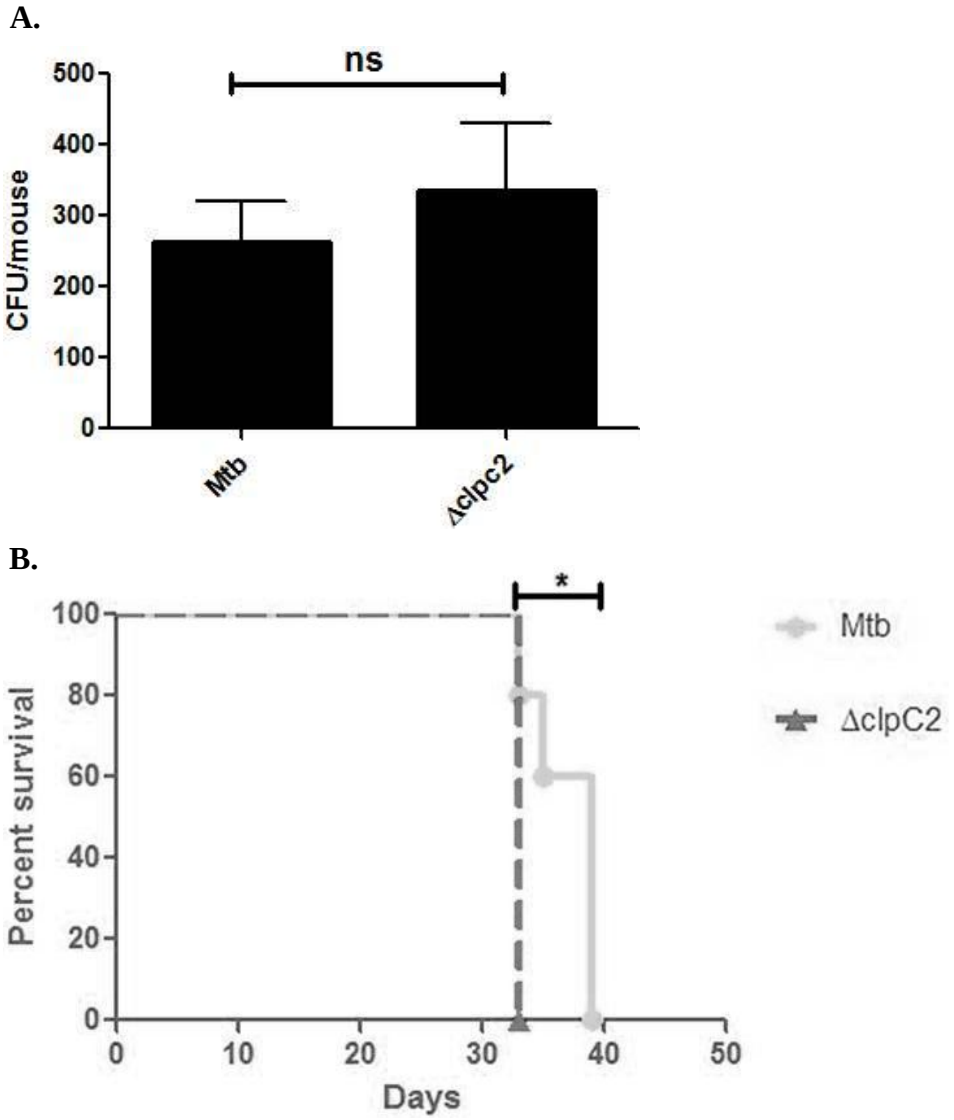


**Figure 26. SCID mice infected with Mtb and Δ*clpC2*.**
8 SCID mice were infected by aerosolized Mtb or Δ*clpC2* bacteria at a low MOI. (A) 3 mice per condition were sacrificed 1 day following infection. Lungs from each mouse were processed to ascertain respective colony forming units (CFUs) for each strain. No significant differences in were seen between Mtb and Δ*clpC2* CFU values. Statistical significance was determined by Student's paired t-test (n=3). (B) Median survival for the 5 mice per condition was 33 days for mice infected with Δ*clpC2* (all sacrificed due to morbidity), while Mtb infected mice had a median survival time of 39 days (3 mice sacrificed due to morbidity at day 39; 1 mouse sacrificed due to morbidity at day 33; 1 mouse perished at day 35) Statistical significance was determined by a Mantel-Cox log-rank test. * p=0.01-0.5 (n=5) (Experiments carried out by SG and BH)

# Chapter 6: Summary and Conclusion

It is well established that the suppression of host apoptosis is a survival strategy of *M. tuberculosis* [53, 90, 91, 117]. Previous members of the Briken lab employed a large gain-of-function screen in an effort to identify genes of the Mtb genome that mediate apoptotic-suppression of a host cell. The screen took 312 randomized gene segments from the virulent *M. tuberculosis* Erdman genome and expressed these regions within the less virulent, fast-growing, high apoptosis-inducing mycobacteria species *M. smegmatis* $mc^2$-155. The transformed $mc^2$-155 were used to infect a human THP-1 cell line, which was screened for a reduction in apoptosis induction relative to THP-1s infected with $mc^2$-155 transformed with an empty-vector control.

One of these genomic regions conferring a GoF phenotype is referred to as "K20" (H37Rv nucleotide region 2,978,367 to 2,990,637, + strand) is 12,271 nt, plus an additional distal genomic region (2,945,437 to 2,946,738, + strand) that is 1,302 nt; K20 contains 19 complete genes). The other anti-apoptosis encoding genetic regions identified in that screen, J21 and M24, were previously reported [53] and characterized. This dissertation has explored and presents new details regarding the hitherto unreported and uncharacterized K20 genomic region of Mtb, with a primary focus on the identification of anti-apoptotic virulence gene(s) of Mtb and a secondary characterization of a hypothetical ATPase subunit of the critically important Clp protease family.

## 6.1 Novel *in vitro* host models identified for the study of Mtb-host apoptosis interactions

Before beginning the identification of the specific anti-apoptotic genes of the region, the K20 anti-apoptotic phenotype was initially validated in human monocyte derived macrophages (HMDMs) and Hartley guinea pig alveolar macrophages; this work established that the phenotype of interest was not solely an artifact of the THP-1 cell line as earlier experimentations had suggested (K.K. Velmurugan, [53], data not shown).

In terms of novel Mtb-host apoptosis modeling systems, these initial K20 validation studies revealed that the use of recombinant human M-CSF cytokine and off-the-clot human serum to differentiate donor provided monocytes into mature, $CD14^{+}$ macrophages produce viable, consistent results. The M-CSF derived human macrophage system was optimized specifically by the author for this dissertation, and the host cells were additionally used by the author to supportively confirm the phenotypes of other anti-apoptotic genes of Mtb, *Rv3165c* and *Rv3167c* (B. Hurley, relevant publication forthcoming). This particular host modeling tool will be quite useful for exploring the Mtb-host apoptosis inhibition interplay in future studies by both the Briken lab and the greater scientific community.

Additionally, the guinea pig has previously been described as the gold-standard animal model for Mtb *in vivo* studies [189], although very little work has been reported describing the usefulness of these macrophages for *in vitro* modeling of Mtb infection. To the best of our knowledge, no circulated reports to date have detailed guinea pig alveolar macrophage apoptotic response to mycobacterial infection. Our experimentations determined that the resident alveolar macrophages of

Hartley guinea pigs are a feasible, plentiful source of macrophages for modeling the Mtb-mediated suppression of host apoptosis *in vitro*. These macrophages were also used by the author to further validate the Rv3167c anti-apoptotic phenotype (Figure 27, B. Hurley, relevant publication forthcoming). This is the first reported use of guinea pig alveolar macrophages for *in vitro* modeling of Mtb-mediated suppression of host apoptosis and the system offers researchers and exciting new tool for future exploration.

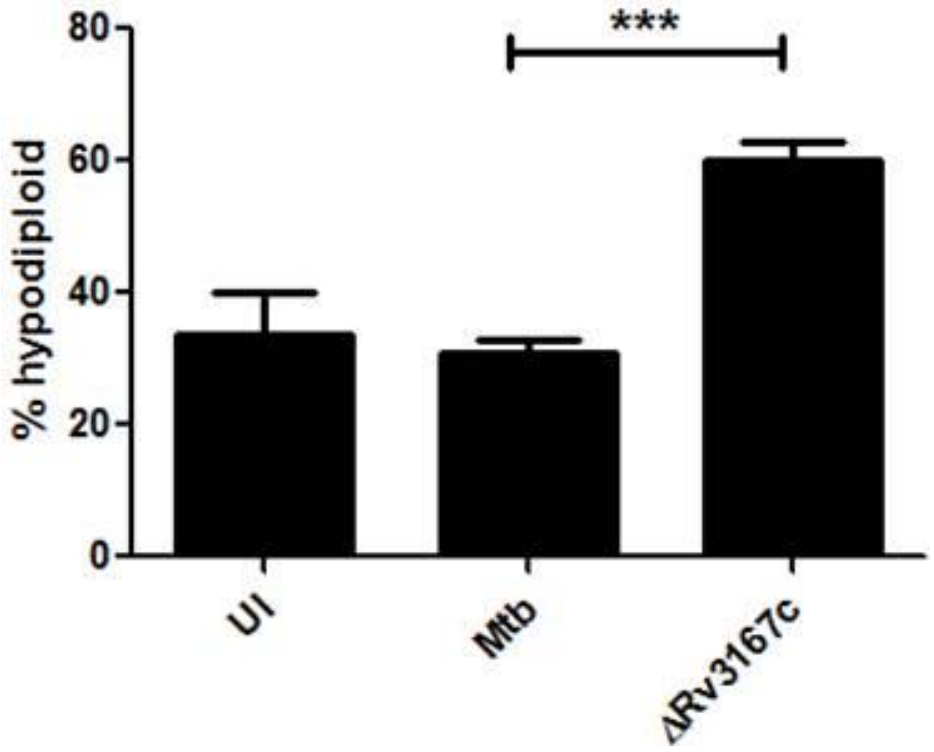


**Figure 27. Infection of Hartley alveolar guinea pig macrophages with WT Mtb and Δ*Rv3167c* indicates significant differences in host apoptosis.**
Significant differences in apoptosis were observed in alveolar macrophages of outbred Hartley guinea pigs infected with WT Mtb and Δ*Rv3167c*. Alveolar macrophages were infected 4 hrs at MOI of 3 followed by a 2 day chase; uninfected (UI) controls were included in all experiments. Results shown are the composite of experiments using alveolar macrophages of 4 unique animals ($n \geq 6$ for all samples). Error bars represent ± SD. Significance bar compares WT Mtb and Δ*Rv3167c*. Statistical analysis employed ANOVA with Tukey post-test.

### 6.1.1 Novel *in vitro* host models identified as impractical/nonviable for the study of Mtb-host apoptosis interactions

At the same time we found the usefulness of the Hartley guinea *alveolar* macrophages, it was determined that guinea pig *peritoneal* macrophages, while obtainable in much greater quantities per animal, are much too sensitive to apoptosis induction to be a feasible modeling system for future *in vitro* Mtb-infection studies.

Furthermore, the immortalized murine alveolar macrophage cell (MH-S) [176, 224] was previously considered to a promising *in vitro* Mtb-host apoptosis modeling system due to the ability to culture the line in very large quantity as well as its many physiological similarities with resident alveolar macrophages (the hallmark host for Mtb). However, testing by the author revealed the cell line was quite impervious to mycobacterial-induced cell death, establishing the MH-S cell line, like guinea pig peritoneal macrophages, as a poor choice for future *in vitro* Mtb-host apoptosis investigations.

## 6.2 Loss-of-gain-of-function screening is a novel and viable method of anti-apoptotic gene identification

A *loss-of-*"gain-of-function" (LoGoF) screen was employed to determine genes that were potentially responsible for the K20 gain-of-function phenotype. As the initial gain-of-function screen previously described (see section 3.3) has been invaluable to the Briken lab, and the relevant techniques and methodology well established, it was decided that the basic approach employed could be exploited to identify the anti-apoptotic gene(s) of interest in a novel way.

In this novel screening tactic, *in vitro* transposon mutagenesis was used to disrupt individual genes of the K20 expressing vector. (This specific portion of this project was previously completed by former Briken lab member, Dr. Serdar Gurses.) A loss of the original K20 gain-of-function effect suggested that the K20-transposon mutant(s) inducing the greatest host-death indicated the particular gene's possible role in the K20 GoF phenotype. The LoGoF screen was repeated several times in the $mc^2$-155 and *M. kansasii* mycobacterial backgrounds, to reproducible ends. Two LoGoF clones were consistently amongst the greatest inducers of host cell death: sg*Rv2666* (*Rv2666* is annotated by most sources as a probable truncated transposase gene) and sg*Rv2667* (*Rv2667* typically annotated as a possible ATP-dependent protease subunit of the Clp family).

Ultimately, we were able to establish the novel LoGoF screen as a valid approach to identification of anti-apoptotic genes of Mtb. The LoGoF approach provides a simple technique and relatively rapid turnaround compared to screening individual gene constructs for a GoF phenotype (traditional forward genetics screen) or screening deletion mutants of Mtb (traditional reverse genetics screen); this is provided that one has access to a pre-fabricated GoF construct to build upon. Additionally, some phenotypes are dependent upon the presence of multiple genes, LoGoF screening allows for the identification of specific gene(s) critical for a phenotype of interest (barring polar effects resulting from transposon insertion). The LoGoF screens employed in this dissertation suggested that Rv2666 and Rv2667 may be novel anti-apoptotic effectors of Mtb, and warranted further investigation.

## 6.3 Identification of *Rv2666* as a novel anti-apoptosis gene of Mtb, and a unique function for a transposase-like gene of Mtb

Having identified both genes of a potential two-gene *Rv2666-Rv2667* operon by LoGoF screening, our attention turned to confirming these findings in an Mtb background. It was determined that using gene-abrogation mutants of Mtb in a loss-of-function (LoF), reverse genetics approach would directly address and confirm our LoGoF screen results, firmly establishing one or both of these genes as responsible for the K20 anti-apoptotic phenotype.

An Mtb *Himar1* transposon mutant of *Rv2666* in the CDC1551 genetic background was obtained through the TARGET (*Tuberculosis Animal Research and Gene Evaluation Taskforce*) project. Experimental results showed the Tn*Rv2666* mutant induced significantly more host apoptosis than the WT CDC1551 strain and the mutant phenotype was successfully complemented with an episomal plasmid carrying *Rv2666*. These results confirm that *Rv2666* acts as an Mtb encoded anti-apoptotic gene. There are no current publications, to the best of our knowledge, suggesting a role for transposase or transposase-like element virulence or anti-apoptotic effects within Mtb, making the findings reported in this dissertation entirely novel.

The specific mechanism of action for Rv2666 is presently unknown, though transposase-turned-transcription factors have been well-established in *Arabidopsis* [192]. Additionally, "domesticated transposases" such as $TnpA_{REP}$ of *E. coli* (indirect transcriptional effects [225]) and TlpA/TlpB of *Clostridium difficile* (transposase-fusion proteins [226, 227]) have been observed in prokaryotes. It is possible, and our present contention, that *Rv2666* effects an anti-apoptotic phenotype by modulating

transcription of factors important for the suppression of host-apoptosis; while no apparent Mtb "anti-apoptosis system" has been presently identified, a multitude of anti-apoptotic genes of Mtb have been characterized (see section 2.4.3) and it is quite possible that Rv2666 may modulate the expression of one or more of these.

## 6.4 *Rv2667 /clpC2* not an anti-apoptotic gene of Mtb, but does affect host IL-1β secretion

The second gene identified by LoGoF screening, *Rv2667*/*clpC2*/*clpX'*, was not available as a TARGET transposon mutant, so a Δ*clpC2* recombinant abrogation mutant was created in the H37Rv genetic background of Mtb. The Δ*clpC2* mutant was confirmed by analysis of both RNA and genomic DNA.

### 6.4.1 *Rv2667 /clpC2* not an anti-apoptotic gene of Mtb

Δ*clpC2* and WT H37Rv were used to infect HMDMs, and relative levels of host-apoptosis induction were not significantly different between the strains; these results held true when the infections were repeated in guinea pig alveolar macrophages. These results suggest *Rv2667*/*clpC2* has no apparent role as anti-apoptotic gene of Mtb. The discrepancy between the Δ*clpC2* results and LoGoF data is possibly the result of evolutionarily conserved redundancy; the anti-apoptotic mechanisms of Mtb may be so important for the survival of the pathogen that numerous backups and fail-safes negate the strong LoF phenotype that was expected of a Δ*clpC2* mutation in Mtb. *M. smegmatis* and *M. kansasii* may lack many of these fail-safes, thus demonstrating the LoGoF phenotype we observed. Alternatively, it

may be possible that ClpC2 has no direct effect on host-apoptosis outcomes whatsoever and that the discrepancy between the LoGoF and Δ*clpC2* studies can be attributed to the involvement of ClpC2 acting in another capacity unrelated to the suppression of host-apoptosis.

### 6.4.2 *Rv2667 /clpC2* affects host IL-1β secretion

Having studied the Δ*clpC2* mutant, we determined that ClpC2 plays no obvious role in the suppression of host macrophages. Further characterization of the Δ*clpC2* mutant was undertaken to confirm or refute a suspected role for ClpC2 in Mtb virulence.

It is known that virulent Mtb modulates host death outcomes in a variety of ways, such as the suppression of host apoptosis (harmful to the pathogen) and the promotion of host necrosis (beneficial to the pathogen). The Mkan/Msmeg LoGoF screens and Δ*clpC2*-LoF experimental discrepancies previously described may be explained by mechanisms that exist outside of Mtb's necrotic promotion pathways, or may be nonessential to a pro-necrosis phenotype but contribute to Mtb host-death mediation in other capacities. Therefore, we examined the Δ*clpC2* mutant for defects in the modulation of host hallmark inflammatory cytokine response to further study this thought.

We found that Δ*clpC2* and WT H37Rv did not vary in their induction of host TNFα release; however, the Δ*clpC2* strain induced significantly more IL-1β secretion by infected host cells ($p \leq 0.001$). The phenotype was partially complemented when Δ*clpC2* was transformed with a plasmid which constitutively expresses ClpC2 and

infections were repeated; this partial, but not complete, complementation may be the result of a burdensome overexpression of ClpC2 by the plasmid-based, *groEL2* promoter carrying pMV261 expression vector or an artifact of overabundant plasmid copy number. Initial *in vitro* growth curve studies (Figure 20) suggested that the pMV261-based complement demonstrated obvious growth defects when grown in minimal media; it may be that the taxing-nature of the episomal plasmid extends to other bacterial processes beyond replication, including the Mtb machinery needed for the suppression of host inflammatory cytokine release following phagocytosis by a macrophage. Further studies will be needed to confirm this.

The reason for the Δ*clpC2* IL-1β secretion phenotype is presently unknown. Given the *in silico* predictions of ATPase/chaperone homology [194], it may be that ClpC2 is an indirect, upstream effector of a protein or system mediating the phenotype. It is quite possible that ClpC2 may aid in Mtb pathogenicity by providing, perhaps indirectly, an effect that allows the pathogen to limit host inflammation thus permitting the infecting mycobacteria a "head start" against the host adaptive immune response. This idea would stand in agreement with real-world clinical findings. It has been determined that at least one prominent difference in Mtb clinical isolates is the difference in the host inflammatory cytokine response they respectively generate. It may be that more virulent strains of Mtb induce lower levels of host-inflammatory response [228, 229], as several research groups have hypothesized; *clpC2* may be the first Mtb gene proven to have a role in the suppression of host IL-1β release by Mtb. In addition to the novelty of our finding, this mutant, and its upstream and downstream effectors, will be quite useful in

studying host IL-1β release, inflammasome activation and the potential virulence link between Mtb-pathogenicity and IL-1β release.

# Chapter 7: Future Directions

This chapter explores the potential future experiments and studies most relevant to the collected data presented in this dissertation.

## 7.1 Future directions: model systems

Much of the material presented within this dissertation has involved the development and characterization of novel Mtb-host apoptosis modeling systems. Some of the new host models described (guinea pig alveolar macrophages and M-CSF differentiated human monocyte-derived macrophages) will be extremely useful in future studies by both the Briken lab and other researchers interested in the host-pathogen interface as it regards the suppression (or induction) of host death by mycobacteria; other host models (guinea pig peritoneal macrophages and the immortalized MH-S, murine alveolar macrophage cell line) should probably be avoided for studies of this nature as they are of limited usefulness in this capacity.

### 7.1.1 Model systems: Hartley guinea pig

As previously stated, our data suggests that Hartley guinea pig alveolar, but not peritoneal, macrophages are an excellent source for an *in vitro* host cell modeling system for studying the induction of cell death by mycobacteria. Alveolar macrophages are the natural host cell of Mtb, but are quite generally quite difficult to obtain from humans (due to an uncomfortable lavage process for donors) and mice (due to a limited number obtainable related to animal size). These guinea pig alveolar

macrophages can be obtained in sufficient quantity for a thorough analysis of host death induction by fluorescence microscopy. Alternatively, given enough animals (4 or more), adequate quantities of alveolar macrophages can be obtained to perform flow cytometry analysis should a researcher wish.

Additionally, our results suggest that the Hartley guinea pig will possibly be a useful model for *in vivo* infection studies of pro-apoptotic mutants of Mtb. The Hartley guinea pig is believed to be one of the most practical animal models for the *in vivo* study of Mtb infection [189]. Our results have extended the usefulness of the model to *in vitro* assays (where alveolar macrophages and Mtb-mediated suppression of apoptosis are concerned). The *in vitro* results we obtained with the pro-apoptotic Tn*Rv2666* mutant of Mtb should be further investigated with an *in vivo*, aerosol infection of Hartley guinea pigs with a full characterization of the mutant's behavior versus WT Mtb in this setting. It will be especially important to note altered animal survival/morbidity, host granuloma formation (particularly useful information can be gleaned from granuloma histology in guinea pigs as compared to the Briken lab's usual murine *in vivo* model) and relative CFU counts to establish the critical importance of Rv2666 for *in vivo* fitness of Mtb.

### 7.1.2 Model systems: human monocyte-derived macrophages (HMDMs)

A large portion of the data presented in this dissertation was generated in a HMDM host cell model system. These HMDMs were driven to macrophage maturity by culturing with off-the-clot human serum and M-CSF. In order to maximize the

potential for this modeling system, a steady supply of monocytes will be required; this was an unfortunate limiting step in the course of this particular thesis project.

This is less an experimental issue than one of logistics, however, Mtb is already one of the slowest growing bacterial species commonly studied and a deficiency of consistent macrophages for the modeling of host infection greatly exacerbates the timelines for all laboratory work of this nature. A steady source of HMDMs would be a tremendous boon for research output by both the Briken lab and all other researchers studying Mtb and other slow-growing mycobacteria. The monocytes used to generate the HMDMs used in this dissertation were generously provided by Dr. Alan Sher (NIH, Bethesda, MD), though this source of monocytes is limited by the availability of blood donors at the NIH campus and the technical issues of monocyte transport following collection. In order to maximize efficiency (both time and financial), the HMDM differentiation process and protocol should be retooled for smaller scale studies employing a lower quantity of monocytes obtained from "local" donors. A smaller pool of monocytes can be readily obtained from an on-campus donor, and used to quickly generate sufficient HMDMs for infection and subsequent analysis by fluorescence microscopy.

Also, as described above (see section 2.2.2) human monocytes can be differentiated into mature macrophages with M-CSF or GM-CSF. It has been suggested that these different cytokines will generate macrophages of different morphological and behavioral characteristics [59, 66], and that differentiation with GM-CSF may generate a mature macrophage with greater similarity to alveolar macrophages. While optimization studies determined that the M-CSF cytokine was

superior for our purposes of host apoptosis study, it may be prudent to reevaluate this cytokine differentiation approach for the further detailing and characterization of Δ*clpC2*, the host IL-1β-secretion-affecting mutant of Mtb. Monocyte differentiation with GM-CSF may provide a more accurate representation of resident alveolar macrophages, thus providing a superior *in vitro* model for Mtb infections and a cleaner phenotype in terms of host IL-1β secretion variations between Δ*clpC2* and WT Mtb infection outcomes.

## 7.2 Future directions: screens to identify anti-apoptotic genes of Mtb

Much of the work that identified the K20 genomic region of Mtb as "anti-apoptotic" was completed several years prior to the beginning of this particular thesis project. Additionally, the important K20 loss-of-gain-of-function (LoGoF) transposon mutant pool was generated by Dr. Serdar Gurses prior to this author's endeavors to identify the specific anti-apoptotic gene(s) of the K20 region. However, future studies to identify additional anti-apoptosis genes of Mtb may employ these methods and a thorough understanding of the pros and cons involved will be quite beneficial to future researchers.

### 7.2.1 Future screens: gain-of-function (GoF) screens to identify anti-apoptotic genes of Mtb

The initial GoF screen used to identify the K20 region is described above (see section 5.1, first paragraph). The major benefit of this assay was a rapid turnaround on a relatively large scale approach (work with mycobacteria often progresses quite

slowly due to longer replication times and the necessity of additional lab safety precautions). From a pool of 312 initial genomic regions, 3 regions were definitively established as conferring an anti-apoptotic phenotype to Msmeg $mc^2$-155. On the downside of this particular screening approach, many relevant anti-apoptosis genes will likely be overlooked (proof of this screening-gap exists in the identification of Mtb anti-apoptosis genes, such as *pknE, secA2, sodA,* etc., that do not occur in the 3 GoF genomic regions identified). The reason for these "gaps" may be due to a number of causes. It is possible the genetic background of Msmeg $mc^2$-155 varies significantly enough from Mtb that the Msmeg is unable to implement the GoF genes to their full anti-apoptotic potential. Or it is possibly that many of the anti-apoptotic genes of Mtb are an integral part of a yet unidentified anti-apoptosis system, and are encoded at distally positioned intervals on the Mtb chromosome, thus a GoF screen of this nature would miss these genes entirely.

If time and financial cost were less of an issue, a more thorough GoF screen and analysis to identify anti-apoptotic genes of Mtb would involve a similar repetition of the initial GoF approach in a mycobacterial model species more closely related to Mtb would be quite useful. Additionally, the initial screen was carried out in a THP-1 cell line. Repetition of the screen in primary macrophages would be a much better approximation of real-world Mtb-host interactions. For example, the GoF library pool could be used to transform *M. kansasii*. GoF-transformed *M. kansasii* may then be used to infect bovine alveolar macrophages or bovine monocyte-derived macrophages [230], readily available in enormous quantity through collaborators at USDA, Beltsville, MD. However, a screen of this magnitude would be a

considerable investment of time and would probably be more practical if carried out by a laboratory technician(s) rather than a doctoral student(s) seeking to generate self-publications during their academic career.

### 7.2.2 Future screens: Improvements to LoGoF screening

The previously described LoGoF screen (see section 3.3) was successfully employed to identify an individual anti-apoptotic gene of Mtb, *Rv2666*. This particular screening strategy was a novel and direct way of identifying a gene that was critical for the K20 GoF phenotype.

However, the LoGoF screen also suggested that *Rv2667*/*clpC2* was a potential anti-apoptotic gene; further testing with a Δ*clpC2* abrogation mutant of Mtb proved this to be untrue. It is possible this false positive resulted from a polar effect generated by transposon insertion into *clpC2* acting on *Rv2666* expression. Additionally, it may be that ClpC2 does have some anti-apoptotic role in Mtb, though it is rendered nonessential due to genetic redundancy within the Mtb background. There are 2 other Clp ATPases encoded by Mtb and the suppression of host apoptosis is critical for the survival of Mtb *in vivo*, so it stands to reason that such an important tactic will have evolutionarily selected backups and fail-safes. Finally, the *clpC2* gene of the K20 GoF vector may have indirectly conferred an anti-apoptotic phenotype to the Msmeg and Mkan model species by acting in some yet unknown, novel pathway that is not present or simply unimportant for the phenotype of interest within Mtb.

Future studies may employ the LoGoF screening approach to identify anti-apoptotic genes or potentially study other phenotypes of interest. In order to avoid false positives in the future, a number of approaches may be employed.

Multiple LoGoF clones should be screened for each gene of interest. Each individual clone will diminish the odds of polar effects generating false positives in nearby genes as well as bolstering the evidence supporting identified, true positives. Also, it may be worthwhile to simultaneously screen individual genes (or smaller subsets of genes) of interest in a GoF approach to validate the LoGoF findings. One would expect these GoF clones to demonstrate a phenotype opposed to their corresponding LoGoF mutant(s). Additionally, RT-PCR may identify and control for aberrant and undesired alterations of LoGoF mutant gene expression that may lead to false positives. Furthermore, screens carried out in a mycobacterial genetic background more closely related to Mtb (such as the *M. bovis* species) may avoid some of these issues altogether.

Finally, the LoGoF screening approach may be retained but, rather than employing random *in vitro* transposon mutagenesis, genes of interest that are carried on the vector may be disrupted by a process of targeted homologous recombination. This would provide clean, specific LoGoF mutants and would limit instances in which the only available LoGoF mutant for a given gene has an insertion point in the final portion of the gene, potentially leaving a functional gene intact (Supplemental Table ST2).

## 7.3 Future directions: *Rv2666*, an anti-apoptotic gene of Mtb

This dissertation has identified a novel anti-apoptotic gene of Mtb, *Rv2666*, by LoGoF screening and study of a *Himar1* transposon mutant of the gene. This subsection explores potential future directions for the characterization of Rv2666.

### 7.3.1 *Rv2666*: confirmation of phenotype in H37Rv, gene deletion background

As previously mentioned, a transposon mutant of *Rv2666* in the CDC1551 clinical isolate background of Mtb was revealed to have a pro-apoptotic phenotype when used to infect HMDMs. This phenotype was completely restored to WT behavior by complementation of the mutant with an expression plasmid carrying the *Rv2666* gene.

The first future step in the further study of Rv2666 will be the creation and confirmation of a specifically targeted *Rv2666* deletion mutant in the H37Rv laboratory strain of Mtb. This will be important as homologous-recombination mutants (and phenotype complementation) are the gold-standard for genetic assessment and characterization of interesting mutants of Mtb. Importantly, CDC1551 is a less commonly employed strain of Mtb used for laboratory work, and a mutant in the H37Rv genetic background will be essential for widespread acceptance, and recreation, of our findings. Also, an H37Rv-based Δ*Rv2666* mutant will allow researchers to experiment in a relatively well-characterized genetic background with a much larger pool of (potentially related) anti-apoptotic Mtb mutants and correlated genetic tools of interest.

### 7.3.1 *Rv2666*: confirmation of phenotype by *in vivo* studies within animal model

Once an *Rv2666* mutant in the H37Rv genetic background of Mtb has been generated and confirmed, it will be important to assess the mutant's relevance for the *in vivo* virulence of Mtb. Not all *in vitro* phenotypes have clinical significance. As one of major goals of this line of research is the identification of Mtb genes that may be useful for the future creation of a pro-apoptotic vaccine, it is essential to establish a baseline for Δ*Rv2666* virulence (or lack thereof) in an animal model. As mentioned above (see Chapter 7.1.1), the Hartley guinea pig should make an excellent animal model for this study. Aerosol infections of Hartley guinea pigs with Δ*Rv2666*, the complemented mutant and WT H37Rv (and possibly a better-characterized pro-apoptotic mutant of Mtb such as Δ*nuoG*) followed by detailed analysis of outcomes will establish the relative importance of Rv2666. Additionally, this dissertation has established the validity of guinea pig alveolar macrophages for *in vitro* analysis of Mtb-host apoptosis response; this research opens the avenue of exploration to a broad range of *in vitro* analyses involving Δ*Rv2666* corresponding to and supporting the *in vivo* studies proposed above.

### 7.3.1 *Rv2666*: confirmation of potential role as a transcription factor of anti-apoptotic genes of Mtb

Understanding the regulation of *Rv2666* will be quite important, as is the establishment of our hypothesized transcriptional factor role for the gene product. As work by other research groups has suggested *Rv2666* expression is upregulated when

Mtb is maintained in macrophages [179], this may be an excellent place to begin analysis of the gene.

Currently, the groundwork for an extensive RNA-seq analysis of Mtb in a variety of conditions (including intra-macrophage conditions) is being undertaken by Briken lab member Jeff Quigley. From these future results, analysis of the data generated may reveal many interesting details about *Rv2666* regulation that can act as a basis for the design of future studies. Additionally, it may be beneficial to see why Mtb-genes similar to *Rv2666* (other transposase-like Mtb genes) are not upregulated in the same conditions [179]. Specifically, this will drive at the question of why *Rv2666* is so unique amongst seemingly similar genes (beyond or including its predicted "truncation").

Ideally, this RNA-seq data may be able to suggest strong correlations between Rv2666 transcription and other known anti-apoptotic genes of Mtb; this will hopefully provide future researchers with a "short-list" of candidate genes for identifying effector proteins directly involved in host cell apoptosis inhibition. Should future work link Rv2666 to regulation of known, or presently unknown, anti-apoptosis effectors of Mtb, our hypothesis that Rv2666 (encoded by a MULE-like, "domesticated" transposase-like gene) acts as a transcription factor of Mtb will have been proven correct.

## 7.4 Future directions: *Rv2667*/*clpC2*, an Mtb gene affecting host-IL-1β secretion

This dissertation has identified a gene of Mtb, *Rv2667*/*clpC2*, that affects host IL-1β secretion. This subsection explores potential future directions for the characterization of Rv2667/ClpC2.

### 7.4.1 *Rv2667*/*clpC2*: confirmation, and possible extension, of host cytokine secretion phenotype of interest

The confirmation of the Δ*clpC2* effect on IL-1β-secretion in additional host backgrounds should be paramount for future studies. For *in vitro* cell culture studies, this additional confirmation should be carried out by way of additional HMDM infections (each monocyte donor has a unique genetic disposition that may affect the final ELISA readout) as well as extending experimentation to identify a suitable human cell line for future investigations (such as THP-1s). Additionally, our *in vivo* SCID mouse infection results such be replicated and include controls to bolster our hypothesized link between Δ*clpC2* infection and hyperinflammation in host animals.

Additional HMDM infections will allow future researchers to add statistical weight to our original data set and provide added assurance that the IL-1β secretion phenotype reported is not a solely donor-dependent effect. This may be important as *clpC2* may be the first identified Mtb gene shown to suppress host IL-1β release, thus precedent-setting and subject to a higher degree of scrutiny. Furthermore, as the phenotype has been previously observed in HMDMs, future investigators should be able to run additional ELISAs using infection supernatants to detect other factors important in inflammasome-linked cytokine secretion (such as the mature form of IL-

18). The long term goals for the study of ClpC2 will certainly entail an assessment of its place within the increasingly understood and critically important host-inflammasome pathways. It will be interesting to identify whether the *clpC2* phenotype in question is IL-1β-specific, or if it generates a wider-ranging host-response than what is demonstrated by our findings. It will be important to establish this early in the characterization of this particular phenotype as ELISA is a measure of "final outcome" as far as our present investigative intentions have been concerned. Ultimately, the result of these experiments should provide clues as to how broadly acting ClpC2 truly is, thus priming future expectations and experimental design.

In terms of further characterizations, the finite supply of HMDMs will inevitably mandate a need for a host model available in plentiful quantity for work with Western blotting and similar "high-input" assays. Briken lab member Swati Shah has recently begun the experimental process of Δ*clpC2* infection of THP-1s and her work should establish the feasibility of that particular cell line for use in future studies of ClpC2.

Finally, our SCID mouse infection should be repeated with the complemented mutant, specifically the *attB*-integrated complement as initial studies suggest that the pMV261 plasmid-based *clpC2* complement strain may have fitness issues under higher burden conditions (Figure 20).

The SCID mouse results presented in this dissertation come from a single experiment and should be validated before definitive conclusions are drawn. Future experimentation should employ additional animals and make the most of these additional data points by use of a range of bacterial dosages (ideally high-, mid- and

low-dose infections that generate corresponding responses in terms of animal mortality/morbidity), and any additional infections should attempt to further validate our hypothesized link between *clpC2* deletion in Mtb and increased host IL-1β release. This could be accomplished using IL-1 receptor-deficient or IL-1converting enzyme (ICE)-deficient mice (or alternatively, in SCID mice dosed with anti-IL-1β in a range of concentrations) and infecting them with Δ*clpC2*, WT Mtb or complemented mutant, and then observing for a diminished morbidity/mortality in Δ*clpC2*-infected animals due to an absence of hyperinflammation.

### 7.4.2 *Rv2667*/*clpC2*: studying potential ATPase or chaperone activity

One of the questions raised by this dissertation regards the specific mechanism of action of ClpC2. *In silico* analysis [194] suggests ClpC2 is an ATP-dependent subunit of a Clp-family protease, or potentially acts in a chaperone capacity.

It will be interesting to see if ClpC2 interacts with other Clp-family members. The Clp ATPase subunits of most bacteria possess a VGF consensus sequence which interacts with ClpP (the protease proteolytic subunit) to form a functional protease. Mtb is somewhat unique in that it possesses 2 proteolytic subunits (ClpP1 and ClpP2) and its verified Clp ATPases (ClpX and ClpC1) have a LGF-interaction loop. ClpC2 lacks this LGF-sequence but does have a LGV sequence which may substitute. In order to establish the potential for ClpC2 interaction with other Clp-family members, a two-hybrid screening approach can be used to investigate this further; this would

also be an ideal time to further examine potential ClpC2-FtsZ interactions as per ClpX-FtsZ interactions [140], described above (see section 5.1.1).

Alternatively (or additionally) to two-hybrid analysis, ClpC2 can be HIS-tagged and relevant protein-protein interactions may be determined by co-immunoprecipitation and subsequent mass spectrometry analysis. Such experiments would reveal a bit more about the general role of ClpC2 in Mtb, potentially answering the question of whether the protein acts as a protease subunit, a chaperone, a broadly acting ATPase or perhaps acting in some completely novel, unexpected capacity.

*In silico* analysis of ClpC2 also suggests regions of ATP-binding homology. The predicted ATPase activity of ClpC2 should be verified. This can be accomplished by incubation of purified ClpC2 (HIS-tagged and nickel-column purified) and ATP; several colorimetric and fluorescence assays exist that will quantify ATP hydrolysis (free-phosphate production) in a rapid, sensitive manner. The known Mtb ATPases ClpC1 and ClpX may be used as controls. Ultimately, establishing whether predicted ATPase activity is truly occurring *in vitro* will greatly assist in steering the specific direction future investigations of this protein should take.

### 7.4.3 *Rv2667*/*clpC2*: study gene expression and regulation with respect to Mtb virulence

ClpC2 has been predicted to be upregulated upon reaeration following extended periods of hypoxia [194], very similar to conditions one might expect upon rupture of a granuloma and sudden reactivation of a latent-stage Mtb infection. As

mentioned above (see section 7.3.1), Briken lab member Jeff Quigley is presently engaged in the early-stages of a sizable RNA-seq analysis of Mtb under a variety of conditions. An extensive examination of the completed data set for *clpC2* transcription may be one of the simplest, yet productive, early-stage studies a future investigator may attempt. At a minimum, we would hope that the RNA-seq data will decrease the initial investment of time required for optimization studies, rapidly identifying the ideal experimental conditions needed for a thorough characterization of ClpC2 and its link to host IL-1β secretion.

# Supplemental Figures

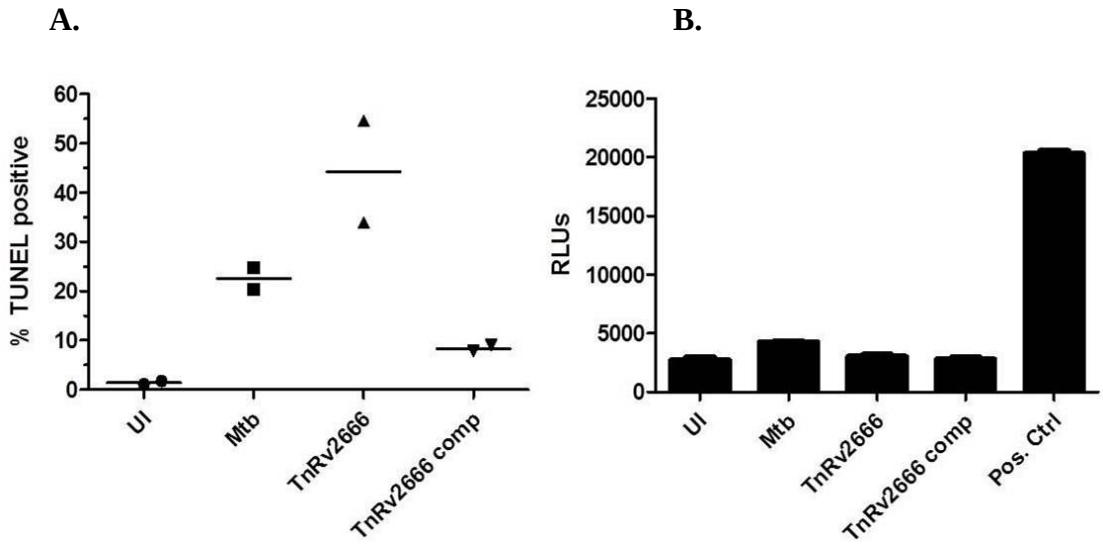


**Figure S1. THP-1 cell line infection with Tn*Rv2666* mutant and complement confirm host anti-apoptosis phenotype and exclude necrosis.**

**A.** THP-1 cells differentiated overnight with PMA were infected at MOI of 3 for 4 hrs, followed by a 3 day chase; uninfected (UI) THP-1s were included in all experiments. Cells were lifted, fixed with 4% PFA and apoptosis was quantified by TUNEL staining and flow cytometry. Figure results presented are representative of the experimental trend and come from a single trial with 2 data points per condition. Bars indicate mean value for the each condition. (*Figure S1A* data generated by Briken lab member Swati Shah)

**B.** THP-1 cells differentiated overnight with PMA were infected at MOI of 3 for 4 hrs, followed by a 3 day chase; uninfected (UI) THP-1s were included in all experiments. Supernatants were collected and an AK release assay was performed to evaluate host necrotic death as indicated by degree of cellular lysis, quantified as relative light units (RLUs) emitted. Results presented are representative of the experimental trend and come from a single experiment with 3 replicates per condition. Error bars indicate ± SD for each condition.

**A.**

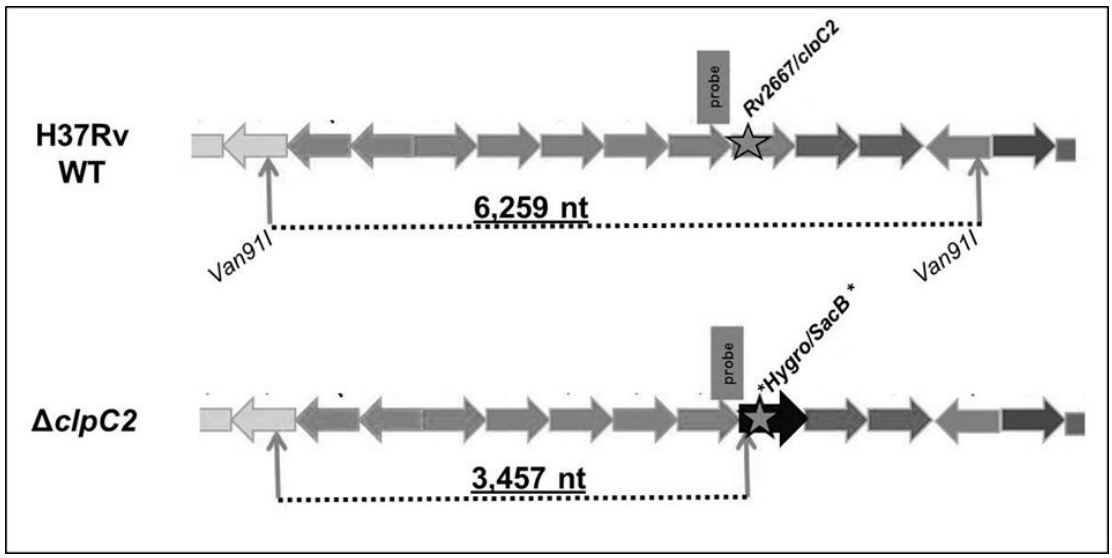


**B.**

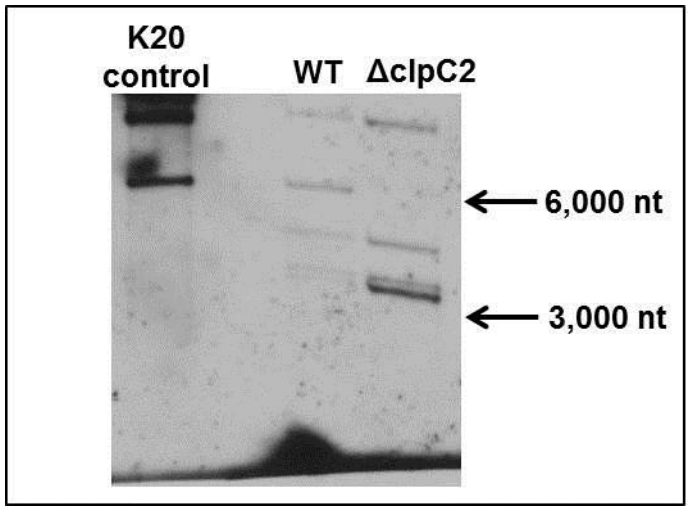


**Figure S2. Southern blot confirmation of *clpC2* gene abrogation.**

A. Theoretical sizes (nt) of WT H37Rv and Δ*clpC2* genomic DNA digested with Van91I. The original K20 GoF vector was also cut as a control for the WT *clpC2* gene.

B. Southern blot confirming abrogation of the *clpC2* gene in the hypothetical knock-out.**note*: additional background bands between 3,000-6,000 nt are a byproduct of a nonspecific probe binding.

```
  1  atg acc tct tct cat ctt atc gac acc gag cag ctt ctg gct gac caa ctc gca

 55  cag gcg agc ccg gat ctg ctg cgc ggg ctg ctc tcg acg ttc atc gcc gcc ttg

109  atg ggg gct gaa gcc gac gcc ctg tgc ggg gcg ggc tac cgc gaa cgc agc gat

163  gag cgg tcc aat cag cgc aac ggc tac cgc cac cgt gat ttc gac acc cgt gcc

217  gca acc atc gac gtc gcg atc ccc aag ctg cgc cag ggc agc tat ttc ccg gac

271  tgg ctg ctg cag cgc cgc aag cga gct gaa cgc gca ctg acc agc gtg gtg gcg
                                                          TnRv2666 >

325  acc tgc tac ctg ctg gga gta tcc act cgc cgg atg gag cgc ctg gtc gaa aca

379  ctt ggt gtg aca aag ctt tcc aag tcg caa gtg tcg atc atg gcc aaa gag ctc

433  gac gaa gcc gta gag gcg ttt cgg acc cgc ccg ctc gat gcc ggc ccg tat acc

487  ttc ctc gcc gcc gac gcc ctg gtg ctc aag gtg cgc gag gca ggc cgc gtc gtc

541  ggg gtg cac acc ttg atc gcc acc ggc gtc aac gcc gag ggc tac cga gag atc
               LoGoF sgRv2666 >

595  ctg ggc atc cag gtc acc tcc gcc gag gac ggg gcc ggc tgg ctg gcg ttc ttc

649  cgc gac ctg gtc gcc cgc ggc ctg tcc ggg gtc gcg ctg gtc acc agc gac gcc

703  cac gcc ggc ctg gtg gcc gcg atc ggc gcc acc ctg ccc gca gcg gcc tgg cag

757  cgc tgc aga acc cac tac gca gcc aat cac ggt cga cac aat gca taa
```

**Figure S3. sg*Rv2666* LoGoF and Tn*Rv2666* insertion points.**
Figure presents gene sequence of *Rv2666* with labeled transposon insertions for both the LoGoF transposon mutant within the K20 vector (see section 3.3) and the TARGET project-generated mutant (see section 3.1.2)

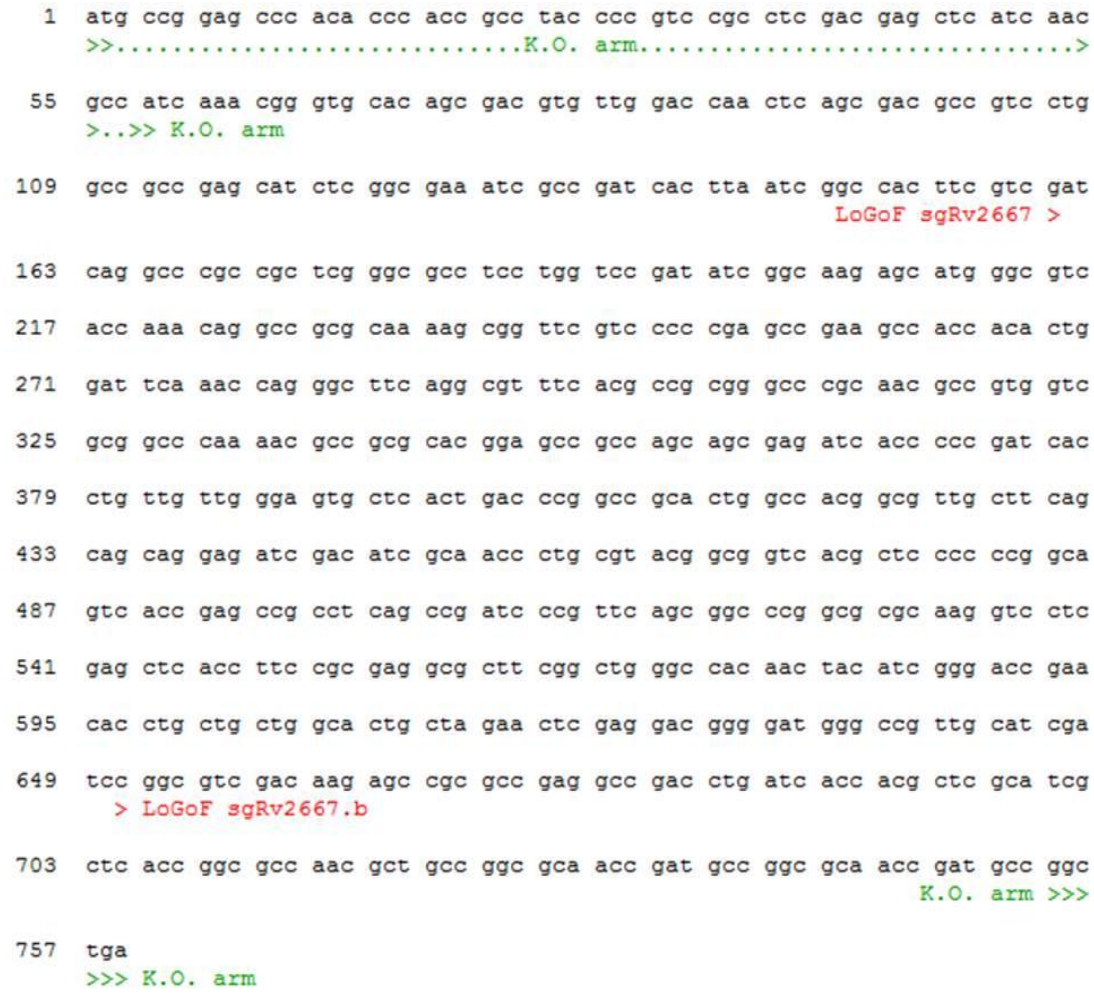


**Figure S4. sg*Rv2667* LoGoF clone insertion points and location of targeted homologous recombination arms within *Rv2667*/*clpC2* interior.**
Figure presents gene sequence of *Rv2667*/*clpC2* with labeled transposon insertions for both the LoGoF transposon mutant within the K20 vector (see section 3.3) and targeting arms of the homologous recombinant mutant of H37Rv generated by specialized phage transduction (see section 3.2.1, Figure 3).

# Supplemental Tables

| Gene | Length (nt) | Position on H37Rv (+ strand) | Orientation | Predicted function |
|---|---|---|---|---|
| *Rv2617c* | 441 | 2945847..2946287 | - | PROBABLE TRANSMEMBRANE PROTEIN |
| *Rv2656c* | 393 | 2978660..2979052 | - | POSSIBLE phiRv2 PROPHAGE PROTEIN |
| *Rv2657c* | 261 | 2979049..2979309 | - | PROBABLE phiRv2 PROPHAGE PROTEIN |
| *Rv2658c* | 363 | 2979326..2979688 | - | POSSIBLE PROPHAGE PROTEIN |
| *Rv2659c* | 1128 | 2979691..2980818 | - | PROBABLE phiRv2 PROPHAGE INTEGRASE |
| *Rv2660c* | 228 | 2980963..2981190 | - | HYPOTHETICAL PROTEIN |
| *Rv2662* | 273 | 2981482..2981754 | + | HYPOTHETICAL PROTEIN |
| *Rv2661c* | 390 | 2981187..2981576 | - | HYPOTHETICAL PROTEIN |
| *Rv2663* | 234 | 2981853..2982086 | + | HYPOTHETICAL PROTEIN |
| *Rv2664* | 255 | 2982097..2982351 | + | HYPOTHETICAL PROTEIN |
| *Rv2665* | 282 | 2982699..2982980 | + | HYPOTHETICAL ARGININE RICH PROTEIN |
| *Rv2666* | 804 | 2983071..2983874 | + | PROBABLE TRANSPOSASE FOR I IS1081 |
| *clpC2* | 759 | 2983896..2984654 | + | POSSIBLE ATP-DEP. PROTEASE CLPC2 |
| *Rv2668* | 522 | 2984733..2985254 | + | POSSIBLE EXPORTED PROTEIN |
| *Rv2669* | 471 | 2985283..2985753 | + | GCN5-RELATED N-ACETYLTRANSFERASE |
| *ribD* | 777 | 2986839..2987615 | + | POSSIBLE RIBOFLAVIN BIOSYNTH. |
| *Rv2670c* | 1110 | 2985731..2986840 | - | CONSERVED HYPOTHETICAL PROTEIN |
| *Rv2672* | 1587 | 2987682..2989268 | + | POSSIBLE SECRETED PROTEASE |
| *Rv2673* | 1302 | 2989291..2990592 | + | POSSIBLE INTEGRAL MEMBRANE PROTEIN |

**Supplemental Table ST1. Genes of the K20 Region: size, position, orientation and predicted function.**

| Gene | Gene Orientation | Tn point-of-insertion (x of x nt) | Gene position (H37Rv, + strand) | Tn position (H37Rv, + strand) |
|---|---|---|---|---|
| *Rv2657c* | - | 49 of 261 | 2979049..2979309 | 2979260 |
| *Rv2658c* | - | 88 of 363 | 2979326..2979688 | 2979600 |
| *Rv2659c* | - | 114 of 1128 | 2979691..2980818 | 2980704 |
| *Rv2660c* | - | 162 of 228 | 2980963..2981190 | 2981028 |
| *Rv2663* | + | 192 of 234 | 2981853..2982086 | 2982045 |
| *Rv2665* | + | 133 of 282 | 2982699..2982980 | 2982832 |
| *Rv2666* | + | 560 of 804 | 2983071..2983874 | 2983631 |
| *clpC2* | + | 160 of 759 | 2983896..2984654 | 2984056 |
| *clpC2** | + | 651 of 759 | 2983896..2984654 | 2984547 |
| *Rv2668* | + | 153 of 522 | 2984733..2985254 | 2984886 |
| *Rv2669* | + | 422 of 471 | 2985283..2985753 | 2985705 |
| *ribD* | + | 213 of 777 | 2986839..2987615 | 2987056 |
| *Rv2670c* | - | 293 of 1110 | 2985731..2986840 | 2986547 |
| *Rv2672* | + | 838 of 1587 | 2987682..2989268 | 2988520 |
| *Rv2673* | + | 496 of 1302 | 2989291..2990592 | 2989787 |

**Supplemental Table ST2. Individual LoGoF mutants.**
Table presents the individual LoGoF clones selected for use in the initial screen in the Msmeg $mc^2$-155 background. Table features gene name, gene orientation with respect to + or – strand of Mtb chromosome, point-of-insertion for each transposon within its respective gene, gene position within the Mtb chromosome and transposon insertion point with respect to the Mtb genome. (Note: Additional LoGoF clones were generated, though not employed in the assay; the respective LoGoF mutant generating the largest predicted gene-truncations were selected for use in the assay where possible. Not all genes were interrupted by a transposon insertion.) *clpC2** indicates a secondary LoGoF clone for *clpC2* which was employed at one point to verify the primary LoGoF clone for the gene.

# Bibliography


[1] M. C. Gutierrez, S. Brisse, R. Brosch, M. Fabre, B. Omaïs, M. Marmiesse, P. Supply, and V. Vincent, "Ancient origin and gene mosaicism of the progenitor of *Mycobacterium tuberculosis*," *PLoS Pathog.*, vol. 1, no. 1, p. e5, Sep. 2005.

[2] G. Trueba and M. Dunthorn, "Many Neglected Tropical Diseases May Have Originated in the Paleolithic or Before: New Insights from Genetics," *PLoS Neglected Tropical Diseases*, vol. 6, no. 3, p. e1393, Mar. 2012.

[3] T. Wirth, F. Hildebrand, C. Allix-Béguec, F. Wölbeling, T. Kubica, K. Kremer, D. van Soolingen, S. Rüsch-Gerdes, C. Locht, S. Brisse, A. Meyer, P. Supply, and S. Niemann, "Origin, Spread and Demography of the *Mycobacterium tuberculosis* Complex," *PLoS Pathog*, vol. 4, no. 9, p. e1000160, 2008.

[4] B. M. Rothschild, L. D. Martin, G. Lev, H. Bercovier, G. K. Bar-Gal, C. Greenblatt, H. Donoghue, M. Spigelman, and D. Brittain, "*Mycobacterium tuberculosis* complex DNA from an extinct bison dated 17,000 years before the present," *Clin. Infect. Dis.*, vol. 33, no. 3, pp. 305–311, Aug. 2001.

[5] I. Hershkovitz, H. D. Donoghue, D. E. Minnikin, G. S. Besra, O. Y.-C. Lee, A. M. Gernaey, E. Galili, V. Eshed, C. L. Greenblatt, E. Lemma, G. K. Bar-Gal, and M. Spigelman, "Detection and molecular characterization of 9,000-year-old *Mycobacterium tuberculosis* from a Neolithic settlement in the Eastern Mediterranean," *PLoS ONE*, vol. 3, no. 10, p. e3426, 2008.

[6] A. R. Zink, C. Sola, U. Reischl, W. Grabner, N. Rastogi, H. Wolf, and A. G. Nerlich, "Characterization of *Mycobacterium tuberculosis* complex DNAs from Egyptian mummies by spoligotyping," *J. Clin. Microbiol.*, vol. 41, no. 1, pp. 359–367, Jan. 2003.

[7] N. Konomi, E. Lebwohl, K. Mowbray, I. Tattersall, and D. Zhang, "Detection of mycobacterial DNA in Andean mummies," *J. Clin. Microbiol.*, vol. 40, no. 12, pp. 4738–4740, Dec. 2002.

[8] A. K. Tyagi and N. Dhar, "Recent advances in tuberculosis research in India," *Adv. Biochem. Eng. Biotechnol.*, vol. 84, pp. 211–273, 2003.

[9] J. A. Myers, "Development of Knowledge of Unity of Tuberculosis and of the Portals of Entry of Tubercle Bacilli," *Journal of the History of Medicine and Allied Sciences*, vol. XXIX, no. 2, pp. 213–228, 1974.

[10] A. Zumla, "The white plague returns to London—with a vengeance," *The Lancet*, vol. 377, no. 9759, pp. 10–11, 1.

[11] K. Byrne, *Tuberculosis and the Victorian Literary Imagination*. Cambridge University Press, 2010.

[12] S. S. Deshpande, R. Mehta, and M. Yagnik, "Short term analysis of healed post-tubercular kyphosis in younger children based on principles of congenital kyphosis," *Indian J Orthop*, vol. 46, no. 2, pp. 179–185, 2012.

[13] D. S. Jones, S. H. Podolsky, and J. A. Greene, "The burden of disease and the changing task of medicine," *N. Engl. J. Med.*, vol. 366, no. 25, pp. 2333–2338, Jun. 2012.

[14] World Health Organization, "WHO | Global tuberculosis control 2011." [Online]. Available: http://www.who.int/tb/publications/global_report/en/. [Accessed: 17-Jun-2012].

[15] D. G. Russell, P.-J. Cardona, M.-J. Kim, S. Allain, and F. Altare, “Foamy macrophages and the progression of the human tuberculosis granuloma,” *Nat. Immunol.*, vol. 10, no. 9, pp. 943–948, Sep. 2009.
[16] D. G. Russell, “Who puts the tubercle in tuberculosis?,” *Nat. Rev. Microbiol.*, vol. 5, no. 1, pp. 39–47, Jan. 2007.
[17] D. G. Russell, C. E. Barry 3rd, and J. L. Flynn, “Tuberculosis: what we don’t know can, and does, hurt us,” *Science*, vol. 328, no. 5980, pp. 852–856, May 2010.
[18] P. Peyron, J. Vaubourgeix, Y. Poquet, F. Levillain, C. Botanch, F. Bardou, M. Daffé, J.-F. Emile, B. Marchou, P.-J. Cardona, C. de Chastellier, and F. Altare, “Foamy macrophages from tuberculous patients’ granulomas constitute a nutrient-rich reservoir for M. tuberculosis persistence,” *PLoS Pathog.*, vol. 4, no. 11, p. e1000204, Nov. 2008.
[19] I. L. Leeds, M. J. Magee, E. V. Kurbatova, C. Del Rio, H. M. Blumberg, M. K. Leonard, and C. S. Kraft, “Site of Extrapulmonary Tuberculosis is Associated with HIV Infection,” *Clin. Infect. Dis.*, vol. 55, no. 1, pp. 75–81, Jul. 2012.
[20] A. Jauregui-Amezaga, F. Turon, I. Ordás, M. Gallego, F. Feu, E. Ricart, and J. Panés, “Risk of developing tuberculosis under anti-TNF treatment despite latent infection screening,” *Journal of Crohn’s & colitis*, Jun. 2012.
[21] V. Kumar and D. Pandey, “Isolated hepatosplenic tuberculosis,” *HBPD INT*, vol. 7, no. 3, pp. 328–330, Jun. 2008.
[22] H. Li, W. Liu, and C. You, “Central nervous system tuberculoma,” *J Clin Neurosci*, vol. 19, no. 5, pp. 691–695, May 2012.
[23] A. L. K. Elnaim, “Bilateral Psoas Abscess and Extensive Soft Tissue Involvement Due to Late Presentation of Pott’s Disease of the Spine,” *Indian J Surg*, vol. 73, no. 2, pp. 161–162, Apr. 2011.
[24] C. K. Kwan and J. D. Ernst, “HIV and tuberculosis: a deadly human syndemic,” *Clin. Microbiol. Rev.*, vol. 24, no. 2, pp. 351–376, Apr. 2011.
[25] K. Lönnroth, K. G. Castro, J. M. Chakaya, L. S. Chauhan, K. Floyd, P. Glaziou, and M. C. Raviglione, “Tuberculosis control and elimination 2010-50: cure, care, and social development,” *Lancet*, vol. 375, no. 9728, pp. 1814–1829, May 2010.
[26] R. C. Maulitz and S. R. Maulitz, “The King’s Evil in Oxfordshire.,” *Med Hist*, vol. 17, no. 1, pp. 87–89, Jan. 1973.
[27] S. A. Knopf, *A history of the National tuberculosis association: the anti-tuberculosis movement in the United States*. National Tuberculosis Association, 1922.
[28] T. H. M. Ottenhoff and S. H. E. Kaufmann, “Vaccines against Tuberculosis: Where Are We and Where Do We Need to Go?,” *PLoS Pathog.*, vol. 8, no. 5, p. e1002607, May 2012.
[29] A. Keyser, J. M. Troudt, J. L. Taylor, and A. A. Izzo, “BCG sub-strains induce variable protection against virulent pulmonary *Mycobacterium tuberculosis* infection, with the capacity to drive Th2 immunity,” *Vaccine*, vol. 29, no. 50, pp. 9308–9315, Nov. 2011.

[30] P. E. M. Fine and E. Vynnycky, “The effect of heterologous immunity upon the apparent efficacy of (e.g. BCG) vaccines,” *Vaccine*, vol. 16, no. 20, pp. 1923–1928, Dec. 1998.
[31] M. A. Behr, “BCG--different strains, different vaccines?,” *Lancet Infect Dis*, vol. 2, no. 2, pp. 86–92, Feb. 2002.
[32] J. F. Murray, “A Century of Tuberculosis,” *Am. J. Respir. Crit. Care Med.*, vol. 169, no. 11, pp. 1181–1186, Jun. 2004.
[33] Z. Taylor, C. M. Nolan, and H. M. Blumberg, “Controlling tuberculosis in the United States. Recommendations from the American Thoracic Society, CDC, and the Infectious Diseases Society of America,” *MMWR Recomm Rep*, vol. 54, no. RR-12, pp. 1–81, Nov. 2005.
[34] J. C. Sacchettini, E. J. Rubin, and J. S. Freundlich, “Drugs versus bugs: in pursuit of the persistent predator *Mycobacterium tuberculosis*,” *Nat. Rev. Microbiol.*, vol. 6, no. 1, pp. 41–52, Jan. 2008.
[35] L. K. Altman, “TB Patient Is Isolated After Taking Two Flights,” *The New York Times*, 30-May-2007.
[36] D. Frosch, “Traveler With TB Is Released After Treatment in Denver,” *The New York Times*, 27-Jul-2007.
[37] C. Hoffmann, A. Leis, M. Niederweis, J. M. Plitzko, and H. Engelhardt, “Disclosure of the mycobacterial outer membrane: cryo-electron tomography and vitreous sections reveal the lipid bilayer structure,” *Proc. Natl. Acad. Sci. U.S.A.*, vol. 105, no. 10, pp. 3963–3967, Mar. 2008.
[38] S. T. Cole, R. Brosch, J. Parkhill, T. Garnier, C. Churcher, D. Harris, S. V. Gordon, K. Eiglmeier, S. Gas, C. E. Barry 3rd, F. Tekaia, K. Badcock, D. Basham, D. Brown, T. Chillingworth, R. Connor, R. Davies, K. Devlin, T. Feltwell, S. Gentles, N. Hamlin, S. Holroyd, T. Hornsby, K. Jagels, A. Krogh, J. McLean, S. Moule, L. Murphy, K. Oliver, J. Osborne, M. A. Quail, M. A. Rajandream, J. Rogers, S. Rutter, K. Seeger, J. Skelton, R. Squares, S. Squares, J. E. Sulston, K. Taylor, S. Whitehead, and B. G. Barrell, “Deciphering the biology of *Mycobacterium tuberculosis* from the complete genome sequence,” *Nature*, vol. 393, no. 6685, pp. 537–544, Jun. 1998.
[39] T. Miyoshi-Akiyama, K. Matsumura, H. Iwai, K. Funatogawa, and T. Kirikae, “Complete annotated genome sequence of *Mycobacterium tuberculosis* Erdman,” *J. Bacteriol.*, vol. 194, no. 10, p. 2770, May 2012.
[40] D. J. V. Beste, M. Espasa, B. Bonde, A. M. Kierzek, G. R. Stewart, and J. McFadden, “The genetic requirements for fast and slow growth in mycobacteria,” *PLoS ONE*, vol. 4, no. 4, p. e5349, 2009.
[41] S. E. Valway, M. P. Sanchez, T. F. Shinnick, I. Orme, T. Agerton, D. Hoy, J. S. Jones, H. Westmoreland, and I. M. Onorato, “An outbreak involving extensive transmission of a virulent strain of *Mycobacterium tuberculosis*,” *N. Engl. J. Med.*, vol. 338, no. 10, pp. 633–639, Mar. 1998.
[42] C. Manca, L. Tsenova, C. E. Barry 3rd, A. Bergtold, S. Freeman, P. A. Haslett, J. M. Musser, V. H. Freedman, and G. Kaplan, “*Mycobacterium tuberculosis* CDC1551 induces a more vigorous host response in vivo and in vitro, but is not more virulent than other clinical isolates,” *J. Immunol.*, vol. 162, no. 11, pp. 6740–6746, Jun. 1999.

[43] J. M. Grange, "*Mycobacterium bovis* infection in human beings," *Tuberculosis*, vol. 81, no. 1–2, pp. 71–77, Feb. 2001.
[44] K. N. Lewis, R. Liao, K. M. Guinn, M. J. Hickey, S. Smith, M. A. Behr, and D. R. Sherman, "Deletion of RD1 from *Mycobacterium tuberculosis* mimics bacille Calmette-Guérin attenuation," *J. Infect. Dis.*, vol. 187, no. 1, pp. 117–123, Jan. 2003.
[45] B. S. A. Kabeer, A. Raja, B. Raman, S. Thangaraj, M. Leportier, G. Ippolito, E. Girardi, P. H. Lagrange, and D. Goletti, "IP-10 response to RD1 antigens might be a useful biomarker for monitoring tuberculosis therapy," *BMC Infect. Dis.*, vol. 11, p. 135, 2011.
[46] C. Wang, R. Fu, Z. Chen, K. Tan, L. Chen, X. Teng, J. Lu, C. Shi, and X. Fan, "Immunogenicity and Protective Efficacy of a Novel Recombinant BCG Strain Overexpressing Antigens Ag85A and Ag85B," *Clin. Dev. Immunol.*, vol. 2012, p. 563838, 2012.
[47] K. Jensen, U. D. K. Ranganathan, K. K. A. Van Rompay, D. R. Canfield, I. Khan, R. Ravindran, P. A. Luciw, W. R. Jacobs Jr, G. Fennelly, M. Larsen, and K. Abel, "A recombinant attenuated *Mycobacterium tuberculosis* vaccine strain is safe in immunosuppressed SIV-infected infant macaques," *Clinical and vaccine immunology: CVI*, Jun. 2012.
[48] M. H. Larsen, W. R. Jacobs, S. A. Porcelli, J. Kim, U. D. K. Ranganathan, and G. J. Fennelly, "Balancing safety and immunogenicity in live-attenuated mycobacterial vaccines for use in humans at risk for HIV: response to misleading comments in Ranganathan et al. 'recombinant pro-apoptotic *Mycobacterium tuberculosis* generates CD8+ T cell responses against human immunodeficiency virus type 1 Env and M. tuberculosis in neonatal mice'," *Vaccine*, vol. 28, no. 21, pp. 3633–3634, May 2010.
[49] C. Aagaard, T. Hoang, J. Dietrich, P.-J. Cardona, A. Izzo, G. Dolganov, G. K. Schoolnik, J. P. Cassidy, R. Billeskov, and P. Andersen, "A multistage tuberculosis vaccine that confers efficient protection before and after exposure," *Nat. Med.*, vol. 17, no. 2, pp. 189–194, Feb. 2011.
[50] P. L. Lin, J. Dietrich, E. Tan, R. M. Abalos, J. Burgos, C. Bigbee, M. Bigbee, L. Milk, H. P. Gideon, M. Rodgers, C. Cochran, K. M. Guinn, D. R. Sherman, E. Klein, C. Janssen, J. L. Flynn, and P. Andersen, "The multistage vaccine H56 boosts the effects of BCG to protect cynomolgus macaques against active tuberculosis and reactivation of latent *Mycobacterium tuberculosis* infection," *J. Clin. Invest.*, vol. 122, no. 1, pp. 303–314, Jan. 2012.
[51] M. U. Shiloh and P. A. DiGiuseppe Champion, "To catch a killer. What can mycobacterial models teach us about *Mycobacterium tuberculosis* pathogenesis?," *Curr Opin Microbiol*, vol. 13, no. 1, pp. 86–92, Feb. 2010.
[52] S. B. Snapper, R. E. Melton, S. Mustafa, T. Kieser, and W. R. Jacobs Jr, "Isolation and characterization of efficient plasmid transformation mutants of *Mycobacterium smegmatis*," *Mol. Microbiol.*, vol. 4, no. 11, pp. 1911–1919, Nov. 1990.
[53] K. Velmurugan, B. Chen, J. L. Miller, S. Azogue, S. Gurses, T. Hsu, M. Glickman, W. R. Jacobs Jr, S. A. Porcelli, and V. Briken, "*Mycobacterium*

*tuberculosis* nuoG is a virulence gene that inhibits apoptosis of infected host cells," *PLoS Pathog.*, vol. 3, no. 7, p. e110, Jul. 2007.
[54] M. J. M. Vaerewijck, G. Huys, J. C. Palomino, J. Swings, and F. Portaels, "Mycobacteria in drinking water distribution systems: ecology and significance for human health," *FEMS Microbiology Reviews*, vol. 29, no. 5, pp. 911–934, 2005.
[55] E. Tortoli, "*Mycobacterium kansasii*, species or complex? Biomolecular and epidemiological insights," *Kekkaku*, vol. 78, no. 11, pp. 705–709, Nov. 2003.
[56] E. Chimara, L. Ferrazoli, S. Y. M. Ueky, M. C. Martins, A. M. Durham, R. D. Arbeit, and S. C. Leão, "Reliable identification of mycobacterial species by PCR-restriction enzyme analysis (PRA)-hsp65 in a reference laboratory and elaboration of a sequence-based extended algorithm of PRA-hsp65 patterns," *BMC Microbiol.*, vol. 8, p. 48, 2008.
[57] R. M. Thomson, "Changing epidemiology of pulmonary nontuberculous mycobacteria infections," *Emerging Infect. Dis.*, vol. 16, no. 10, pp. 1576–1583, Oct. 2010.
[58] S. Tsuchiya, M. Yamabe, Y. Yamaguchi, Y. Kobayashi, T. Konno, and K. Tada, "Establishment and characterization of a human acute monocytic leukemia cell line (THP-1)," *Int. J. Cancer*, vol. 26, no. 2, pp. 171–176, Aug. 1980.
[59] I. Komuro, N. Keicho, A. Iwamoto, and K. S. Akagawa, "Human alveolar macrophages and granulocyte-macrophage colony-stimulating factor-induced monocyte-derived macrophages are resistant to H2O2 via their high basal and inducible levels of catalase activity," *J. Biol. Chem.*, vol. 276, no. 26, pp. 24360–24364, Jun. 2001.
[60] Mantovani, Sica, and M. Locati, "Macrophage Polarization Comes of Age," *Immunity*, vol. 23, no. 4, pp. 344–346, Oct. 2005.
[61] C. A. Dinarello, "Blocking IL-1 in Systemic Inflammation," *J Exp Med*, vol. 201, no. 9, pp. 1355–1359, May 2005.
[62] W. Noël, G. Raes, G. Hassanzadeh Ghassabeh, P. De Baetselier, and A. Beschin, "Alternatively activated macrophages during parasite infections," *Trends in Parasitology*, vol. 20, no. 3, pp. 126–133, Mar. 2004.
[63] K. Nakata, K. S. Akagawa, M. Fukayama, Y. Hayashi, M. Kadokura, and T. Tokunaga, "Granulocyte-Macrophage Colony-Stimulating Factor Promotes the Proliferation of Human Alveolar Macrophages in Vitro.," *J Immunol*, vol. 147, no. 4, pp. 1266–1272, Aug. 1991.
[64] S.-I. Hashimoto, T. Suzuki, H.-Y. Dong, N. Yamazaki, and K. Matsushima, "Serial Analysis of Gene Expression in Human Monocytes and Macrophages," *Blood*, vol. 94, no. 3, pp. 837–844, Aug. 1999.
[65] F. A. W. Verreck, T. D. Boer, D. M. L. Langenberg, M. A. Hoeve, M. Kramer, E. Vaisberg, R. Kastelein, A. Kolk, R. D. Waal-Malefyt, and T. H. M. Ottenhoff, "Human IL-23-Producing Type 1 Macrophages Promote but IL-10-Producing Type 2 Macrophages Subvert Immunity to (myco)bacteria," *PNAS*, vol. 101, no. 13, pp. 4560–4565, Mar. 2004.
[66] I. Komuro, T. Yasuda, A. Iwamoto, and K. S. Akagawa, "Catalase plays a critical role in the CSF-independent survival of human macrophages via

regulation of the expression of BCL-2 family," *J. Biol. Chem.*, vol. 280, no. 50, pp. 41137–41145, Dec. 2005.
[67] JAX, (2012)., "Jackson Laboratory Mice and Services Database. http://jaxmice.jax.org/." [Online]. Available: http://jaxmice.jax.org/. [Accessed: 18-Jun-2012].
[68] A. Apt and I. Kramnik, "Man and mouse TB: Contradictions and solutions," *Tuberculosis*, vol. 89, no. 3, pp. 195–198, May 2009.
[69] J. G. McCaskill, K. D. Chason, X. Hua, I. P. Neuringer, A. J. Ghio, W. K. Funkhouser, and S. L. Tilley, "Pulmonary immune responses to Propionibacterium acnes in C57BL/6 and BALB/c mice," *Am. J. Respir. Cell Mol. Biol.*, vol. 35, no. 3, pp. 347–356, Sep. 2006.
[70] R. Chatelain, K. Varkila, and R. L. Coffman, "IL-4 induces a Th2 response in *Leishmania major*-infected mice," *J. Immunol.*, vol. 148, no. 4, pp. 1182–1187, Feb. 1992.
[71] P. L. Lin, J. Yee, E. Klein, and N. W. Lerche, "Immunological concepts in tuberculosis diagnostics for non-human primates: a review," *J. Med. Primatol.*, vol. 37 Suppl 1, pp. 44–51, Feb. 2008.
[72] P. J. Converse, P. C. Karakousis, L. G. Klinkenberg, A. K. Kesavan, L. H. Ly, S. S. Allen, J. H. Grosset, S. K. Jain, G. Lamichhane, Y. C. Manabe, D. N. McMurray, E. L. Nuermberger, and W. R. Bishai, "Role of the dosR-dosS two-component regulatory system in *Mycobacterium tuberculosis* virulence in three animal models," *Infect. Immun.*, vol. 77, no. 3, pp. 1230–1237, Mar. 2009.
[73] J. L. Flynn, S. V. Capuano, D. Croix, S. Pawar, A. Myers, A. Zinovik, and E. Klein, "Non-human primates: a model for tuberculosis research," *Tuberculosis (Edinb)*, vol. 83, no. 1–3, pp. 116–118, 2003.
[74] S. A. Sharpe, H. McShane, M. J. Dennis, R. J. Basaraba, F. Gleeson, G. Hall, A. McIntyre, K. Gooch, S. Clark, N. E. R. Beveridge, E. Nuth, A. White, A. Marriott, S. Dowall, A. V. S. Hill, A. Williams, and P. D. Marsh, "Establishment of an aerosol challenge model of tuberculosis in rhesus macaques and an evaluation of endpoints for vaccine testing," *Clin. Vaccine Immunol.*, vol. 17, no. 8, pp. 1170–1182, Aug. 2010.
[75] Y. C. Manabe, A. K. Kesavan, J. Lopez-Molina, C. L. Hatem, M. Brooks, R. Fujiwara, K. Hochstein, M. L. M. Pitt, J. Tufariello, J. Chan, D. N. McMurray, W. R. Bishai, A. M. Dannenberg Jr, and S. Mendez, "The aerosol rabbit model of TB latency, reactivation and immune reconstitution inflammatory syndrome," *Tuberculosis (Edinb)*, vol. 88, no. 3, pp. 187–196, May 2008.
[76] M. S. Jassal, G. G. Nedeltchev, J. Osborne, and W. R. Bishai, "A modified scoring system to describe gross pathology in the rabbit model of tuberculosis," *BMC Microbiol.*, vol. 11, p. 49, 2011.
[77] H. Cho, R. de Haas, A. Jeevan, and D. N. McMurray, "Differential activation of alveolar and peritoneal macrophages from BCG-vaccinated guinea pigs," *Tuberculosis (Edinb)*, vol. 88, no. 4, pp. 307–316, Jul. 2008.
[78] A. S. Dharmadhikari and E. A. Nardell, "What animal models teach humans about tuberculosis," *Am. J. Respir. Cell Mol. Biol.*, vol. 39, no. 5, pp. 503–508, Nov. 2008.

[79] D. Ordway, G. Palanisamy, M. Henao-Tamayo, E. E. Smith, C. Shanley, I. M. Orme, and R. J. Basaraba, "The Cellular Immune Response to *Mycobacterium tuberculosis* Infection in the Guinea Pig," *J Immunol*, vol. 179, no. 4, pp. 2532–2541, Aug. 2007.
[80] I. Vergne, J. Chua, S. B. Singh, and V. Deretic, "Cell biology of *Mycobacterium tuberculosis* phagosome," *Annu. Rev. Cell Dev. Biol.*, vol. 20, pp. 367–394, 2004.
[81] R. Bryk, P. Griffin, and C. Nathan, "Peroxynitrite reductase activity of bacterial peroxiredoxins," *Nature*, vol. 407, no. 6801, pp. 211–215, Sep. 2000.
[82] A. Gupta, A. Kaul, A. G. Tsolaki, U. Kishore, and S. Bhakta, "*Mycobacterium tuberculosis*: Immune evasion, latency and reactivation," *Immunobiology*, vol. 217, no. 3, pp. 363–374, Mar. 2012.
[83] A. Walburger, A. Koul, G. Ferrari, L. Nguyen, C. Prescianotto-Baschong, K. Huygen, B. Klebl, C. Thompson, G. Bacher, and J. Pieters, "Protein kinase G from pathogenic mycobacteria promotes survival within macrophages," *Science*, vol. 304, no. 5678, pp. 1800–1804, Jun. 2004.
[84] C. A. Scanga, V. P. Mohan, K. Tanaka, D. Alland, J. L. Flynn, and J. Chan, "The inducible nitric oxide synthase locus confers protection against aerogenic challenge of both clinical and laboratory strains of *Mycobacterium tuberculosis* in mice," *Infect. Immun.*, vol. 69, no. 12, pp. 7711–7717, Dec. 2001.
[85] R. Bryk, C. D. Lima, H. Erdjument-Bromage, P. Tempst, and C. Nathan, "Metabolic enzymes of mycobacteria linked to antioxidant defense by a thioredoxin-like protein," *Science*, vol. 295, no. 5557, pp. 1073–1077, Feb. 2002.
[86] K. H. Darwin, S. Ehrt, J.-C. Gutierrez-Ramos, N. Weich, and C. F. Nathan, "The proteasome of *Mycobacterium tuberculosis* is required for resistance to nitric oxide," *Science*, vol. 302, no. 5652, pp. 1963–1966, Dec. 2003.
[87] S. Saikolappan, K. Das, S. J. Sasindran, C. Jagannath, and S. Dhandayuthapani, "OsmC proteins of *Mycobacterium tuberculosis* and *Mycobacterium smegmatis* protect against organic hydroperoxide stress," *Tuberculosis (Edinb)*, vol. 91 Suppl 1, pp. S119–127, Dec. 2011.
[88] R. Colangeli, A. Haq, V. L. Arcus, E. Summers, R. S. Magliozzo, A. McBride, A. K. Mitra, M. Radjainia, A. Khajo, W. R. Jacobs Jr, P. Salgame, and D. Alland, "The multifunctional histone-like protein Lsr2 protects mycobacteria against reactive oxygen intermediates," *Proc. Natl. Acad. Sci. U.S.A.*, vol. 106, no. 11, pp. 4414–4418, Mar. 2009.
[89] E. L. Summers, K. Meindl, I. Usón, A. K. Mitra, M. Radjainia, R. Colangeli, D. Alland, and V. L. Arcus, "The Structure of the Oligomerization Domain of Lsr2 from *Mycobacterium tuberculosis* Reveals a Mechanism for Chromosome Organization and Protection," *PLoS ONE*, vol. 7, no. 6, p. e38542, 2012.
[90] J. Keane, M. K. Balcewicz-Sablinska, H. G. Remold, G. L. Chupp, B. B. Meek, M. J. Fenton, and H. Kornfeld, "Infection by *Mycobacterium tuberculosis* promotes human alveolar macrophage apoptosis," *Infect. Immun.*, vol. 65, no. 1, pp. 298–304, Jan. 1997.
[91] J. Keane, H. G. Remold, and H. Kornfeld, "Virulent *Mycobacterium tuberculosis* strains evade apoptosis of infected alveolar macrophages," *J. Immunol.*, vol. 164, no. 4, pp. 2016–2020, Feb. 2000.

[92] A. Spira, J. D. Carroll, G. Liu, Z. Aziz, V. Shah, H. Kornfeld, and J. Keane, "Apoptosis genes in human alveolar macrophages infected with virulent or attenuated *Mycobacterium tuberculosis*: a pivotal role for tumor necrosis factor," *Am. J. Respir. Cell Mol. Biol.*, vol. 29, no. 5, pp. 545–551, Nov. 2003.

[93] M. L. Arcila, M. D. Sánchez, B. Ortiz, L. F. Barrera, L. F. García, and M. Rojas, "Activation of apoptosis, but not necrosis, during *Mycobacterium tuberculosis* infection correlated with decreased bacterial growth: role of TNF-alpha, IL-10, caspases and phospholipase A2," *Cell. Immunol.*, vol. 249, no. 2, pp. 80–93, Oct. 2007.

[94] L. Danelishvili, Y. Yamazaki, J. Selker, and L. E. Bermudez, "Secreted *Mycobacterium tuberculosis* Rv3654c and Rv3655c Proteins Participate in the Suppression of Macrophage Apoptosis," *PLoS ONE*, vol. 5, no. 5, p. e10474, May 2010.

[95] M. Chen, H. Gan, and H. G. Remold, "A mechanism of virulence: virulent *Mycobacterium tuberculosis* strain H37Rv, but not attenuated H37Ra, causes significant mitochondrial inner membrane disruption in macrophages leading to necrosis," *J. Immunol.*, vol. 176, no. 6, pp. 3707–3716, Mar. 2006.

[96] W. W. Navarre and A. Zychlinsky, "Pathogen-induced apoptosis of macrophages: a common end for different pathogenic strategies," *Cell. Microbiol.*, vol. 2, no. 4, pp. 265–273, Aug. 2000.

[97] S. M. Behar, C. J. Martin, C. Nunes-Alves, M. Divangahi, and H. G. Remold, "Lipids, apoptosis, and cross-presentation: links in the chain of host defense against *Mycobacterium tuberculosis*," *Microbes Infect.*, vol. 13, no. 8–9, pp. 749–756, Aug. 2011.

[98] R. Simeone, A. Bobard, J. Lippmann, W. Bitter, L. Majlessi, R. Brosch, and J. Enninga, "Phagosomal rupture by *Mycobacterium tuberculosis* results in toxicity and host cell death," *PLoS Pathog.*, vol. 8, no. 2, p. e1002507, Feb. 2012.

[99] K.-W. Wong and W. R. Jacobs Jr, "Critical role for NLRP3 in necrotic death triggered by *Mycobacterium tuberculosis*," *Cell. Microbiol.*, vol. 13, no. 9, pp. 1371–1384, Sep. 2011.

[100] M. Divangahi, M. Chen, H. Gan, D. Desjardins, T. T. Hickman, D. M. Lee, S. Fortune, S. M. Behar, and H. G. Remold, "*Mycobacterium tuberculosis* evades macrophage defenses by inhibiting plasma membrane repair," *Nat. Immunol.*, vol. 10, no. 8, pp. 899–906, Aug. 2009.

[101] A. Welin, D. Eklund, O. Stendahl, and M. Lerm, "Human Macrophages Infected with a High Burden of ESAT-6-Expressing *M. tuberculosis* Undergo Caspase-1- and Cathepsin B-Independent Necrosis," *PLoS ONE*, vol. 6, no. 5, p. e20302, May 2011.

[102] S.-G. Cho and E.-J. Choi, "Apoptotic signaling pathways: caspases and stress-activated protein kinases," *J. Biochem. Mol. Biol.*, vol. 35, no. 1, pp. 24–27, Jan. 2002.

[103] U. E. Schaible, F. Winau, P. A. Sieling, K. Fischer, H. L. Collins, K. Hagens, R. L. Modlin, V. Brinkmann, and S. H. E. Kaufmann, "Apoptosis facilitates antigen presentation to T lymphocytes through MHC-I and CD1 in tuberculosis," *Nat. Med.*, vol. 9, no. 8, pp. 1039–1046, Aug. 2003.

[104] F. Winau, S. H. E. Kaufmann, and U. E. Schaible, “Apoptosis paves the detour path for CD8 T cell activation against intracellular bacteria,” *Cell. Microbiol.*, vol. 6, no. 7, pp. 599–607, Jul. 2004.
[105] F. Winau, S. Weber, S. Sad, J. de Diego, S. L. Hoops, B. Breiden, K. Sandhoff, V. Brinkmann, S. H. E. Kaufmann, and U. E. Schaible, “Apoptotic vesicles crossprime CD8 T cells and protect against tuberculosis,” *Immunity*, vol. 24, no. 1, pp. 105–117, Jan. 2006.
[106] J. Hinchey, B. Y. Jeon, H. Alley, B. Chen, M. Goldberg, S. Derrick, S. Morris, W. R. Jacobs Jr, S. A. Porcelli, and S. Lee, “Lysine auxotrophy combined with deletion of the SecA2 gene results in a safe and highly immunogenic candidate live attenuated vaccine for tuberculosis,” *PLoS ONE*, vol. 6, no. 1, p. e15857, 2011.
[107] D. Kumar and S. Narayanan, “pknE, a serine/threonine kinase of *Mycobacterium tuberculosis* modulates multiple apoptotic paradigms,” *Infect. Genet. Evol.*, vol. 12, no. 4, pp. 737–747, Jun. 2012.
[108] N. K. Dutta, S. Mehra, A. N. Martinez, X. Alvarez, N. A. Renner, L. A. Morici, B. Pahar, A. G. Maclean, A. A. Lackner, and D. Kaushal, “The stress-response factor SigH modulates the interaction between *Mycobacterium tuberculosis* and host phagocytes,” *PLoS ONE*, vol. 7, no. 1, p. e28958, 2012.
[109] J. L. Miller, K. Velmurugan, M. J. Cowan, and V. Briken, “The type I NADH dehydrogenase of *Mycobacterium tuberculosis* counters phagosomal NOX2 activity to inhibit TNF-alpha-mediated host cell apoptosis,” *PLoS Pathog.*, vol. 6, no. 4, p. e1000864, Apr. 2010.
[110] D. Jayakumar, W. R. Jacobs Jr, and S. Narayanan, “Protein kinase E of *Mycobacterium tuberculosis* has a role in the nitric oxide stress response and apoptosis in a human macrophage model of infection,” *Cell. Microbiol.*, vol. 10, no. 2, pp. 365–374, Feb. 2008.
[111] J. T. Sullivan, E. F. Young, J. R. McCann, and M. Braunstein, “The *Mycobacterium tuberculosis* SecA2 system subverts phagosome maturation to promote growth in macrophages,” *Infect. Immun.*, vol. 80, no. 3, pp. 996–1006, Mar. 2012.
[112] R. Jain, B. Dey, A. Khera, P. Srivastav, U. D. Gupta, V. M. Katoch, V. D. Ramanathan, and A. K. Tyagi, “Over-expression of superoxide dismutase obliterates the protective effect of BCG against tuberculosis by modulating innate and adaptive immune responses,” *Vaccine*, vol. 29, no. 45, pp. 8118–8125, Oct. 2011.
[113] M. Niki, M. Niki, Y. Tateishi, Y. Ozeki, T. Kirikae, A. Lewin, Y. Inoue, M. Matsumoto, J. L. Dahl, H. Ogura, K. Kobayashi, and S. Matsumoto, “A novel mechanism of growth phase-dependent tolerance to isoniazid in mycobacteria,” *The Journal of biological chemistry*, May 2012.
[114] S. Mehra, N. A. Golden, K. Stuckey, P. J. Didier, L. A. Doyle, K. E. Russell-Lodrigue, C. Sugimoto, A. Hasegawa, S. K. Sivasubramani, C. J. Roy, X. Alvarez, M. J. Kuroda, J. L. Blanchard, A. A. Lackner, and D. Kaushal, “The *Mycobacterium tuberculosis* stress response factor SigH is required for bacterial burden as well as immunopathology in primate lungs,” *J. Infect. Dis.*, vol. 205, no. 8, pp. 1203–1213, Apr. 2012.

[115] L. Danelishvili, J. L. Everman, M. J. McNamara, and L. E. Bermudez, "Inhibition of the Plasma-Membrane-Associated Serine Protease Cathepsin G by *Mycobacterium tuberculosis* Rv3364c Suppresses Caspase-1 and Pyroptosis in Macrophages," *Front Microbiol*, vol. 2, p. 281, 2011.
[116] G. Xu, H. Jia, Y. Li, X. Liu, M. Li, and Y. Wang, "Hemolytic phospholipase Rv0183 of *Mycobacterium tuberculosis* induces inflammatory response and apoptosis in alveolar macrophage RAW264.7 cells," *Can. J. Microbiol.*, vol. 56, no. 11, pp. 916–924, Nov. 2010.
[117] V. Briken and J. L. Miller, "Living on the edge: inhibition of host cell apoptosis by *Mycobacterium tuberculosis*," *Future Microbiol*, vol. 3, no. 4, pp. 415–422, Aug. 2008.
[118] J. Hinchey, S. Lee, B. Y. Jeon, R. J. Basaraba, M. M. Venkataswamy, B. Chen, J. Chan, M. Braunstein, I. M. Orme, S. C. Derrick, S. L. Morris, W. R. Jacobs Jr, and S. A. Porcelli, "Enhanced priming of adaptive immunity by a proapoptotic mutant of *Mycobacterium tuberculosis*," *J. Clin. Invest.*, vol. 117, no. 8, pp. 2279–2288, Aug. 2007.
[119] M. Muñoz-López and J. L. García-Pérez, "DNA transposons: nature and applications in genomics," *Curr. Genomics*, vol. 11, no. 2, pp. 115–128, Apr. 2010.
[120] R. K. Aziz, M. Breitbart, and R. A. Edwards, "Transposases Are the Most Abundant, Most Ubiquitous Genes in Nature," *Nucl. Acids Res.*, Mar. 2010.
[121] P. Prentki, B. Teter, M. Chandler, and D. J. Galas, "Functional promoters created by the insertion of transposable element IS1," *Journal of Molecular Biology*, vol. 191, no. 3, pp. 383–393, Oct. 1986.
[122] D. J. Strand and J. F. McDonald, "Copia Is Transcriptionally Responsive to Environmental Stress," *Nucl. Acids Res.*, vol. 13, no. 12, pp. 4401–4410, Jun. 1985.
[123] R. Lin, L. Ding, C. Casola, D. R. Ripoll, C. Feschotte, and H. Wang, "Transposase-derived transcription factors regulate light signaling in Arabidopsis," *Science*, vol. 318, no. 5854, pp. 1302–1305, Nov. 2007.
[124] C. Casola, D. Hucks, and C. Feschotte, "Convergent domestication of pogo-like transposases into centromere-binding proteins in fission yeast and mammals," *Mol. Biol. Evol.*, vol. 25, no. 1, pp. 29–41, Jan. 2008.
[125] C.-Y. Cheng, A. Vogt, K. Mochizuki, and M.-C. Yao, "A domesticated piggyBac transposase plays key roles in heterochromatin dynamics and DNA cleavage during programmed DNA deletion in Tetrahymena thermophila," *Mol. Biol. Cell*, vol. 21, no. 10, pp. 1753–1762, May 2010.
[126] A. Agrawal, Q. M. Eastman, and D. G. Schatz, "Transposition mediated by RAG1 and RAG2 and its implications for the evolution of the immune system," *Nature*, vol. 394, no. 6695, pp. 744–751, Aug. 1998.
[127] D. G. Schatz and Y. Ji, "Recombination centres and the orchestration of V(D)J recombination," *Nat. Rev. Immunol.*, vol. 11, no. 4, pp. 251–263, Apr. 2011.
[128] J. Stanley and N. Saunders, "DNA insertion sequences and the molecular epidemiology of Salmonella and Mycobacterium," *J. Med. Microbiol.*, vol. 45, no. 4, pp. 236–251, Oct. 1996.

[129] A. Benedetti, D. Menzies, M. A. Behr, K. Schwartzman, and Y. Jin, "How Close Is Close Enough? Exploring Matching Criteria in the Estimation of Recent Transmission of Tuberculosis," *Am. J. Epidemiol.*, vol. 172, no. 3, pp. 318–326, Aug. 2010.
[130] A. Reyes, A. Sandoval, A. Cubillos-Ruiz, K. E. Varley, I. Hernández-Neuta, S. Samper, C. Martín, M. J. Garcia, V. Ritacco, L. López, J. Robledo, M. M. Zambrano Mmz, R. D. Mitra, and P. Del Portillo, "IS-seq: a novel high throughput survey of in vivo IS6110 transposition in multiple *Mycobacterium tuberculosis* genomes," *BMC genomics*, vol. 13, no. 1, p. 249, Jun. 2012.
[131] C. R. E. McEvoy, A. A. Falmer, N. C. Gey van Pittius, T. C. Victor, P. D. van Helden, and R. M. Warren, "The role of IS6110 in the evolution of *Mycobacterium tuberculosis*," *Tuberculosis (Edinb)*, vol. 87, no. 5, pp. 393–404, Sep. 2007.
[132] A. Coros, E. DeConno, and K. M. Derbyshire, "IS6110, a *Mycobacterium tuberculosis* Complex-Specific Insertion Sequence, Is Also Present in the Genome of *Mycobacterium smegmatis*, Suggestive of Lateral Gene Transfer among Mycobacterial Species," *Journal of Bacteriology*, vol. 190, no. 9, pp. 3408–3410, Mar. 2008.
[133] S. Selvaraj, V. Sambandam, D. Sardar, and S. Anishetty, "In silico analysis of DosR regulon proteins of *Mycobacterium tuberculosis*," *Gene*, Jun. 2012.
[134] P. Du, Y. Yang, H. Wang, D. Liu, G. F. Gao, and C. Chen, "A large scale comparative genomic analysis reveals insertion sites for newly acquired genomic islands in bacterial genomes," *BMC Microbiol.*, vol. 11, p. 135, 2011.
[135] A. A. M. Al Mamun and M. Z. Humayun, "Spontaneous mutagenesis is elevated in protease-defective cells," *Mol. Microbiol.*, vol. 71, no. 3, pp. 629–639, Feb. 2009.
[136] J. P. Murry, C. M. Sassetti, J. M. Lane, Z. Xie, and E. J. Rubin, "Transposon site hybridization in *Mycobacterium tuberculosis*," *Methods Mol. Biol.*, vol. 416, pp. 45–59, 2008.
[137] C. M. Sassetti, D. H. Boyd, and E. J. Rubin, "Genes required for mycobacterial growth defined by high density mutagenesis," *Mol. Microbiol.*, vol. 48, no. 1, pp. 77–84, Apr. 2003.
[138] J. E. Griffin, J. D. Gawronski, M. A. Dejesus, T. R. Ioerger, B. J. Akerley, and C. M. Sassetti, "High-resolution phenotypic profiling defines genes essential for mycobacterial growth and cholesterol catabolism," *PLoS Pathog.*, vol. 7, no. 9, p. e1002251, Sep. 2011.
[139] N. P. Kar, D. Sikriwal, P. Rath, R. K. Choudhary, and J. K. Batra, "*Mycobacterium tuberculosis* ClpC1: characterization and role of the N-terminal domain in its function," *FEBS J.*, vol. 275, no. 24, pp. 6149–6158, Dec. 2008.
[140] R. Dziedzic, M. Kiran, P. Plocinski, M. Ziolkiewicz, A. Brzostek, M. Moomey, I. S. Vadrevu, J. Dziadek, M. Madiraju, and M. Rajagopalan, "*Mycobacterium tuberculosis* ClpX interacts with FtsZ and interferes with FtsZ assembly," *PLoS ONE*, vol. 5, no. 7, p. e11058, 2010.
[141] R. M. Raju, M. Unnikrishnan, D. H. F. Rubin, V. Krishnamoorthy, O. Kandror, T. N. Akopian, A. L. Goldberg, and E. J. Rubin, "*Mycobacterium tuberculosis* ClpP1 and ClpP2 function together in protein degradation and are

required for viability in vitro and during infection," *PLoS Pathog.*, vol. 8, no. 2, p. e1002511, Feb. 2012.
[142] J. Ollinger, T. O'Malley, E. A. Kesicki, J. Odingo, and T. Parish, "Validation of the Essential ClpP Protease in *Mycobacterium tuberculosis* as a Novel Drug Target," *J. Bacteriol.*, vol. 194, no. 3, pp. 663–668, Feb. 2012.
[143] H. Ingvarsson, M. J. Maté, M. Högbom, D. Portnoï, N. Benaroudj, P. M. Alzari, M. Ortiz-Lombardía, and T. Unge, "Insights into the inter-ring plasticity of caseinolytic proteases from the X-ray structure of *Mycobacterium tuberculosis* ClpP1," *Acta Crystallogr. D Biol. Crystallogr.*, vol. 63, no. Pt 2, pp. 249–259, Feb. 2007.
[144] S. Gandotra, M. B. Lebron, and S. Ehrt, "The *Mycobacterium tuberculosis* Proteasome Active Site Threonine Is Essential for Persistence Yet Dispensable for Replication and Resistance to Nitric Oxide," *PLoS Pathog*, vol. 6, no. 8, p. e1001040, 2010.
[145] S. Barik, K. Sureka, P. Mukherjee, J. Basu, and M. Kundu, "RseA, the SigE specific anti-sigma factor of *Mycobacterium tuberculosis*, is inactivated by phosphorylation-dependent ClpC1P2 proteolysis," *Mol. Microbiol.*, vol. 75, no. 3, pp. 592–606, Feb. 2010.
[146] S. M. Butler, R. A. Festa, M. J. Pearce, and K. H. Darwin, "Self-compartmentalized bacterial proteases and pathogenesis," *Mol. Microbiol.*, vol. 60, no. 3, pp. 553–562, May 2006.
[147] O. Gaillot, E. Pellegrini, S. Bregenholt, S. Nair, and P. Berche, "The ClpP serine protease is essential for the intracellular parasitism and virulence of *Listeria monocytogenes*," *Mol. Microbiol.*, vol. 35, no. 6, pp. 1286–1294, Mar. 2000.
[148] G. T. Robertson, W.-L. Ng, J. Foley, R. Gilmour, and M. E. Winkler, "Global transcriptional analysis of clpP mutations of type 2 Streptococcus pneumoniae and their effects on physiology and virulence," *J. Bacteriol.*, vol. 184, no. 13, pp. 3508–3520, Jul. 2002.
[149] G. T. Robertson, W.-L. Ng, R. Gilmour, and M. E. Winkler, "Essentiality of clpX, but not clpP, clpL, clpC, or clpE, in *Streptococcus pneumoniae* R6," *J. Bacteriol.*, vol. 185, no. 9, pp. 2961–2966, May 2003.
[150] C. Webb, M. Moreno, M. Wilmes-Riesenberg, R. Curtiss 3rd, and J. W. Foster, "Effects of DksA and ClpP protease on sigma S production and virulence in *Salmonella typhimurium*," *Mol. Microbiol.*, vol. 34, no. 1, pp. 112–123, Oct. 1999.
[151] M. Estorninho, H. Smith, J. Thole, J. Harders-Westerveen, A. Kierzek, R. E. Butler, O. Neyrolles, and G. R. Stewart, "ClgR regulation of chaperone and protease systems is essential for *Mycobacterium tuberculosis* parasitism of the macrophage," *Microbiology (Reading, Engl.)*, vol. 156, no. Pt 11, pp. 3445–3455, Nov. 2010.
[152] A. M. Sherrid, T. R. Rustad, G. A. Cangelosi, and D. R. Sherman, "Characterization of a Clp protease gene regulator and the reaeration response in *Mycobacterium tuberculosis*," *PLoS ONE*, vol. 5, no. 7, p. e11622, 2010.

[153] S. Mehra and D. Kaushal, “Functional genomics reveals extended roles of the *Mycobacterium tuberculosis* stress response factor sigmaH,” *J. Bacteriol.*, vol. 191, no. 12, pp. 3965–3980, Jun. 2009.
[154] E. K. Schmitt, M. Riwanto, V. Sambandamurthy, S. Roggo, C. Miault, C. Zwingelstein, P. Krastel, C. Noble, D. Beer, S. P. S. Rao, M. Au, P. Niyomrattanakit, V. Lim, J. Zheng, D. Jeffery, K. Pethe, and L. R. Camacho, “The natural product cyclomarin kills *Mycobacterium tuberculosis* by targeting the ClpC1 subunit of the caseinolytic protease,” *Angew. Chem. Int. Ed. Engl.*, vol. 50, no. 26, pp. 5889–5891, Jun. 2011.
[155] TARGET, “TARGET: JHU Home.” [Online]. Available: http://webhost.nts.jhu.edu/target/. [Accessed: 21-Jun-2012].
[156] TARGET, “TBVTRM Contract - Transposon Mutant Libraray - Colorado State University.” [Online]. Available: http://www.cvmbs.colostate.edu/mip/tb/tnmutants.htm. [Accessed: 21-Jun-2012].
[157] BEI, “BEI Resources- Mtb.” [Online]. Available: http://www.beiresources.org/tabid/716/stabid/75/PathogenLinkID/55/Default.aspx#Bacteria. [Accessed: 21-Jun-2012].
[158] G. Lamichhane, M. Zignol, N. J. Blades, D. E. Geiman, A. Dougherty, J. Grosset, K. W. Broman, and W. R. Bishai, “A postgenomic method for predicting essential genes at subsaturation levels of mutagenesis: application to *Mycobacterium tuberculosis*,” *Proc. Natl. Acad. Sci. U.S.A.*, vol. 100, no. 12, pp. 7213–7218, Jun. 2003.
[159] S. Bardarov, S. Bardarov Jr Jr, M. S. Pavelka Jr Jr, V. Sambandamurthy, M. Larsen, J. Tufariello, J. Chan, G. Hatfull, and W. R. Jacobs Jr Jr, “Specialized transduction: an efficient method for generating marked and unmarked targeted gene disruptions in *Mycobacterium tuberculosis*, M. bovis BCG and M. smegmatis,” *Microbiology (Reading, Engl.)*, vol. 148, no. Pt 10, pp. 3007–3017, Oct. 2002.
[160] W. R. Jacobs, *Molecular Genetics of Mycobacteria*. ASM Press, 2000.
[161] T. B. K. Reddy, R. Riley, F. Wymore, P. Montgomery, D. DeCaprio, R. Engels, M. Gellesch, J. Hubble, D. Jen, H. Jin, M. Koehrsen, L. Larson, M. Mao, M. Nitzberg, P. Sisk, C. Stolte, B. Weiner, J. White, Z. K. Zachariah, G. Sherlock, J. E. Galagan, C. A. Ball, and G. K. Schoolnik, “TB database: an integrated platform for tuberculosis research,” *Nucleic Acids Research*, vol. 37, no. Database, pp. D499–D508, Jan. 2009.
[162] S. M. Behar, C. J. Martin, M. G. Booty, T. Nishimura, X. Zhao, H.-X. Gan, M. Divangahi, and H. G. Remold, “Apoptosis is an innate defense function of macrophages against *Mycobacterium tuberculosis*,” *Mucosal Immunol*, vol. 4, no. 3, pp. 279–287, May 2011.
[163] S. M. Behar, M. Divangahi, and H. G. Remold, “Evasion of innate immunity by *Mycobacterium tuberculosis*: is death an exit strategy?,” *Nat. Rev. Microbiol.*, vol. 8, no. 9, pp. 668–674, Sep. 2010.
[164] TubercuList, “TubercuList Web Server.” [Online]. Available: http://genolist.pasteur.fr/TubercuList/. [Accessed: 22-Jun-2012].

[165] I. N. Mbawuike and H. B. Herscowitz, "MH-S, a murine alveolar macrophage cell line: morphological, cytochemical, and functional characteristics," *J. Leukoc. Biol.*, vol. 46, no. 2, pp. 119–127, Aug. 1989.
[166] B. Jayashankar, K. P. Mishra, M. S. Y. Kumar, K. Udayasankar, K. Misra, L. Ganju, and S. B. Singh, "A supercritical CO(2) extract from seabuckthorn leaves inhibits pro-inflammatory mediators via inhibition of mitogen activated protein kinase p38 and transcription factor nuclear factor-κB," *Int. Immunopharmacol.*, vol. 13, no. 4, pp. 461–467, Aug. 2012.
[167] S. M. Yeligar, F. L. Harris, C. M. Hart, and L. A. S. Brown, "Ethanol induces oxidative stress in alveolar macrophages via upregulation of NADPH oxidases," *J. Immunol.*, vol. 188, no. 8, pp. 3648–3657, Apr. 2012.
[168] A. Bohsali, H. Abdalla, K. Velmurugan, and V. Briken, "The non-pathogenic mycobacteria *M. smegmatis* and *M. fortuitum* induce rapid host cell apoptosis via a caspase-3 and TNF dependent pathway," *BMC Microbiol.*, vol. 10, p. 237, 2010.
[169] T. van Opijnen, K. L. Bodi, and A. Camilli, "Tn-seq: high-throughput parallel sequencing for fitness and genetic interaction studies in microorganisms," *Nature Methods*, vol. 6, no. 10, pp. 767–772, 2009.
[170] G. Lamichhane, S. Tyagi, and W. R. Bishai, "Designer Arrays for Defined Mutant Analysis To Detect Genes Essential for Survival of *Mycobacterium tuberculosis* in Mouse Lungs," *Infect. Immun.*, vol. 73, no. 4, pp. 2533–2540, Apr. 2005.
[171] M. Pertea, K. Ayanbule, M. Smedinghoff, and S. L. Salzberg, "OperonDB: a comprehensive database of predicted operons in microbial genomes," *Nucleic Acids Research*, vol. 37, no. Database, pp. D479–D482, Jan. 2009.
[172] D. M. Collins and D. M. Stephens, "Identification of an insertion sequence, IS1081, in *Mycobacterium bovis*," *FEMS Microbiol. Lett.*, vol. 67, no. 1, pp. 11–15, Sep. 1991.
[173] D. van Soolingen, P. W. Hermans, P. E. de Haas, and J. D. van Embden, "Insertion element IS1081-associated restriction fragment length polymorphisms in *Mycobacterium tuberculosis* complex species: a reliable tool for recognizing *Mycobacterium bovis* BCG.," *Journal of Clinical Microbiology*, vol. 30, no. 7, p. 1772, Jul. 1992.
[174] G. Lamichhane, J. S. Freundlich, S. Ekins, N. Wickramaratne, S. T. Nolan, and W. R. Bishai, "Essential Metabolites of *Mycobacterium tuberculosis* and Their Mimics," *mBio*, vol. 2, no. 1, pp. e00301–10–e00301–10, Feb. 2011.
[175] R. Gupta, M. Lavollay, J.-L. Mainardi, M. Arthur, W. R. Bishai, and G. Lamichhane, "The *Mycobacterium tuberculosis* protein LdtMt2 is a nonclassical transpeptidase required for virulence and resistance to amoxicillin," *Nat. Med.*, vol. 16, no. 4, pp. 466–469, Apr. 2010.
[176] A. Alahari, L. Alibaud, X. Trivelli, R. Gupta, G. Lamichhane, R. C. Reynolds, W. R. Bishai, Y. Guerardel, and L. Kremer, "Mycolic acid methyltransferase, MmaA4, is necessary for thiacetazone susceptibility in *Mycobacterium tuberculosis*," *Mol. Microbiol.*, vol. 71, no. 5, pp. 1263–1277, Mar. 2009.

[177] "Rv2666 truncated IS1081 transposase [*Mycobacterium tuberculosis* H37Rv] - Gene - NCBI." [Online]. Available: http://www.ncbi.nlm.nih.gov.proxy-um.researchport.umd.edu/gene/888904. [Accessed: 07-Jul-2012].
[178] M. M. Babu, L. M. Iyer, S. Balaji, and L. Aravind, "The natural history of the WRKY-GCM1 zinc fingers and the relationship between transcription factors and transposons," *Nucleic Acids Res.*, vol. 34, no. 22, pp. 6505–6520, 2006.
[179] "M. tuberculosis H37Rv (GB:AL123456): Rv2666 - transposase - TB Genomes." [Online]. Available: http://genome.tbdb.org/annotation/genome/tbdb/GeneDetails.html?sp=S7000000635251931. [Accessed: 23-Jun-2012].
[180] B. Marquina-Castillo, L. García-García, A. Ponce-de-León, M.-E. Jimenez-Corona, M. Bobadilla-Del Valle, B. Cano-Arellano, S. Canizales-Quintero, A. Martinez-Gamboa, M. Kato-Maeda, B. Robertson, D. Young, P. Small, G. Schoolnik, J. Sifuentes-Osornio, and R. Hernandez-Pando, "Virulence, immunopathology and transmissibility of selected strains of *Mycobacterium tuberculosis* in a murine model," *Immunology*, vol. 128, no. 1, pp. 123–133, Sep. 2009.
[181] M.-S. Koo, S. Subbian, and G. Kaplan, "Strain specific transcriptional response in *Mycobacterium tuberculosis* infected macrophages," *Cell Commun. Signal*, vol. 10, no. 1, p. 2, 2012.
[182] M. P. O'Sullivan, S. O'Leary, D. M. Kelly, and J. Keane, "A caspase-independent pathway mediates macrophage cell death in response to *Mycobacterium tuberculosis* infection," *Infect. Immun.*, vol. 75, no. 4, pp. 1984–1993, Apr. 2007.
[183] J. Lee, H. G. Remold, M. H. Ieong, and H. Kornfeld, "Macrophage apoptosis in response to high intracellular burden of *Mycobacterium tuberculosis* is mediated by a novel caspase-independent pathway," *J. Immunol.*, vol. 176, no. 7, pp. 4267–4274, Apr. 2006.
[184] J. Lee, T. Repasy, K. Papavinasasundaram, C. Sassetti, and H. Kornfeld, "*Mycobacterium tuberculosis* induces an atypical cell death mode to escape from infected macrophages," *PLoS ONE*, vol. 6, no. 3, p. e18367, 2011.
[185] I. Nicoletti, G. Migliorati, M. C. Pagliacci, F. Grignani, and C. Riccardi, "A rapid and simple method for measuring thymocyte apoptosis by propidium iodide staining and flow cytometry," *J. Immunol. Methods*, vol. 139, no. 2, pp. 271–279, Jun. 1991.
[186] Z. Darzynkiewicz, D. Galkowski, and H. Zhao, "Analysis of apoptosis by cytometry using TUNEL assay," *Methods*, vol. 44, no. 3, pp. 250–254, Mar. 2008.
[187] D. S. O'Mahony, U. Pham, R. Iyer, T. R. Hawn, and W. C. Liles, "Differential constitutive and cytokine-modulated expression of human Toll-like receptors in primary neutrophils, monocytes, and macrophages," *Int J Med Sci*, vol. 5, no. 1, pp. 1–8, 2008.
[188] M. Kato-Maeda, C. A. Shanley, D. Ackart, L. G. Jarlsberg, S. Shang, A. Obregon-Henao, M. Harton, R. J. Basaraba, M. Henao-Tamayo, J. C. Barrozo, J. Rose, L. M. Kawamura, M. Coscolla, V. Y. Fofanov, H. Koshinsky, S. Gagneux, P. C. Hopewell, D. J. Ordway, and I. M. Orme, "Beijing sublineages of

*Mycobacterium tuberculosis* differ in pathogenicity in the guinea pig," *Clinical and vaccine immunology: CVI*, Jun. 2012.
[189] L. H. Ly and D. N. McMurray, "The Yin-Yang of TNFalpha in the guinea pig model of tuberculosis," *Indian J. Exp. Biol.*, vol. 47, no. 6, pp. 432–439, Jun. 2009.
[190] V. S. Cooper, D. Schneider, M. Blot, and R. E. Lenski, "Mechanisms Causing Rapid and Parallel Losses of Ribose Catabolism in Evolving Populations of Escherichia Coli B," *J. Bacteriol.*, vol. 183, no. 9, pp. 2834–2841, May 2001.
[191] D. M. Stoebel and C. J. Dorman, "The effect of mobile element IS10 on experimental regulatory evolution in Escherichia coli," *Mol. Biol. Evol.*, vol. 27, no. 9, pp. 2105–2112, Sep. 2010.
[192] M. E. Hudson, D. R. Lisch, and P. H. Quail, "The FHY3 and FAR1 genes encode transposase-related proteins involved in regulation of gene expression by the phytochrome A-signaling pathway," *The Plant Journal*, vol. 34, no. 4, pp. 453–471, 2003.
[193] R. Lin, Y. Teng, H.-J. Park, L. Ding, C. Black, P. Fang, and H. Wang, "Discrete and Essential Roles of the Multiple Domains of *Arabidopsis* FHY3 in Mediating Phytochrome A Signal Transduction," *Plant Physiol.*, vol. 148, no. 2, pp. 981–992, Oct. 2008.
[194] "*M. tuberculosis* H37Rv (GB:AL123456): Rv2667 - ATP-dependent protease ATP-binding subunit clpC2 - TB Genomes." [Online]. Available: http://genome.tbdb.org/annotation/genome/tbdb/GeneDetails.html?sp=S7000000635251922. [Accessed: 26-Jun-2012].
[195] E. McElvania Tekippe, I. C. Allen, P. D. Hulseberg, J. T. Sullivan, J. R. McCann, M. Sandor, M. Braunstein, and J. P.-Y. Ting, "Granuloma formation and host defense in chronic *Mycobacterium tuberculosis* infection requires PYCARD/ASC but not NLRP3 or caspase-1," *PLoS ONE*, vol. 5, no. 8, p. e12320, 2010.
[196] L. Ramakrishnan, "Revisiting the role of the granuloma in tuberculosis," *Nat. Rev. Immunol.*, vol. 12, no. 5, pp. 352–366, 2012.
[197] Z. He and J. De Buck, "Cell wall proteome analysis of *Mycobacterium smegmatis* strain MC2 155," *BMC Microbiol.*, vol. 10, p. 121, 2010.
[198] Q. Long, Q. Zhou, L. Ji, J. Wu, W. Wang, and J. Xie, "*Mycobacterium smegmatis* genomic characteristics associated with its saprophyte lifestyle," *Journal of cellular biochemistry*, May 2012.
[199] C.-C. Chen, S.-H. Tsai, C.-C. Lu, S.-T. Hu, T.-S. Wu, T.-T. Huang, N. Saïd-Sadier, D. M. Ojcius, and H.-C. Lai, "Activation of an NLRP3 Inflammasome Restricts *Mycobacterium kansasii* Infection," *PLoS ONE*, vol. 7, no. 4, p. e36292, 2012.
[200] J. L. Camberg, J. R. Hoskins, and S. Wickner, "ClpXP Protease Degrades the Cytoskeletal Protein, FtsZ, and Modulates FtsZ Polymer Dynamics," *PNAS*, vol. 106, no. 26, pp. 10614–10619, Jun. 2009.
[201] V. P. Mohan, C. A. Scanga, K. Yu, H. M. Scott, K. E. Tanaka, E. Tsang, M. C. Tsai, J. L. Flynn, and J. Chan, "Effects of Tumor Necrosis Factor Alpha on Host Immune Response in Chronic Persistent Tuberculosis: Possible Role for

Limiting Pathology," *Infection and Immunity*, vol. 69, no. 3, pp. 1847–1855, Mar. 2001.
[202] S. D. Chakravarty, G. Zhu, M. C. Tsai, V. P. Mohan, S. Marino, D. E. Kirschner, L. Huang, J. Flynn, and J. Chan, "Tumor necrosis factor blockade in chronic murine tuberculosis enhances granulomatous inflammation and disorganizes granulomas in the lungs," *Infect. Immun.*, vol. 76, no. 3, pp. 916–926, Mar. 2008.
[203] J. L. Flynn, M. M. Goldstein, J. Chan, K. J. Triebold, K. Pfeffer, C. J. Lowenstein, R. Schreiber, T. W. Mak, and B. R. Bloom, "Tumor necrosis factor-alpha is required in the protective immune response against *Mycobacterium tuberculosis* in mice," *Immunity*, vol. 2, no. 6, pp. 561–572, Jun. 1995.
[204] I. Dambuza, R. Keeton, N. Allie, N.-J. Hsu, P. Randall, B. Sebesho, L. Fick, V. J. F. Quesniaux, and M. Jacobs, "Reactivation of *M. tuberculosis* infection in trans-membrane tumour necrosis factor mice," *PLoS ONE*, vol. 6, no. 11, p. e25121, 2011.
[205] P. L. Lin, A. Myers, L. Smith, C. Bigbee, M. Bigbee, C. Fuhrman, H. Grieser, I. Chiosea, N. N. Voitenek, S. V. Capuano, E. Klein, and J. L. Flynn, "Tumor necrosis factor neutralization results in disseminated disease in acute and latent *Mycobacterium tuberculosis* infection with normal granuloma structure in a cynomolgus macaque model," *Arthritis Rheum.*, vol. 62, no. 2, pp. 340–350, Feb. 2010.
[206] S. A. Shaikha, K. Mansour, and H. Riad, "Reactivation of Tuberculosis in Three Cases of Psoriasis after Initiation of Anti-TNF Therapy," *Case Rep Dermatol*, vol. 4, no. 1, pp. 41–46, Jan. 2012.
[207] R. K. Maitra, T. Bowling, P. Venkatesan, and C. Maxwell-Armstrong, "Crohn's disease or TB--the perennial question and diagnostic pitfalls," *BMJ Case Rep*, vol. 2012, 2012.
[208] A. Dasgupta, K. Sureka, D. Mitra, B. Saha, S. Sanyal, A. K. Das, P. Chakrabarti, M. Jackson, B. Gicquel, M. Kundu, and J. Basu, "An Oligopeptide Transporter of *Mycobacterium tuberculosis* Regulates Cytokine Release and Apoptosis of Infected Macrophages," *PLoS ONE*, vol. 5, no. 8, p. e12225, Aug. 2010.
[209] J. Kleinnijenhuis, M. Oosting, T. S. Plantinga, J. W. M. van der Meer, L. A. B. Joosten, R. V. Crevel, and M. G. Netea, "Autophagy modulates the *Mycobacterium tuberculosis*-induced cytokine response," *Immunology*, vol. 134, no. 3, pp. 341–348, 2011.
[210] C. M. Fremond, D. Togbe, E. Doz, S. Rose, V. Vasseur, I. Maillet, M. Jacobs, B. Ryffel, and V. F. J. Quesniaux, "IL-1 receptor-mediated signal is an essential component of MyD88-dependent innate response to *Mycobacterium tuberculosis* infection," *J. Immunol.*, vol. 179, no. 2, pp. 1178–1189, Jul. 2007.
[211] R. C. M. Ryan, M. P. O'Sullivan, and J. Keane, "*Mycobacterium tuberculosis* infection induces non-apoptotic cell death of human dendritic cells," *BMC Microbiol.*, vol. 11, p. 237, 2011.
[212] B. B. Mishra, P. Moura-Alves, A. Sonawane, N. Hacohen, G. Griffiths, L. F. Moita, and E. Anes, "*Mycobacterium tuberculosis* protein ESAT-6 is a potent

activator of the NLRP3/ASC inflammasome," *Cell. Microbiol.*, vol. 12, no. 8, pp. 1046–1063, Aug. 2010.
[213] C.-S. Yang, D.-M. Shin, and E.-K. Jo, "The Role of NLR-related Protein 3 Inflammasome in Host Defense and Inflammatory Diseases," *Int Neurourol J*, vol. 16, no. 1, pp. 2–12, Mar. 2012.
[214] A. G. Kinhikar, I. Verma, D. Chandra, K. K. Singh, K. Weldingh, P. Andersen, T. Hsu, W. R. Jacobs Jr, and S. Laal, "Potential role for ESAT6 in dissemination of *M. tuberculosis* via human lung epithelial cells," *Mol. Microbiol.*, vol. 75, no. 1, pp. 92–106, Jan. 2010.
[215] J. C. Betts, P. T. Lukey, L. C. Robb, R. A. McAdam, and K. Duncan, "Evaluation of a nutrient starvation model of *Mycobacterium tuberculosis* persistence by gene and protein expression profiling," *Molecular Microbiology*, vol. 43, no. 3, pp. 717–731, 2002.
[216] Y. Liu and G. Schoolnik, "Liu and Schoolnik- Unpublished Carbon Sources Data provided for public use to TBDM::Rv2667 data." [Online]. Available: http://www.tbdb.org/expressionHistory.shtml?gn=Rv2667. [Accessed: 02-Jul-2012].
[217] M. F. Rodrigues, M. M. Barsante, C. C. S. Alves, M. A. Souza, A. P. Ferreira, G. P. Amarante-Mendes, and H. C. Teixeira, "Apoptosis of macrophages during pulmonary *Mycobacterium bovis* infection: correlation with intracellular bacillary load and cytokine levels," *Immunology*, vol. 128, no. 1 Suppl, pp. e691–699, Sep. 2009.
[218] N. P. Juffermans, S. Florquin, L. Camoglio, A. Verbon, A. H. Kolk, P. Speelman, S. J. van Deventer, and T. van Der Poll, "Interleukin-1 signaling is essential for host defense during murine pulmonary tuberculosis," *J. Infect. Dis.*, vol. 182, no. 3, pp. 902–908, Sep. 2000.
[219] K. Patel, S. S. Jhamb, and P. P. Singh, "Models of latent tuberculosis: their salient features, limitations, and development," *J Lab Physicians*, vol. 3, no. 2, pp. 75–79, Jul. 2011.
[220] A. M. Abdallah, J. Bestebroer, N. D. L. Savage, K. de Punder, M. van Zon, L. Wilson, C. J. Korbee, A. M. van der Sar, T. H. M. Ottenhoff, N. N. van der Wel, W. Bitter, and P. J. Peters, "Mycobacterial secretion systems ESX-1 and ESX-5 play distinct roles in host cell death and inflammasome activation," *J. Immunol.*, vol. 187, no. 9, pp. 4744–4753, Nov. 2011.
[221] D. Portevin, S. Gagneux, I. Comas, and D. Young, "Human macrophage responses to clinical isolates from the *Mycobacterium tuberculosis* complex discriminate between ancient and modern lineages," *PLoS Pathog.*, vol. 7, no. 3, p. e1001307, Mar. 2011.
[222] S. Gagneux and P. M. Small, "Global phylogeography of *Mycobacterium tuberculosis* and implications for tuberculosis product development," *Lancet Infect Dis*, vol. 7, no. 5, pp. 328–337, May 2007.
[223] M. P. Nicol and R. J. Wilkinson, "The clinical consequences of strain diversity in *Mycobacterium tuberculosis*," *Trans. R. Soc. Trop. Med. Hyg.*, vol. 102, no. 10, pp. 955–965, Oct. 2008.

[224] K. Sankaran and H. B. Herscowitz, “Phenotypic and functional heterogeneity of the murine alveolar macrophage-derived cell line MH-S,” *J. Leukoc. Biol.*, vol. 57, no. 4, pp. 562–568, Apr. 1995.
[225] B. Ton-Hoang, P. Siguier, Y. Quentin, S. Onillon, B. Marty, G. Fichant, and M. Chandler, “Structuring the bacterial genome: Y1-transposases associated with REP-BIME sequences,” *Nucleic Acids Res.*, vol. 40, no. 8, pp. 3596–3609, Apr. 2012.
[226] V. Braun, M. Mehlig, M. Moos, M. Rupnik, B. Kalt, D. E. Mahony, and C. Von Eichel-Streiber, “A chimeric ribozyme in *Clostridium difficile* combines features of group I introns and insertion elements,” *Molecular Microbiology*, vol. 36, no. 6, pp. 1447–1459, 2000.
[227] O. Hasselmayer, V. Braun, C. Nitsche, M. Moos, M. Rupnik, and C. von Eichel-Streiber, “*Clostridium difficile* IStron CdISt1: Discovery of a Variant Encoding Two Complete Transposase-Like Proteins,” *Journal of Bacteriology*, vol. 186, no. 8, pp. 2508–2510, Apr. 2004.
[228] B. Mathema, N. Kurepina, G. Yang, E. Shashkina, C. Manca, C. Mehaffy, H. Bielefeldt-Ohmann, S. Ahuja, D. A. Fallows, A. Izzo, P. Bifani, K. Dobos, G. Kaplan, and B. N. Kreiswirth, “Epidemiologic consequences of microvariation in *Mycobacterium tuberculosis*,” *J. Infect. Dis.*, vol. 205, no. 6, pp. 964–974, Mar. 2012.
[229] M. K. Sharma, A. Al-Azem, J. Wolfe, E. Hershfield, and A. Kabani, “Identification of a predominant isolate of *Mycobacterium tuberculosis* using molecular and clinical epidemiology tools and *in vitro* cytokine responses,” *BMC Infect. Dis.*, vol. 3, p. 3, Apr. 2003.
[230] D. A. Magee, M. Taraktsoglou, K. E. Killick, N. C. Nalpas, J. A. Browne, S. D. E. Park, K. M. Conlon, D. J. Lynn, K. Hokamp, S. V. Gordon, E. Gormley, and D. E. MacHugh, “Global gene expression and systems biology analysis of bovine monocyte-derived macrophages in response to *in vitro* challenge with *Mycobacterium bovis*,” *PLoS ONE*, vol. 7, no. 2, p. e32034, 2012.